State University of New York Report

Large Eddy Simulations and Direct Numerical Simulations of High Speed Turbulent Reacting Flows

by

P. Givi, S.H. Frankel, V. Adumitroaie,
G. Sabini, and C.K. Madnia

NAG1-1122

Department of Mechanical and Aerospace Engineering
State University of New York
Buffalo, New York 14260-4400

Semi-Annual Report Submitted to
NASA Langley Research Center

Summary of Activities Supported Under Grant NAG 1-1122

for the Period

August 1, 1992 - January 31, 1993

Contents

Large Eddy Simulations and Direct Numerical Simulations of High Speed Turbulent Reacting Flows

P. Givi, S.H. Frankel, V. Adumitroaie, G. Sabini, and C.K. Madnia
Department of Mechanical and Aerospace Engineering
State University of New York at Buffalo
Buffalo, New York 14260

Abstract

The primary objective of this research is to extend current capabilities of *Large Eddy Simulations* (LES) and *Direct Numerical Simulations* (DNS) for the computational analyses of high speed reacting flows. Our efforts in the first two years of this research have been concentrated on *a priori* investigations of single-point Probability Density Function (PDF) methods for providing subgrid closures in reacting turbulent flows. In the efforts initiated in the third year, our primary focus has been on performing actual LES by means of PDF methods. The approach is based on *assumed* PDF methods and we have performed extensive analysis of turbulent reacting flows by means of LES. This includes simulations of both three-dimensional (3D) isotropic compressible flows and two-dimensional reacting planar mixing layers. In addition to these LES analyses, some work is in progress to assess the extent of validity of our assumed PDF methods. This assessment is done by making detailed companions with recent laboratory data in predicting the rate of reactant conversion in parallel reacting shear flows.

This report provides a summary of our achievements for the first six months of the third year of this program. This research has been supported by NASA Langley Research Center under Grant NAG-1-1122. Dr. J. Philip Drummond, Theoretical Flow Physics Branch (TFPB), Mail Stop 156, Tel: 804-864-2298 is the Technical Monitor of this Grant

1 Recent Progress

In the first two years of this research program, we have been speculating the feasibility of the approach based on probability density function (PDF) methods as a means of accounting for the effects of subgrid scalar fluctuations in large eddy simulations (LES) of turbulent reacting flows. Within this period, we have devoted substantial effort on extending the state-of-the-art on PDF modeling, and on making use of recent developments for the purpose of our investigation. Fortunately, we have been able to make noteworthy progress in understanding the advantages and drawbacks of *all* of the recently available PDF methods. Therefore, in this third year of our activities, we have initiated a strong program in making use of PDF methods for the purpose of LES. In doing so, based on our experience in the first two years, we have initiated a step-by-step procedure which we shall describe below. The advantage of this procedure is the fact that the results of our investigation are also helpful in approaches based on conventional Reynolds averaging methods.

It is well-know that there are two ways by which the PDF methods can be invoked for modeling of scalar fluctuations in a statistical description of turbulent reacting flows [1, 2]: (1) Assumed PDF, (2) PDF obtained by a modeled transport equation. By fluctuations we mean those in either typical Reynolds averaging or within the subgrid in LES. Each of these two PDF methods have certain advantages and drawbacks, as indicated in our previous yearly reports and as also indicated in a number of previous publications, *e.g.* [3, 4, 5].

A noteworthy progress in PDF methods is the recent development of the *Amplitude Mapping Closure* (AMC) by Kraichnan and co-workers [6, 7]. In a number of standard test cases, it has been demonstrated that this closure is somewhat more superior in comparisons with previous PDF methods based on the so called Coalescence/Dispersion (C/D) models [8]. Based on this development, at the initial phase of this research our intention was to make use of AMC for the purpose of subgrid closures. For that, we initiated a research program for the purpose of better understanding the properties of this closure. Based on our work

to date, the results of which are reported in [9, 10], it is shown that the approach provides some advantages over previous models for some "simple" cases. However, it does also have certain drawbacks which limits its use for "practical" applications. In our recent paper [10] (included as Appendix I), a lengthy discussion is presented of all the properties of these methods. Here, we shall summarize some of the difficulties associated with the use of AMC for PDF based LES:

1. The use of the approach is practical for closure only at the single-point level.

2. In its present form, the model cannot take the effects of mixing on migration of scalar bounds into account.

3. The computational implementation of the model for multi-scalar mixing and reaction is virtually impossible.

4. For the cases which the model has been validated, other simpler PDF methods; particularly those belonging to the *Pearson Family* (PF) [11] or *Johnson Edgeworth Translation* (JET) [12, 13] of distribution have been satisfactory.

Considering points (1) and (2), it is safe to conclude that the AMC shares the same limitations as those in assumed PDF methods and in C/D closures. Point (3) advocates the use of other PDF methods until developments of more reliable numerical methods. Based on these three points, and also considering point (4) we decided to "discontinue" further *basic* research on assessing pro's and con's of PDF methods, in favor of extending LES technology by means of PDF methods. This is deemed acceptable, at least at the present stage, since:

(i) Most current PDF methods can be only incorporated at the single-point level. Therefore, closure models for the second order moments (*e.g.* variances and covariance) have to be provided by other means.

(ii) The flexibilities offered by some of the assumed probability distributions, *e.g.* members of PF or JET is very pleasing for accounting the effects of species fluctuations in a stochastic

sense.

(iii) While in Reynolds averaging of reacting flow, the modeling of the PDF is very crucial [14], we speculate that in LES of such flows it is more crucial to have the second order moments of the scalar field predicted correctly.

Based on these points, we have decided to perform extensive LES analyses of homogeneous-isotropic and spatially developing reacting mixing layers. The results of our efforts to-date are described in detail in Appendix II. The summary of our findings is:

(a) We feel that the approach based on a hybrid second-order closure and assumed PDF methods provides the most promising and practical means of performing LES of reacting flows, at least presently. The appropriate form of the closure that can be used is based on a $k - \Delta - \mathrm{g}$ model. Here, k = kinetic energy of velocity fluctuations within the subgrid, Δ = the width of the filter, and g = the "covariance" vector.

(b) It is impossible to make use of zero-order models (equivalent of Prandtl's mixing length hypothesis) in LES. The implementation of this model results in wrong predictions.

(c) The second order methodology is significantly different from that used in conventional Reynolds averaging procedures. The primary difference is due to modeling of convective transport and also the "diminished" degree of freedom because of the lack of a transport equation for Δ.

(d) After significant analyses (see Appendix II), we now have a reasonable k equation. This equation works well if a combination of both the "strain rate tensor" and the "rotation tensor" are used in modeling the turbulent viscosity.

(e) In simple reacting systems, assumed PDF's of PF and JET [10] provide a reasonable means of accounting for the scalar fluctuations within the subgrid. For example, in the chemistry of $A + B \rightarrow$ Product, the Logit-Normal density and the Beta density of first kind are reasonable for the chemistry under equilibrium conditions. Under non-equilibrium

conditions, the use of Dirichlet distribution can be justified.

(f) The model described above can be used effectively if k and g are predicted accurately. The usual practice is to use gradient diffusion modeling for the effects of convective transport in the g equation. While this model has been somewhat satisfactory in Reynolds averaging procedures, it does not work in LES (see Appendix II). In fact, even in a simple non-reacting flow, the scalar g (not in the vector form) cannot be precited well. This is expected considering the different form of k equation which had to be used. Nevertheless, if this parameter is modeled accurately the LES procedure can be implemented very effectively.

We do not yet know how to modify the g equation in a form appropriate for LES. This issue is currently being investigated.

The next step in our work in this direction is to replace the assumed PDF method with the approach based on a transport equation for the PDF. For that we plan to make use of C/D models for modeling of the molecular mixing term. Our purpose for doing so is due to two factors: (1) C/D closure can be incorporated into the numerical procedure rather easily, and (2) The problem associated with the lack of boundary migration is less severe in C/D in comparison to AMC.

The summary of all our achievements are highlighted in the appendices. These appendices are self explanatory. Therefore, there is no need for further elaboration here.

2 Recent Publications

Within the first half of our activities in the third year, we have produced the following publications: A journal article to appear *Comb. Sci. and Tech.* [10] (Appendix I), a paper to be presented at the LES conference at the ASME meeting in June 1993 (Appendix II), and an article to be submitted for publication shortly (Appendix III).

References

[1] O'Brien, E. E., The Probability Density Function (PDF) Approach to Reacting Turbulent Flows, in Libby, P. A. and Williams, F. A., editors, *Turbulent Reacting Flows*, chapter 5, pp. 185–218, Springer-Verlag, Heidelberg, 1980.

[2] Pope, S. B., PDF Methods for Turbulent Reacting Flows, *Prog. Energy Combust. Sci.*, **11**:119–192 (1985).

[3] Givi, P., Model Free Simulations of Turbulent Reactive Flows, *Prog. Energy Combust. Sci.*, **15**:1–107 (1989).

[4] Kollmann, W., The pdf Approach to Turbulent Flow, *Theoret. Comput. Fluid Dynamics*, **1**:249–285 (1990).

[5] Pope, S. B., Computations of Turbulent Combustion: Progress and Challenges, in *Proceedings of 23rd Symp. (Int.) on Combustion*, pp. 591–612, The Combustion Institute, Pittsburgh, PA, 1990.

[6] Kraichnan, R. H., Closures for Probability Distributions, *Bull. Amer. Phys. Soc.*, **34**:2298 (1989).

[7] Chen, H., Chen, S., and Kraichnan, R. H., Probability Distribution of a Stochastically Advected Scalar Field, *Phys. Rev. Lett.*, **63**(24):2657–2660 (1989).

[8] Pope, S. B., Mapping Closures for Turbulent Mixing and Reaction, *Theoret. Comput. Fluid Dynamics*, **2**:255–270 (1991).

[9] Madnia, C. K., Frankel, S. H., and Givi, P., Reactant Conversion in Homogeneous Turbulence: Mathematical Modeling, Computational Validations and Practical Applications, *Theoret. Comput. Fluid Dynamics*, **4**:79–93 (1992).

[10] Miller, R. S., Frankel, S. H., Madnia, C. K., and Givi, P., Johnson-Edgeworth Translation for Probability Modeling of Binary Mixing in Turbulent Flows, *Combust. Sci. and Tech.*, (1993), In press.

[11] Pearson, K., Contributions to the Mathematical Theory of Evolution: II. Skew Variations in Homogeneous Material, *Philos. Trans. of the Royal Soc. of London, Series A.*, **186**:343–414 (1895).

[12] Johnson, N. L., Systems of Frequency Curves Generated by Methods of Translation, *Biometrika*, **36**:149–176 (1949a).

[13] Edgeworth, F. Y., On the Representation of Statistical Frequency by a Series, *Journal of the Royal Statistical Society, Series A.*, **70**:102–106 (1907).

[14] Libby, P. A. and Williams, F. A., editors, *Turbulent Reacting Flows, Topics in Applied Physics*, Vol. 44, Springer-Verlag, Heidelberg, 1980.

3 Appendix I

This appendix provides a summary of our work on assumed PDF methods. In addition to explaining many important mathematical characteristics of all the available PDF methods, this paper also provides a comparative assessment of these closure for practical applications. The major point of the report, as relevant to our LES analyses, is the comparison of the properties of PF and JET generated PDF's with those of AMC.

The work reported here makes a logical extension of our previous work reported in [9].

CST 92-08-14

Combust. Sci. and Tech., 1993, Vol. XX, pp. 1-32
Photocopying permitted by license only

Johnson-Edgeworth Translation for Probability Modeling of Binary Scalar Mixing in Turbulent Flows

R. S. MILLER, S. H. FRANKEL, C. K. MADNIA, and P. GIVI *Department of Mechanical and Aerospace Engineering, State University of New York, Buffalo, NY 14260*

(Received August 14, 1992; in final form November 2, 1992)

Abstract—A family of Probability Density Functions (PDF's) generated by *Johnson-Edgeworth* Translation (JET) is used for statistical modeling of the mixing of an initially binary scalar in isotropic turbulence. The frequencies obtained by this translation are shown to satisfy some of the characteristics of the PDF's generated by the *Amplitude Mapping* Closure (AMC) (Kraichnan, 1989; Chen *et al.*, 1989). In fact, the solution obtained by one of the members of this family is shown to be identical to that developed by the AMC (Pope, 1991). Due to this similarity and due to the demonstrated capabilities of the AMC, a justification is provided for the use of other members of JET frequencies for the modeling of the binary mixing problem. This similarity also furnishes the reasoning for the applicability of the *Pearson Family* (PF) of frequencies for modeling of the same phenomena. The mathematical requirements associated with the applications of JET in the modeling of the binary mixing problem are provided, and all the results are compared with data generated by Direct Numerical Simulations (DNS). These comparisons indicate that the *Logit-Normal* frequency portrays some subtle features of the mixing problem better than the other closures. However, none of the models considered (JET, AMC, and PF) are capable of predicting the evolution of the conditional expected dissipation and/or the conditional expected diffusion of the scalar field in accordance with DNS. It is demonstrated that this is due to the incapability of the models to account for the variations of the scalar bounds as the mixing proceeds. A remedy is suggested for overcoming this problem which can be useful in probability modeling of turbulent mixing, especially when accompanied by chemical reactions. While in the context of a single-point description the evolution of the scalar bounds cannot be predicted, the qualitative analytical-computational results portray a physically plausible behavior.

1 INTRODUCTION

The problem of binary mixing in turbulent flows has been the subject of widespread investigations over the past two decades (Dopazo, 1973; Pope, 1979; Pope, 1985; Pope, 1990; Givi, 1989; Kollmann, 1990). This problem has been particularly useful in assessing the extent of validity of the closures developed within this period for modeling of turbulent mixing by Probability Density Function (PDF) methods (Dopazo, 1973; Pope, 1976; Pope, 1979; Janicka *et al.*, 1979; Pope, 1982; Kosaly and Givi, 1987; Norris and Pope, 1991). Usually the problem is considered in the setting of a spatially homogeneous turbulent flow in which the temporal evolution of the PDF is considered. In this setting, development of a closure which can accurately predict the evolution of the PDF has been the main objective of these investigations (for recent reviews see Pope (1990); Kollmann (1990); Givi (1989)).

Computational experiments based on Direct Numerical Simulations (DNS) have proven very useful in evaluating the performance of new closures (Givi, 1989; Pope, 1990). The binary mixing problem is well-suited for DNS investigation, and current computational capabilities allow consideration of flows at sufficiently large Reynolds numbers in which the behavior of the models can be assessed (Eswaran and Pope, 1988; Givi and McMurtry, 1988; McMurtry and Givi, 1989; Madnia and Givi, 1992). The results of all the previous work on DNS of the binary mixing problem portray a clear picture of the PDF evolution, at least at the single-point level. A successful closure is one which can predict all the stages of mixing, as depicted by DNS, from an initially binary state (total segregated) to a final mixed condition.

NOTE: This is not a reprint. It is a Page Proof, and Contains many spelling errors. Some of the equations are also type-set wrong... P. Givi

Amongst the models developed in the literature, the recent Amplitude Mapping Closure (AMC) (Kraichnan, 1989; Chen *et al.*, 1989; Pope, 1991) has proven effective in producing a physically correct PDF evolution. In the application of this model to the problem of binary mixing it has been demonstrated that the closure is capable of approximating a reasonably correct evolution at all stages of mixing (Pope, 1991). Namely, the evolution from an initial double delta PDF to an asymptotic Gaussian distribution. This is a trend which has been observed in DNS (Eswaran and Pope, 1988; Givi and McMurtry, 1988; McMurtry and Givi, 1989; Madnia and Givi, 1992) and also corroborated by experimental investigations (Miyawaki *et al.*, 1974). However, it is shown by Gao (1991); O'Brien and Jiang (1991) that the PDF adopts an asymptotic Gaussian-like distribution only near the mean scalar value, and the conditional expected dissipation does not correspond to that of a Gaussian field everywhere within the composition domain.

Our first objective in this work is to present another means by which the AMC can be viewed. It is demonstrated that in the binary mixing problem, this closure can be considered as a member of the family of frequencies generated by the method of Johnson-Edgeworth Translation (JET). In fact, it is shown that the result produced by the AMC is identical to that generated by one of the members of this translation. With this observation, a justification for employing other simpler "assumed" frequencies is provided. Our second objective is to make a detailed examination of the conditional expected dissipation and the conditional expected diffusion of the scalar variable as predicted by the closures. This examination provides an effective means of demonstrating the deficiencies of these models in reproducing the correct physical behavior as depicted by DNS results. With the development of analytical relations for some of these closures, a remedy is suggested for overcoming the model deficiencies.

1.1 Outline

In the next section, the problem of binary mixing and its solution via the AMC is briefly reviewed. In Section 3, the Johnson-Edgeworth Translation is introduced with a highlight on the mathematical constraints associated with its application for the modeling of the mixing problem. Due to the previously established similarity of the JET frequencies with those based on the Pearson Family (PF), the Beta density of the first kind is also presented in this section. The PDF's generated by these three models (AMC, JET and PF) are compared against each other and also with data generated by Direct Numerical Simulations (DNS) in Section 4. The results for the conditional expected scalar dissipation, and the conditional expected scalar dissipations for all the closures are discussed, respectively, in Section 5 and in Section 6. In Section 7, some theoretical remarks pertaining to the evolution of the scalar in an isotropic field are presented. With this presentation, the problems associated with all three closures become more clear. In Sections 2-7, the discussions are limited to those associated with the transport of a passive scalar from an initially symmetric binary state in isotopic turbulence. Therefore, in Section 8 some discussions are presented of the applications of the models for treating more general problems. This paper is drawn to a conclusion in Section 9.

2 BINARY MIXING PROBLEM

We consider the mixing of a scalar variable $\phi = \phi(\mathbf{x}, t)$($\mathbf{x}$ is the position vector, and t denotes time) from an initially symmetric binary state within the bounds $\phi_\ell \leq \phi \leq \phi_u$. In this section, we assume that the lower and the upper bounds of the scalar range remain fixed (*i.e.* $\phi_u, \phi_e ll$ are constant). Within this domain, the single-point PDF of the variable ϕ at initial time is given by

$$P_1(\phi, t = 0) = \frac{1}{2}[\delta(\phi - \phi_\ell) + \delta(\phi - \phi_u)], \tag{1}$$

DVIAPS ATLIS Publishing, Inc.
4 TeX output 1993.01.21:1426 (3)

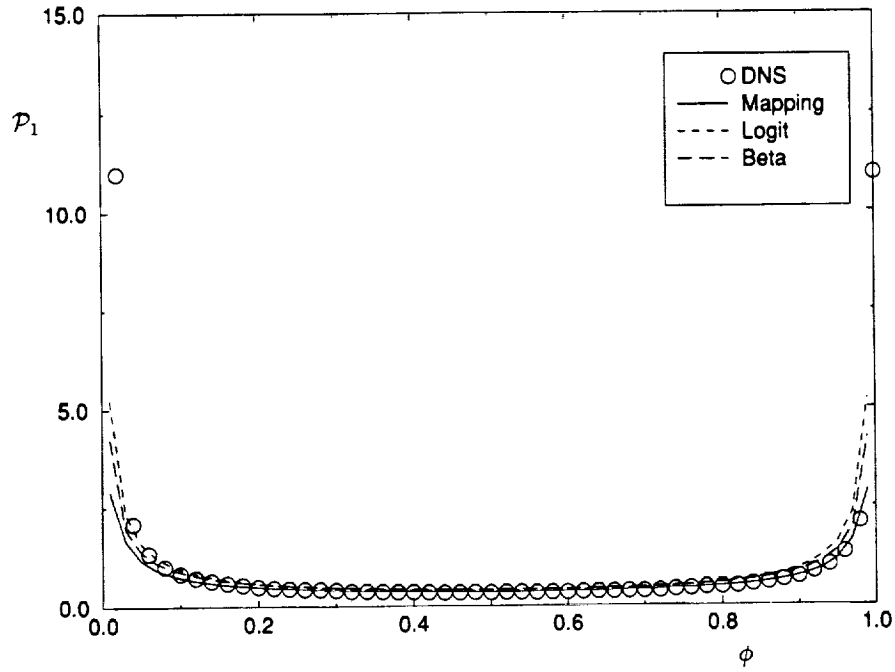

FIGURE 1a The comparison of the PDF's as predicted by the models with DNS data. (a) $\sigma^2 = 0.173$.

which obviously infers the following relations for the mean and the variance

$$< \phi >= (\phi_u + \phi_\ell)/2, < \phi'^2 >= \sigma^2 = \frac{1}{4}(\phi_u - \phi_\ell)^2. \tag{2}$$

Here, ¡ ¿ indicates the probability mean, σ^2 denotes the variance, and the prime represents the instantaneous deviation from the mean. In isotropic incompressible turbulence, the evolution of the PDF is governed by the transport equation

$$\frac{\partial P_1}{\partial t} + \frac{\partial^2(\varepsilon P_1)}{\partial \phi^2} = 0, \partial_\ell \leq \phi \leq \partial_u \tag{3}$$

where ε represents the expected value of the scalar dissipation with diffusion coefficient Γ, $\xi(= \Gamma \nabla\phi \cdot \nabla\phi)$, conditioned on the value of the scalar $\phi(\mathbf{x}, t)$,

$$\varepsilon = \varepsilon(\phi, t) =< \xi | \phi(\mathbf{x}, t) > . \tag{4}$$

Equation (3) can alternatively be expressed by

$$\frac{\partial P_1}{\partial t} + \frac{\partial(DP_1)}{\partial \phi} = 0, \phi_\ell \leq \phi \leq \phi_u, \tag{5}$$

where D denotes the conditional expected value of the scalar diffusion

$$D = D(\phi, t) \ < \Gamma \nabla^2 \phi | \phi(\mathbf{x}, t) > . \tag{6}$$

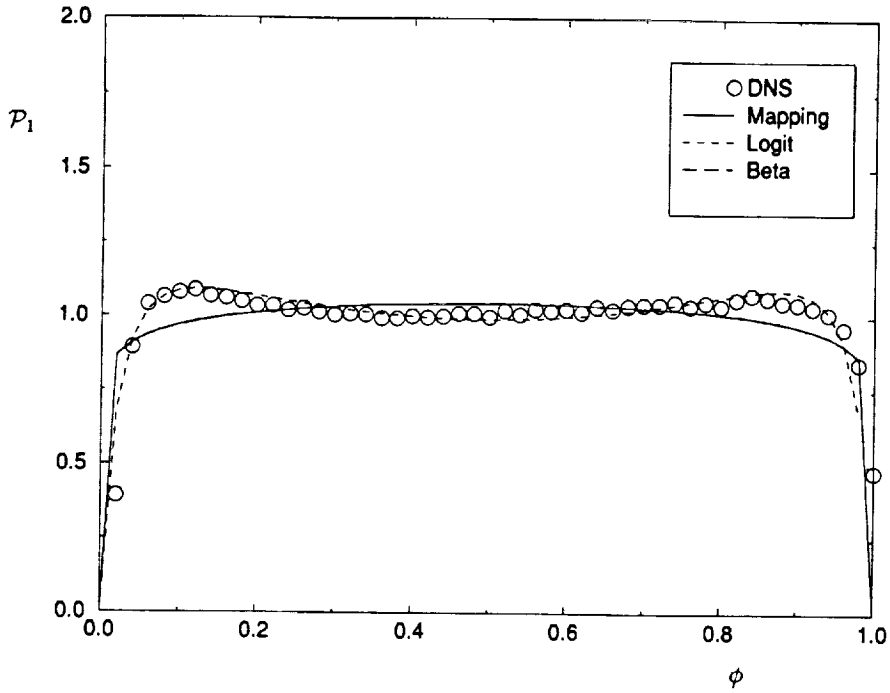

FIGURE 1b The comparison of the PDF's as predicted by the models with DNS data. (b) $\sigma^2 = 0.079$.

The closure problem in determining the PDF, P_1, is associated with the unknown conditional expected dissipation, ε, and/or the conditional expected diffusion, D. These two are related through Eqs. (1)-(6),

$$D(\phi, t) = \frac{1}{P_1(\phi, t)} \frac{\partial(\varepsilon P_1)}{\partial \phi}. \tag{7}$$

At the single-point level neither the conditional mean dissipation nor the conditional mean diffusion are known (neither are their unconditional mean values). Their specifications require external information.

With the application of the AMC, this external information is obtained in an implicit manner. As explained in detail by Pope (1991), the AMC involves a *mapping* of the random field of interest ϕ to a stationary Gaussian reference field ϕ_0, via a transformation $\phi = \chi(\phi_0, t)$. Once this relation is established, the PDF of the random variable ϕ, $P_1(\phi)$, is related to that of a Gaussian distribution. In a domain with fixed upper and lower bounds, *i.e.* fixed ϕ_ℓ, ϕ_u, the corresponding form of the mapping function is obtained by Pope (1991). The solution for a symmetric field with zero mean, $< \phi >= 0, \phi_u = -\phi_\ell$, is represented in terms of an unknown time τ

$$\chi(\phi_0, \tau) = \phi_u erf\left(\frac{\phi_0}{\sqrt{2}G}\right), G(\tau) = \sqrt{\exp(2\tau) - 1}. \tag{8}$$

With this transformation, the PDF is determined from the physical requirement

$$P_1(\chi(\phi_0, \tau), \tau) d\chi = P_G(\phi_0) d\phi_0, \tag{9}$$

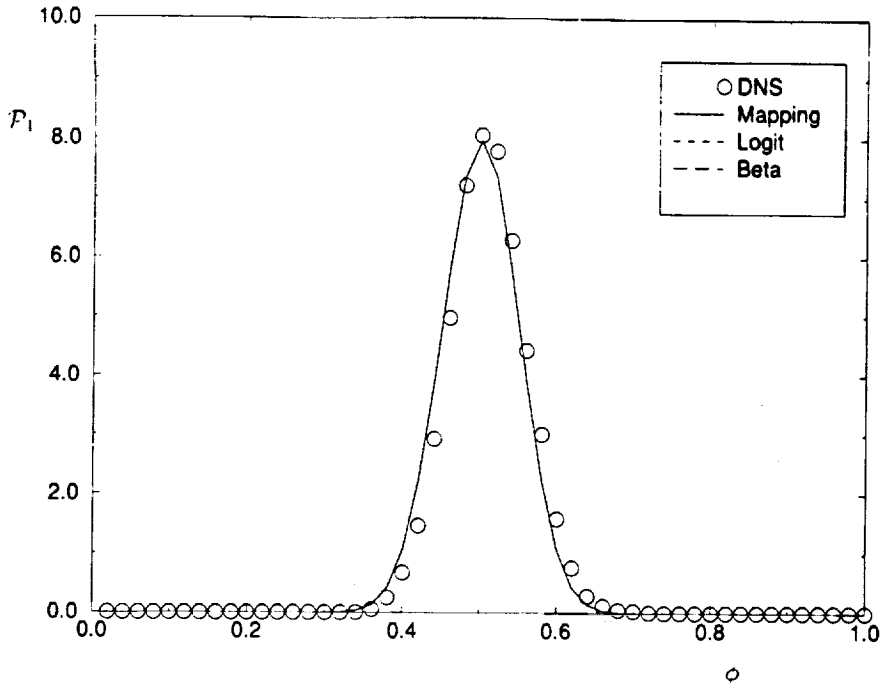

FIGURE 1c The comparison of the PDF's as predicted by the models with DNS data. (c) $\sigma^2 = 0.00247$.

where P_G denotes the PDF of a standardized Gaussian distribution, *i.e.* $P_G(\phi_0) = \frac{1}{\sqrt{2\pi}} \exp(-\phi_0^2/2)$. A combination of Eq. (8) and Eq. (9) yields

$$P_1(\phi,\tau) = \frac{G}{2\phi_u} \exp\left\{-(G^2-1)\left[erf^{-1}(\frac{\phi}{\phi_u})\right]^2\right\}. \tag{10}$$

In these equations, the relation between τ and the physical time t is unknown in the context of a single-point description. This relation can be obtained only through knowledge of the higher order statistical properties of the scalar field. For example, it is shown by Madnia *et al.* (1992); Frankel *et al.* (1992a) that the mapping closure yields the algebraic relation for the normalized variance,

$$\frac{<\sigma^2>(\tau)}{<\sigma^2>(0)} = \frac{2}{\pi} \arctan\left(\frac{1}{G\sqrt{G^2+2}}\right), \tag{11}$$

in which the variance is related to the unknown mean dissipation $\epsilon(t)$ by integrating Eq. (3),

$$\sigma \frac{d\sigma}{dt} = -\epsilon(t), \tag{12}$$

where,

$$\epsilon(t) = \int_{\phi_l}^{\phi u} P_1(\phi,t)\varepsilon(\phi,t)d\phi = -\int^{\phi u} -\phi_l \phi P_1(\phi,t)D(\phi,t)d\phi. \tag{13}$$

3 JOHNSON-EDGEWORTH TRANSLATION

The AMC captures some of the basic features of the binary mixing problem as described by Pope (1991). Namely, the inverse diffusion of the PDF in the composition domain from a double delta distribution to an asymptotic Gaussian distribution centered around $< \phi >$, as $\sigma^2 \to 0$ (or $G \to \infty$). This asymptotic Gaussian distribution near the mean scalar value cannot be realized in any of the previous mixing models based on the so called Coalescence/Dispersion (C/D) closures (Curl, 1963; Janicka *et al.*, 1979; Pope, 1982; Kosaly and Givi, 1987). And those modified C/D models which do yield such an asymptotic state, *e.g.* Pope (1982), do not predict the initial stages of mixing correctly (Kosaly, 1986). This deficiency of the C/D models in yielding asymptotic Gaussianity has been a motivating factor for recent investigations resulting in the development of the AMC (Pope, 1991).

In the spirit of "mapping" to a specified reference field, it is speculated that there are perhaps other means of "driving" the PDF toward Gaussianity in a physically acceptable manner. In fact, this subject has been of major interest to statisticians and biometricians within the last century since the early work of Edgeworth (1907). The scheme was referred to by Edgeworth as the Method of Translation, and was later detailed by Johnson (1949a). In today's literature of statistics and biometrics, the scheme is known as Johnson-Edgeworth frequency generation, and has many applications in statistical analysis.

The essential element of Johnson-Edgeworth Translation (JET) is similar to that of the AMC. Namely, it involves the transformation of the random physical field, here, ϕ, to a fixed standard Gaussian reference field by means of a translation (or mapping) of the form

$$\phi = Z\left[\frac{\phi_0}{\gamma(t)}\right],$$

$$\gamma(t=0) = 0 \leq \gamma(t) \leq \gamma(t \to \infty) \to \infty. \tag{14}$$

In this equation, the function $\gamma(t)$ plays a role similar to that of G in the AMC. With an appropriate form for the function Z, the scalar PDF is determined from Eq. (9). For application in the problem of mixing from an initially symmetric binary state of zero mean within a fixed domain $\phi_\ell = -\phi_u \leq \phi \leq \phi_u$, the appropriate JET must satisfy the following physical constraints:

$$(i) Lim_{(\gamma \to 0)} Z(\frac{\phi_0}{\gamma}) \approx H(\phi_0).$$

$$(ii) Lim_{(\gamma \to \infty)} Z(\frac{\phi_0}{\gamma}) \approx C\phi_0 + O(\phi_0^3) + \ldots$$

(iii) $Z(\frac{\phi_0}{\gamma})$ is an odd function with respect to the scalar mean for any value of σ^2. (iv) $Z(\frac{\phi_0}{\gamma})$ is bounded and is a non-decreasing function of ϕ_0, and $-\phi_u \leq Z \leq \phi_u$ at all times.

(15)

In these relations, H denotes the Heaviside function, and C is constant. Constraint (i) implies an initially symmetric and segregated binary state. The second constraint ensures an asymptotic Gaussian distribution for $P_1(\phi)$ near the mean scalar value. Condition (iii) preserves the symmetry of the PDF around the mean value at all times, and constraint (iv) implies the boundedness of the scalar field, *i.e.* $-\phi_u \leq \phi \leq \phi_u$. A function Z

which satisfies all the above constraints, is therefore expected to provide an acceptable means of approximating the PDF. An example is the *Logit*-Normal (or $\tanh^{-1}$-Normal) distribution, as originally proposed by Johnson (1949a). For the symmetric problem within a fixed domain, this distribution is produced by a mapping of the form[1]

$$Z = \phi_u \tanh\left(\frac{\phi_0}{\gamma}\right). \tag{16}$$

With this mapping, together with Eq. (9), the PDF of the scalar adopts the form,

$$P_1(\phi, t) = \frac{\gamma}{\sqrt{2\pi}\left(\frac{1-(\frac{\phi}{\phi_u})^2}{}\right)} \exp\left\{-\frac{\gamma^2}{2}\left[\tanh^{-1}(\frac{\phi}{\phi_u})\right]^2\right\}. \tag{17}$$

It is easily verified that this frequency satisfies the physical constraints of the symmetric binary mixing problem (Eq. (15)). At $t = 0$, the PDF is approximately composed of two delta functions at $\phi = \pm\phi_u$, and as $t \to \infty$ the PDF adopts an approximate Gaussian-like distribution centered around the zero mean. These features are similar to those portrayed by the PDF generated by the AMC (Eq. 10)).

This example demonstrates that with the satisfaction of the above indicated constraints, several other frequencies can be generated for effective modeling of the binary mixing problem. In fact, it is easy to show that the solution generated by the AMC can also be viewed as a member of the JET family. This is demonstrated by considering a translation of the form

$$Z = \phi_u erf\left(\frac{\phi_0}{\gamma}\right), \tag{18}$$

From Eq. (9), this translation yields the PDF

$$P_1(\phi, t) = \frac{\gamma}{2\sqrt{2}\phi_u} \exp\left\{-(\frac{\gamma^2}{2} - 1)\left[erf^{-1}(\frac{\phi}{\phi_u})\right]^2\right\}. \tag{19}$$

This frequency can be termed the erf^{-1}-Normal distribution and is identical to the form presented by Eq. (10). The difference is due to the terms containing G and γ. But this is unimportant since in the context of single-point statistics neither of the two parameters can be determined by the PDF. Therefore, with $G \equiv \frac{\gamma}{\sqrt{2}}$, both expressions are equivalent. With this equivalence, the closed form relation for the variance of the erf^{-1}-Normal distribution has the same algebraic form given by Eq. (11). It is easy to show that many other distributions can be generated to display similar characteristics. In the discussions to follow, we only consider the Logit-Normal and the erf^{-1}-Normal distributions, the latter being identical to the distribution generated by AMC.

Pearson Family

The similarity of the AMC and JET in generating equivalent PDF's is also useful in explaining the applicability of the frequencies generated by the Pearson family (Pearson, 1895). For a "bimodal" distribution, a physically acceptable frequency is the Pearson

[1] In recent literature, the Logit-Normal is usually expressed by the mapping $Z = \phi_u 2[1 + exp(\phi_0/\gamma)]^{-1} - 1$.

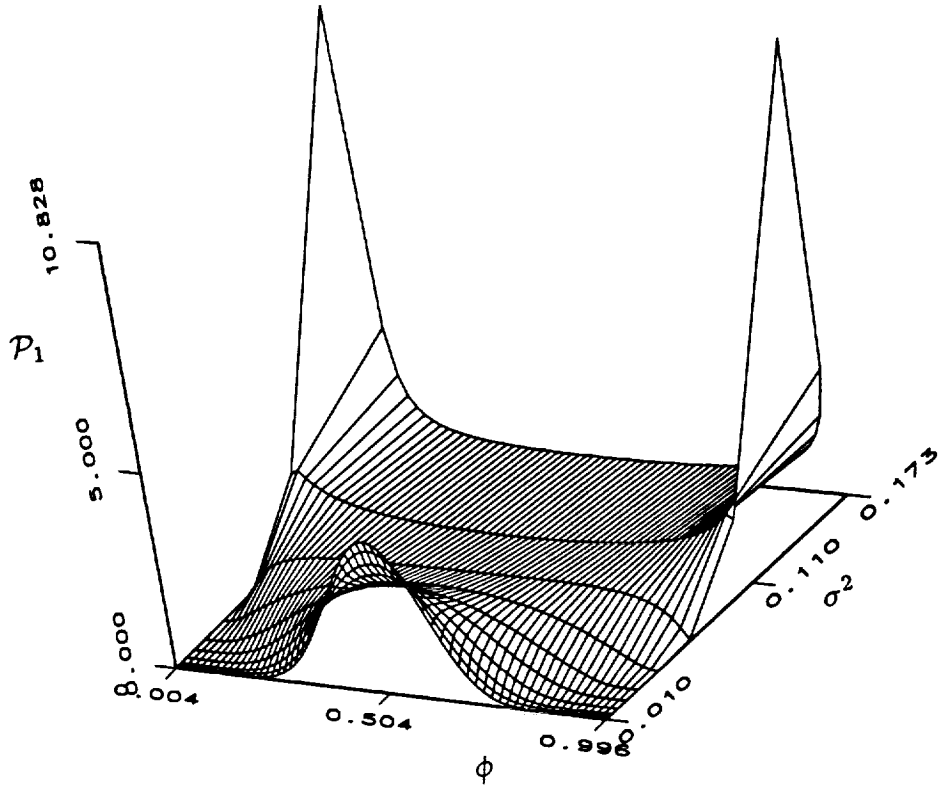

FIGURE 2 Temporal evolution of the Logit-Normal PDF.

Type I, known as the general form of the "Beta density of the first kind". This density is typically expressed in a fixed domain within the range $0 \leq \phi \leq 1$,

$$P_1(\phi) = \frac{1}{B(\beta_1, \beta_2)} \phi^{\beta_1 - 1}(1 - \phi)^{\beta_2 - 1}, 0 \leq \phi \leq 1. \tag{20}$$

Here B denotes the Beta function, and the parameters β_1 and β_2 are determined from the knowledge of the mean and the variance of the random variable. In a symmetric field within [0,1], $< \phi >= \frac{1}{2}$, $\beta_1 = \beta_2 = \beta$, and thus the PDF is characterized by the variance alone.

The similarity of the Pearson distributions and the JET frequencies is well recognized in the statistics literature (see Johnson (1949a)). Therefore, with the equivalence of the AMC and the JET as demonstrated above, it is not surprising that the Beta density and the AMC are also similar. This similarity, without a mathematical proof, has been recognized in previous works (Madnia *et al.*, 1991b; Madnia and Givi, 1992).

4 COMPARATIVE ASSESSMENTS

The probability distributions obtained from the three frequency generation methods described above are all capable of providing a reasonable stochastic approximation of

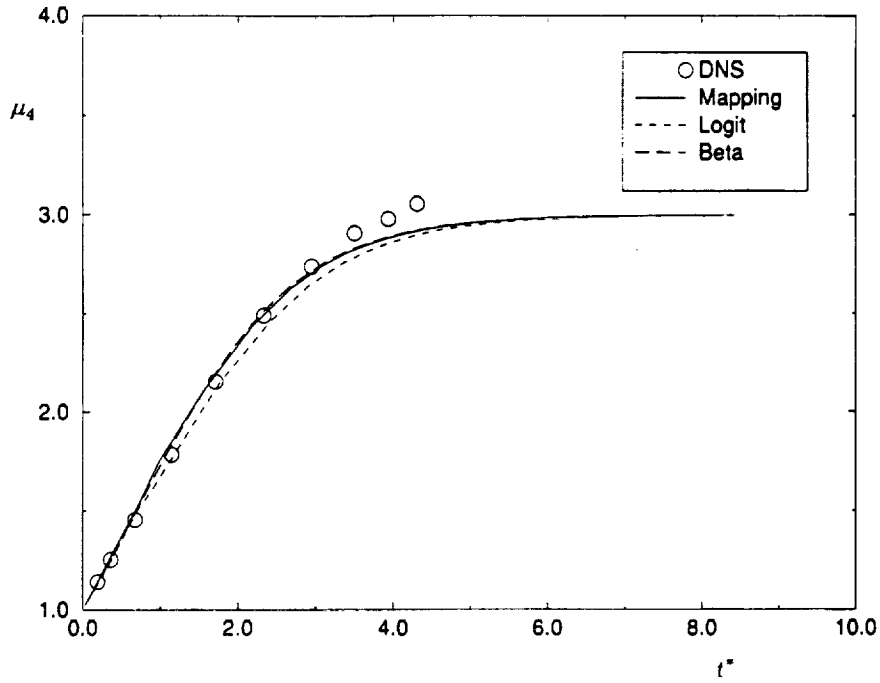

FIGURE 3a Temporal evolution of the centralized moments of the scalar variable as predicted by the models and the comparison with DNS data. (a) μ_4 vs. t^*.

the mixing problem from an initially binary state. Namely, an approximate double delta distribution at $t = 0$, and an approximate Gaussian-like distribution as $t \to \infty$. The former can be realized in the limit of unity normalized variance $\sigma^2(t)/\sigma^2(0) = 1$. In a fixed composition domain, this corresponds to $G = 0$ for AMC ($\gamma = 0$ in JET), and to $\beta = 0$ for the Beta density. The latter is realized in the limit $G, \gamma, \beta \to \infty$. The limiting Gaussian distribution for the AMC has been asserted by Pope (1991). For the JET, the criterion (ii) in Eq. (15) guarantees this condition. For the Beta density, the assertion of an asymptotic Gaussian distribution in the limit of zero variance is established in elementary texts on statistics (*e.g.* Casella and Berger (1990)). At the intermediate stages, however, the PDF's are not identical. It is easily verified by Eqs. (10), (20) that the AMC and the Beta distributions become constant ($P_1(\phi)$ = constant - $\frac{1}{2}\phi_u$) for $G = \beta = 1$. However, the Logit-Normal PDF does not yield a uniform distribution at any stage of its evolution. Also, as indicated by Johnson (1949a) it is not possible to provide a closed form algebraic expression similar to Eq. (11) for the variance of the Logit-Normal distribution.

In order to make comparative assessments of the models, the frequencies generated by the three methods (AMC, JET, and PF) are compared with each other, and also with PDF's generated by Direct Numerical Simulations (DNS). The DNS procedure is similar to that of previous simulations of this type. Since these simulations are not the major focus of this paper, only a brief outline of the procedure is described; for a detailed discussion we refer the reader to Madnia and Givi (1992). The subject of the DNS is a three-dimensional periodic homogeneous box flow carrying a passive scalar variable. The initial scalar field is composed of square waves with maximum and minimum values of 1 and 0, respectively. These limiting values are arbitrary, and can be translated to

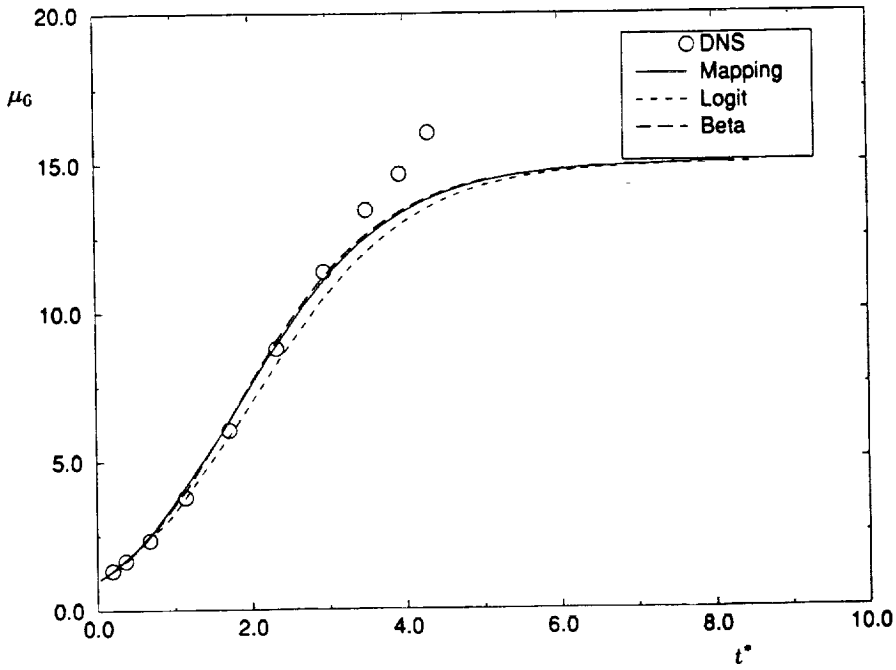

FIGURE 3b Temporal evolution of the centralized moments of the scalar variable as predicted by the models and the comparison with DNS data. (b) μ_6 vs. t^*.

appropriate ϕ_u, ϕ_l for comparison to each of the models. At time zero, in most regions of the flow, the scalar adopts these limiting values (with equal probability), and the spatial regions between the initial maxima and minima are smoothed by a polynomial fit. The degree of this smoothing is minimized, but limited by the computational resolution, to ensure an approximate initial double delta distribution. The computational scheme is based on a spectral-collocation procedure using Fourier basis functions developed by Erlebacher *et al.* (1990a); Erlebacher *et al.* (1987); Erlebacher *et al.* (1990b). The hydrodynamic field is assumed isotropic and is initialized in a similar manner to that by Erlebacher *et al.* (1990a); Passot and Pouquet (1987). The code is capable of simulating flows with different levels of compressibility (Hussaini *et al.*, 1990). Here, only the results obtained for a low compressible case are discussed. The resolution consists of 96 collocation points in each direction. Therefore, at each time step 96^3 is the sample size for statistical analysis. With this resolution, simulations with a Reynolds number (based on the Taylor microscale) of $Re_\lambda \approx 41$ are attainable. The value of the molecular Schmidt number is set equal to unity.

As indicated in Section 1, in order to compare the model predictions with DNS results a matching is required of the higher order statistics of the field as generated by each method. Here, this matching is done through the variance of the conserved scalar. These results are presented in Fig. 1. This figure indicates that at initial times, $\frac{\sigma^2(t)}{\sigma^2(0)} \approx 1$, all the PDF's are approximately composed of two delta functions at $\phi = 0,1$ indicating the initial binary state. At longer times, the PDF's evolve through an inverse-like diffusion in the composition space. The heights of the delta functions decrease and the PDF's are redistributed at other ϕ values within the range [0,1]. At very long times, the PDF's

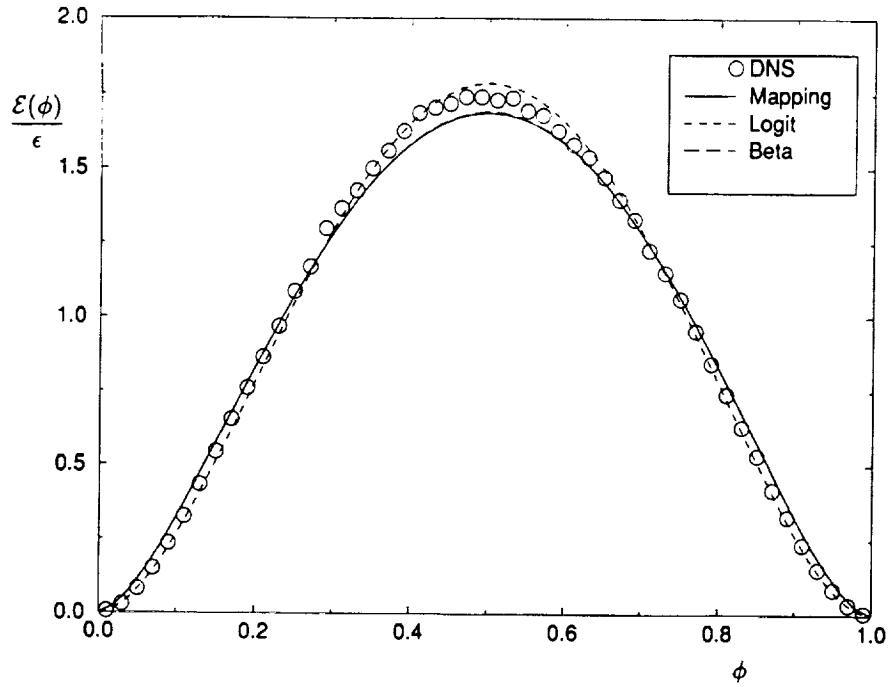

FIGURE 4a Comparisons of the normalized conditional dissipation as predicted by the three models with the DNS data. (a) $\sigma^2 = 0.079$.

become asymptotically concentrated around the mean value in a manner that can be approximated by a Gaussian distribution.

An interesting feature captured in Fig.1(b), is the capability of the Logit-Normal distribution in depicting a subtle behavior in the frequency distribution. This feature is the double "hump" characteristic of the DNS data at intermediate times and cannot be realized by the AMC or the PF generated frequencies. All the previous DNS results including those of Eswaran and Pope (1988); Givi and McMurtry (1988); Pope (1991) portray this feature. The PDF's generated by the AMC, and the Beta distributions adopt a constant value (of 1/2) when $\sigma^2 = \frac{1}{12}$ (for $0 \leq \phi \leq 1$). This corresponds to $G = 1, \gamma = \sqrt{2}, \beta = 1$. This uniform distribution is not exactly realized in any previous or present DNS results. Therefore, it can be speculated that in the absence of a better alternative, the Logit-Normal distribution may provide the simplest means of providing an *assumed* distribution for the statistical modeling of the symmetric binary mixing problem. The complete evolution of the Logit-Normal PDF is shown in Fig.2.

Further quantification of the agreements noted above are made by comparing the higher moments of the scalar field. This comparison is made in Fig.3. In this figure, results are presented for the temporal variations of the kurtosis (μ_4) and the superskewness (μ_6) of the scalar variable ϕ. For the Beta density, the higher order moments are obtained analytically based on the knowledge of the variance. For the AMC, the analytical-numerical results by Jiang *et al.* (1992) are used, while for the Logit-Normal PDF the moments are calculated strictly by numerical means. This figure shows that initially, all these moments are close to unity, and monotonically increase as mixing proceeds. For all the models, the magnitudes of the moments asymptotically approach the limiting values of 3 and 15, respectively, corresponding to those of a Gaussian distribution. The DNS

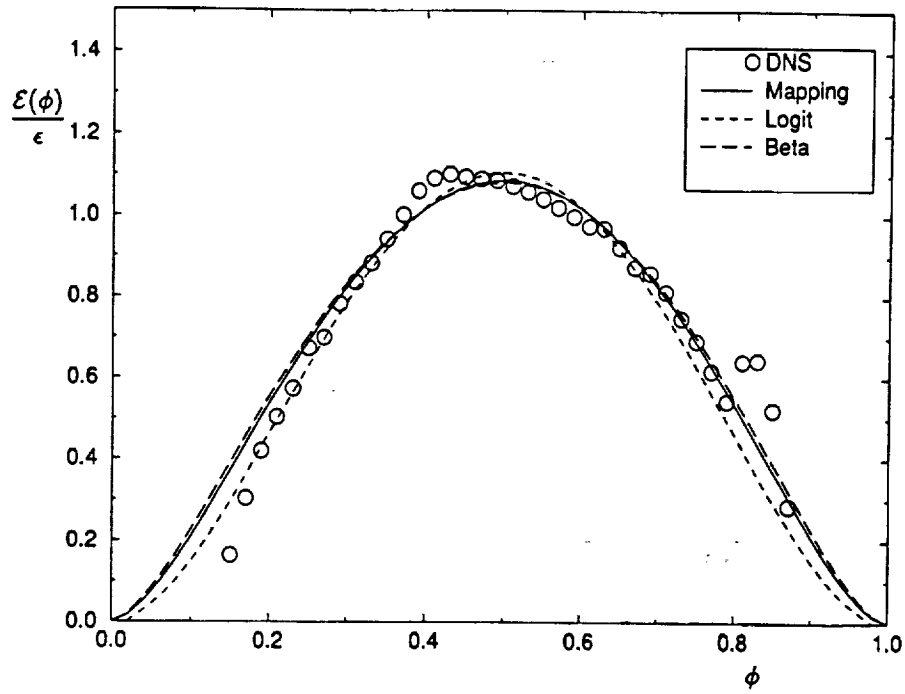

FIGURE 4b Comparisons of the normalized conditional dissipation as predicted by the three models with the DNS data. (b) $\sigma^2 = 0.013$.

results are in good agreement with the model predictions at all times. However, due to obvious numerical difficulties, the simulations could not be continued until the variance approaches zero identically.

5 SCALAR DISSIPATION

The results presented above indicate a good agreement between the model predicted single-point statistics (PDF's and high-order moments) and the DNS data at all the stages of mixing. These results also suggest an approximate asymptotic Gaussian state for all the closure PDF's and those of the DNS. Here, it will be demonstrated that the agreement between the DNS and the model predictions is very good at the initial and the intermediate stages of mixing. However, the agreement worsens at the final stages. Also it will be shown that none of the closures yield "exact" Gaussian distributions at the final stages of mixing. In doing so, it is useful to note that a Gaussian PDF is defined, and is only valid, for an unbounded domain. The frequencies generated here, are all defined within a *fixed and finite* domain. For AMC, it has been established (Gao, 1991; O'Brien and Jiang, 1991) that the finite boundary size at the initial time "maintains" its influence at *all* the subsequent stages of mixing. In other words, the PDF adopts a Gaussian distribution in the limit of zero variance only near the mean value of the scalar. In order to show the departure from Gaussianity at scalar values away from the mean, the conditional expected dissipation of the scalar field is considered.

Given the PDF, as is the case here, Eq. (3) can be used to determine the expected conditional dissipation. It has been shown by Girimaji (1992) (and will be discussed in

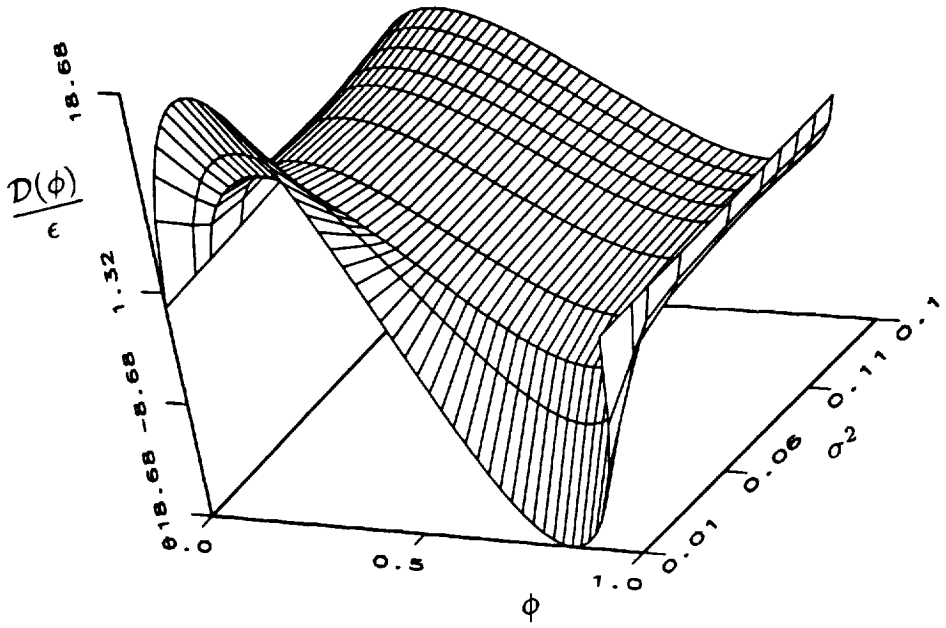

FIGURE 5a Temporal evolution of the conditional expected diffusion normalized with the total dissipation. (a) erf^{-1}-Normal.

detail in Section 7) that for a valid PDF within a defined range, $-\phi_u \leq \phi \leq \phi_u$, the expected conditional scalar dissipation is given by

$$\varepsilon(\phi,t) = -\frac{1}{P_1(\phi,t)}\frac{\partial}{\partial t}\left(\int_{-\phi_u}^{\phi} F(\psi,t)d\psi\right), \tag{21}$$

where F denotes the cumulative distribution function (CDF)

$$F(\phi,t) = \int_{-\phi u}^{\phi} P_1(\psi,t)d\psi. \tag{22}$$

With Eq. (21), the expected conditional dissipation can be evaluated for a given PDF. For example, for a Gaussian distribution of zero mean, $P_G(\phi,\sigma^2) = \frac{1}{\sqrt{2\pi}\sigma}\exp(-\frac{\sigma^2}{2\sigma^2}, -\infty = -\sigma_u \leq \sigma \leq \sigma_u = \infty$, with a non-stationary variance, $\sigma^2 = \sigma^2(t)$, it is easily shown that,

$$\varepsilon(\phi,t) = \left[\frac{1}{P_G(\phi,\sigma^2)}\right]\frac{\partial}{\partial t}\left(\frac{\phi}{2} + \frac{\phi}{2}erf(\frac{\phi}{\sqrt{2}\sigma}) + \frac{\sigma}{\sqrt{2\pi}}\exp(-\frac{\phi^2}{2\sigma^2})\right), -\infty \leq \phi \leq \infty \tag{23}$$

Noting that ϕ is an independent variable (of t), and evaluating the derivatives on the RHS of Eq. (23) yields, after some simple manipulations,

$$\varepsilon(\phi,t) = constant = -\sigma\frac{d\sigma}{dt}, \tag{24}$$

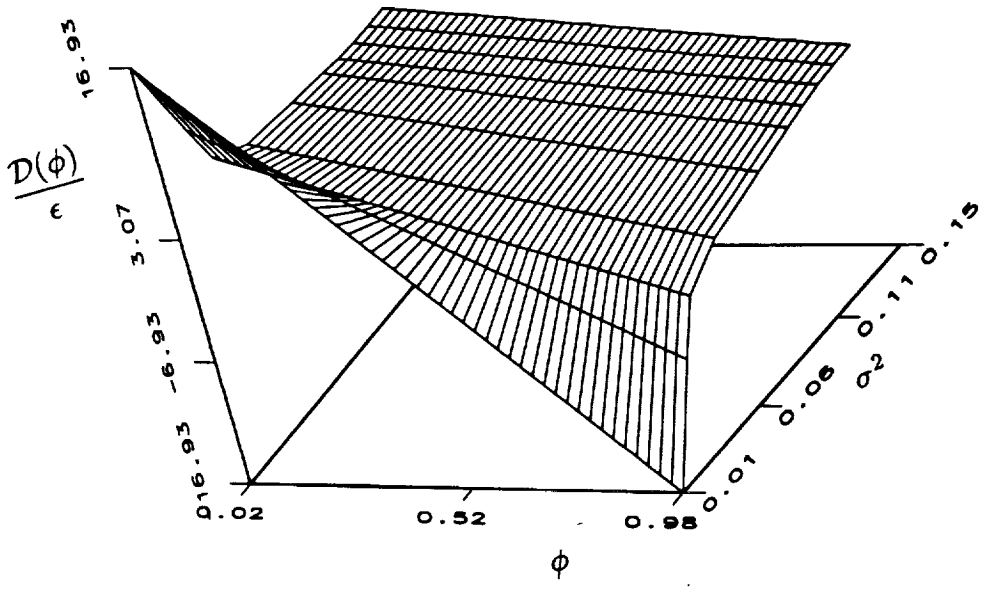

FIGURE 5b Temporal evolution of the conditional expected diffusion normalized with the total dissipation. (b) LMSE.

with the implications (derived from Eqs. (12)-(13)),

$$\frac{\epsilon(\phi,t)}{\epsilon(t)} = constant = 1, \tag{25}$$

at all times for *all phi* values in the range $-\infty$ to $+\infty$. Equations (24-25) indicate the independence of the conditional scalar dissipation and the composition domain for a Gaussian field. These results have also been obtained by Gao (1991); O'Brien and Jiang (1991) by following a different mathematical procedure.

The conditional expected dissipation predicted by the models can be obtained by following a similar course. For the AMC and the PF distribution, the conditional dissipation fields have been obtained by Gao (1991); O'Brien and Jiang (1991) and by Girimaji (1992), respectively. For the purpose of the discussions to follow, these results are presented here in a different form for all three closures. For the erf^{-1}-Normal distribution, the instantaneous CDF is given by

$$F(\phi,t) = \frac{1}{2}\left(1 + erf\left[\frac{\gamma}{\sqrt{2}} ert^{-1}\left(\frac{\phi}{\phi_u}\right)\right]\right). \tag{26}$$

Therefore, with Eq. (21), the conditional dissipation can be expressed in terms of the corresponding PDF,

$$\epsilon(\phi,t) = -\frac{1}{P_1(\phi,t)}\frac{\partial}{\partial t}\left\{\frac{1}{2}\int_{-\phi_u}^{\phi} erf\left[\frac{\gamma}{\sqrt{2}} erf^{-1}\left(\frac{\phi}{\phi_u}\right)\right] d\phi + \frac{1}{2}(\phi+\phi_u)\right\}. \tag{27}$$

Again, with an independence of ϕ and t this equation reduces to,

$$\varepsilon(\phi,t) = -\frac{1}{P_1(\phi,t)}\frac{\partial H}{\partial t}, \tag{28}$$

where,

$$H = \frac{\phi_u}{\sqrt{\pi}}\int^{erf^{-1}} (\frac{\phi}{\phi_u})_{-\phi_u} erf(\frac{\gamma}{\sqrt{2}}z)\exp(-z^2)dz. \tag{29}$$

For a PDF within a fixed domain, the integration procedure becomes simplified by evaluating the time derivatives inside the integral. In this way, the results can be expressed analytically. After some manipulations,

$$\frac{dH}{dt} = \frac{-\sqrt{2}\phi_u \frac{d\gamma}{dt}}{\pi(2+\gamma^2)}\exp\left\{-(1+\frac{\gamma^2}{2})\left[erf^{-1}(\frac{\phi}{\phi_u})\right]^2\right\}, \tag{30}$$

and, therefore

$$\varepsilon(\phi,t) = \frac{4\phi_u^2 \frac{d\gamma}{dt}}{\pi\gamma(2+\gamma^2)}\exp\left\{-2\left[erf^{-1}(\frac{\phi}{\phi_u})\right]^2\right\}. \tag{31}$$

From this equation, the total dissipation is obtained by direct integration of the conditional mean dissipation field. The results, after significant algebraic manipulations yield

$$\epsilon(t) = \frac{4\phi_u^2 \frac{d\gamma}{dt}}{\pi(2+\gamma^2)\sqrt{4+\gamma^2}}, \tag{32}$$

$$\frac{\varepsilon(\phi,t)}{\epsilon(t)} = \left(\sqrt{\frac{1+\sin\left[\frac{\pi\sigma^2(t)}{2\sigma^2(0)}\right]}{1-\sin\left[\frac{\pi\sigma^2(t)}{2\sigma^2(0)}\right]}}\right)\exp\left\{-2\left[erf^{-1}(\frac{\phi}{\phi_u})\right]^2\right\}. \tag{33}$$

In the form presented above, Eqs. (31)-(33) portray several insightful features of the solution. First, Eq. (33) indicates that the conditional dissipation is always dependent on the magnitude of the scalar, and it maintains the same self-similar functional form of dependence $\exp\left\{-2\left[erf^{-1}(\frac{\phi}{\phi_u})\right]^2\right\}$. This has been previously indicated by Gao (1991); O'Brien and Jiang (1991). Here, the amplitude $\varepsilon(\phi=0,t)$ can be conveniently expressed in terms of the variance decay, which is very useful for further manipulations. Second, it is interesting to note the similarity of Eqs. (31) and (33) with the results obtained for the instantaneous dissipation of Fickian mixing of a conserved scalar in laminar non-homogeneous flows (such as the typical shear flows (Spalding, 1961; Liñan, 1974; Peters, 1984)). This similarity further asserts the "permanent" influence of the boundaries since in non-homogeneous mixing, the scalar bounds are "fixed" due to the physical constraints. Finally, Eq. (32) suggests an infinitely large dissipation at time zero, *i.e.* when $\sigma^2(t)/\sigma^2(0) = 1$, and the asymptotic behavior

$$Lim_{(\sigma^2\to 0)}\frac{\varepsilon(\phi)}{\epsilon}|_{\phi=0} = 1. \tag{34}$$

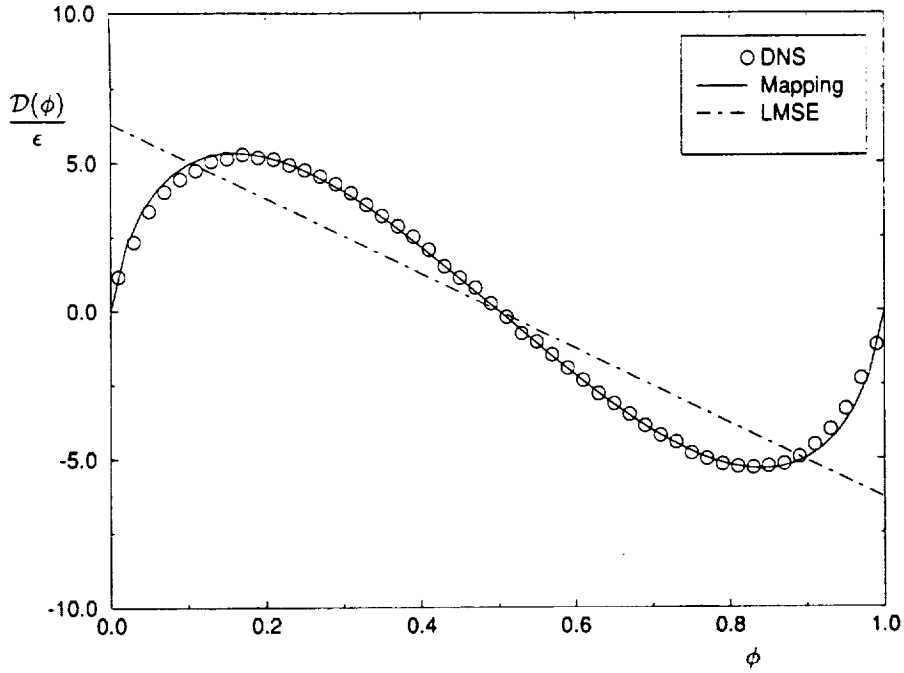

FIGURE 6a Comparisons of the normalized conditional diffusion as predicted by the three models and the LMSE closure, with the DNS data. (a) $\sigma^2 = 0.079$.

This limiting behavior near zero indicates the Gaussianity of the PDF only at the mean value of the scalar.

Following a similar procedure, the conditional expected dissipation can be obtained for the other closures. For the Beta density in the range $0 \leq \phi \leq 1$, the final results can be expressed as

$$\varepsilon(\phi, t) = -\frac{1}{P_1(\phi, t)} \frac{\partial}{\partial t} \left(\int_0^{\phi} I_{\phi}(\beta, \beta) d\phi \right), \tag{35}$$

where, I denotes the Incomplete Beta Function (Abramowitz and Stegun, 1972). For the Logit-Normal distribution, the corresponding form is

$$\varepsilon(\phi, t) = -\frac{1}{P_1(\phi, t)} \frac{\partial}{\partial t} \left\{ \frac{1}{2} \int_{-\phi_u}^{\phi} erf \left[\frac{\gamma}{\sqrt{2}} \ln \left(\frac{1 + \frac{\phi}{\phi_u}}{1 - \frac{\phi}{\phi_u}} \right) \right] d\phi \right\}. \tag{36}$$

Neither of the equations (35-36) can be simplified further. Therefore, in order to evaluate the conditional expected dissipation (and the total dissipation), these equations must be evaluated numerically.

In Fig. 4, the evolution of the conditional expected dissipation (normalized by the total dissipation) is presented for the models and the DNS data. This figure shows the similarity of the conditional expected dissipation for all of the models. The bell shape distribution is evident in all the figures with a maximum amplitude near the mean value. Also, as the variance decreases and the PDF becomes concentrated near the mean, the

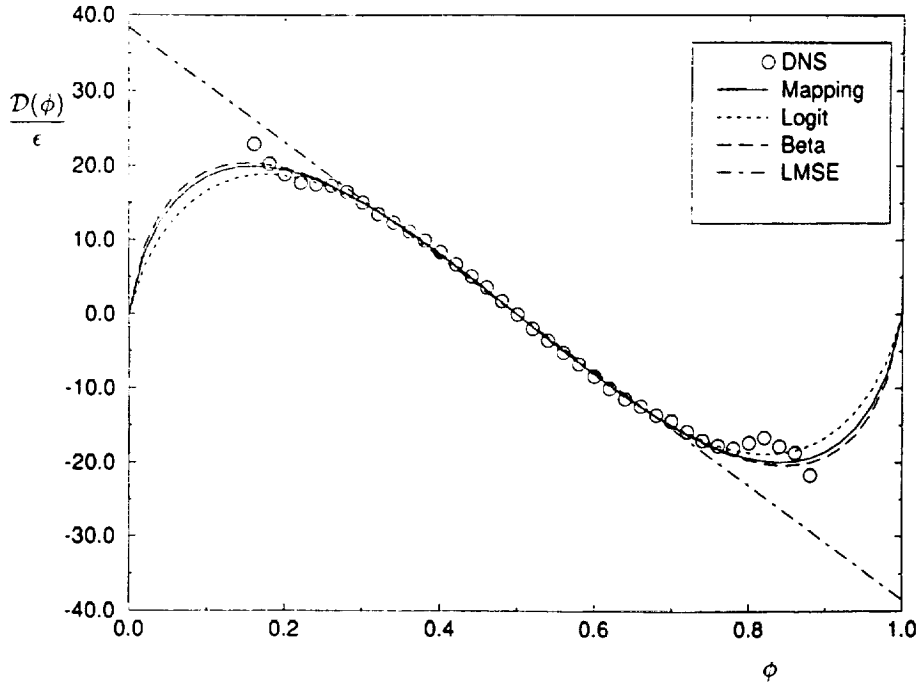

FIGURE 6b Comparisons of the normalized conditional diffusion as predicted by the three models and the LMSE closure, with the DNS data. (b) $\sigma^2 = 0.013$.

amplitude tends to unity. This shape is typical of that observed in previous DNS results of Eswaran and Pope (1988); Nomura and Elgobashi (1992).

The results in Fig.4 show the ϕ dependency of the results at *all* the stages of mixing. That is, the PDF asymptotically adopts an apparent Gaussian-like distribution only near the mean value of the scalar, and the conditional dissipation does not become independent of the scalar everywhere. For the AMC, this has been discussed by Gao (1991); O'Brien and Jiang (1991). Considering the similarity of the three models, it is therefore concluded that all three models yield the same characteristics. These results also suggest a poor agreement between the model predicted conditional expected dissipations and the DNS data. Note that at the initial stages of mixing, the predicted results compare well with DNS data. However, with mixing progression, at smaller variance values, the agreement is only good near the mean scalar value and worsens near the bounds of the composition domain. This, as described above, is due to the permanent influence of the scalar boundaries at all the stages of mixing.

6 SCALAR DIFFUSION

Albeit directly related to the conditional expected dissipation (Eq. 7), it is useful to examine the behavior of the conditional expected diffusion in light of the discussions above. Given the PDF, again within the fixed range $-\phi_u \leq \phi \leq \phi_u$, the conditional expected diffusion can be determined from

$$D(\phi, t) = -\frac{1}{P_1(\phi, t)} \frac{\partial F}{\partial t}. \tag{37}$$

This equation is very useful in illustrating the properties of the PDF. For example, for a Gaussian distribution within an infinite domain

$$\frac{\partial F}{\partial t} = -\frac{\phi}{\sqrt{2\pi\sigma^2}} \frac{d\sigma^2}{dt} \exp(-\frac{\phi^2}{2\phi^2}), \tag{38}$$

and consequently

$$\frac{D(\phi,t)}{\epsilon(t)} = \frac{-\phi}{\sigma^2(t)}. \tag{39}$$

It is noted that Eq. (39) is in accord with the Linear Mean Square Estimation (LMSE) closure (O'Brien, 1980).

The mean conditional diffusion can be determined for the three models considered. For the erf^{-1}-Normal PDF with zero mean

$$\frac{\partial F}{\partial t} = \frac{1}{\sqrt{2\pi}} \frac{d\gamma}{dt} \exp\left\{-\frac{\gamma^2}{2}\left[erf^{-1}(\frac{\phi}{\phi_u})\right]^2\right\} erf^{-1}(\frac{\phi}{\phi_u}) \tag{40}$$

Again with explicit equations for the total dissipation and the variance, it is possible to obtain an algebraic expression for the conditional expected diffusion. The results after substantial algebraic manipulations yield

$$\frac{D(\phi,t)}{\epsilon(t)} = \left(\frac{-\sqrt{\pi}}{\sin\left[\frac{\pi\sigma^2(g)}{2\sigma^2(0)}\right]} \sqrt{\frac{1+\sin\left[\frac{\pi\sigma^2(t)}{2\sigma^2(0)}\right]}{1-\sin\left[\frac{\pi\sigma^2(t)}{2\sigma^2(0)}\right]}}\right) \exp\left\{-\left[erf^{-1}(\frac{\phi}{\phi_u})\right]^2\right\} erf^{-1}(\frac{\phi}{\phi_u}). \tag{41}$$

In this form Eq. (41) is very pleasing since it does reveal the (t,ϕ) separability, and thus the self-similarity, of the diffusion field. The terms inside the parenthesis on the RHS are time dependent, whereas the remaining terms depend explicitly on ϕ only. As indicated by O'Brien and Jiang (1991), this separability cannot be easily deduced from Eq. (5), but is possible with the analytical procedure followed above. The temporal evolution of the conditional expected diffusion for the erf^{-1}-Normal distribution, and its comparison with that of the LMSE closure is presented in Fig.5.

By following the procedure above, analogous expressions are obtained for the other two closures. Namely,

$$\frac{D(\phi,t)}{\epsilon(t)} = \frac{2\phi_u}{\gamma} \frac{d\gamma}{d\sigma^2} \left[1-\left(\frac{\phi}{\phi_u}\right)^2\right] \tanh^{-1}(\frac{\phi}{\phi_u}), \tag{42}$$

for the Logit-Normal distribution of zero mean, and

$$\frac{D(\phi,t)}{\epsilon(t)} = \frac{2}{P_1(\phi,t)} \frac{\partial I_\phi(\beta,\beta)}{\partial\sigma^2} \tag{43}$$

for the symmetric Beta density within [0,1]. Equations (42)-(43) cannot be simplified further due to the lack of an explicit analytical relation for the variance of the Logit-Normal distribution (Johnson, 1949a), and the unknown analytical form of the derivatives of the Incomplete Beta Function.

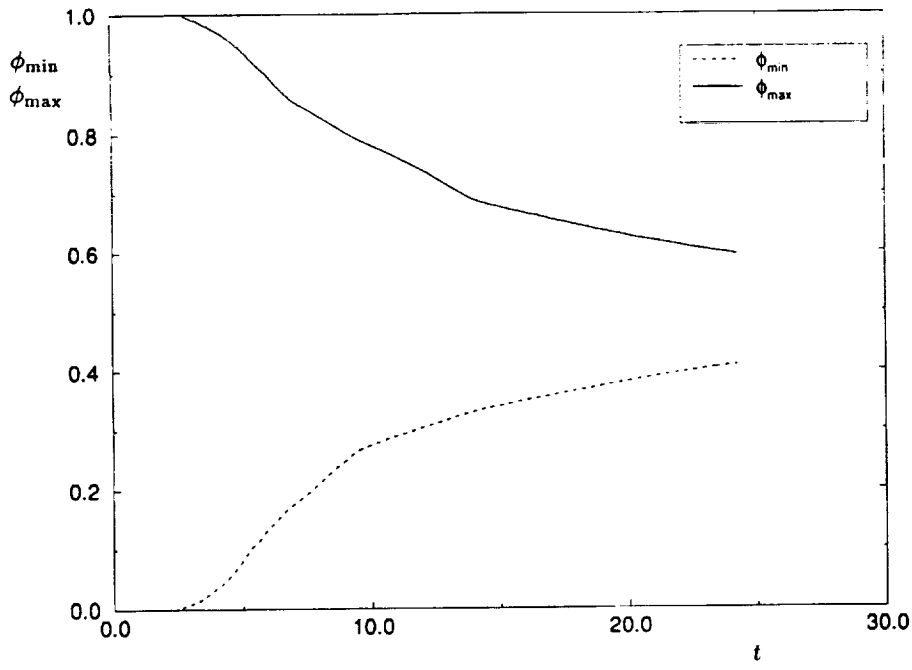

FIGURE 7 The temporal variations of ϕ_{max} and ϕ_{min} generated by DNS.

In Fig. 6, results are presented of the conditional expected diffusion as predicted by the three models, and also that of the LMSE closure. In these figures, the DNS data are also provided at several variance values. The similarity of the modelled results are once again revealed in these figures, which is expected in view of the PDF similarities. At all times, the conditional diffusion field has an odd distribution near the mean scalar value. On the right half of the composition domain, all three closures yield a monotonic decrease of D to an instantaneous minimum, and then a monotonic increase to zero at the upper bound of the scalar. The location and the magnitude of the instantaneous maxima and minima is not the same for the three closures. Also, as Eqs. (41)-(43) indicate, the zeroes of D can only be realized at $\phi = 0, \pm\phi_u$. At the initial times, *i.e.* large variances, all three closures agree reasonably well with the DNS data. This agreement is better for the three models than for the LMSE closure. However, as the variance becomes smaller, the agreement between the model predictions and the DNS data worsens. It is noted that as the variance becomes small, all the closures yield a Gaussian-like PDF near the mean value of the scalar. This is shown in the figures near $\phi =< \phi >$ ($= \frac{1}{2}$ for DNS), where the predicted results are in accord with the LMSE closure, *i.e.* linear profiles of similar slopes. In this region, the results are also in accord with DNS data for all the closures including the LMSE. However, again, the predicted results deviate from the DNS data away from the mean value. It is clearly noted that the DNS generated D values do not go to zero at the scalar bounds.

7 EVOLUTION OF THE SCALAR FIELD

The problems described at the conclusion of the previous two sections stem from a lack of capability of all of the models in accounting for the variations of the scalar

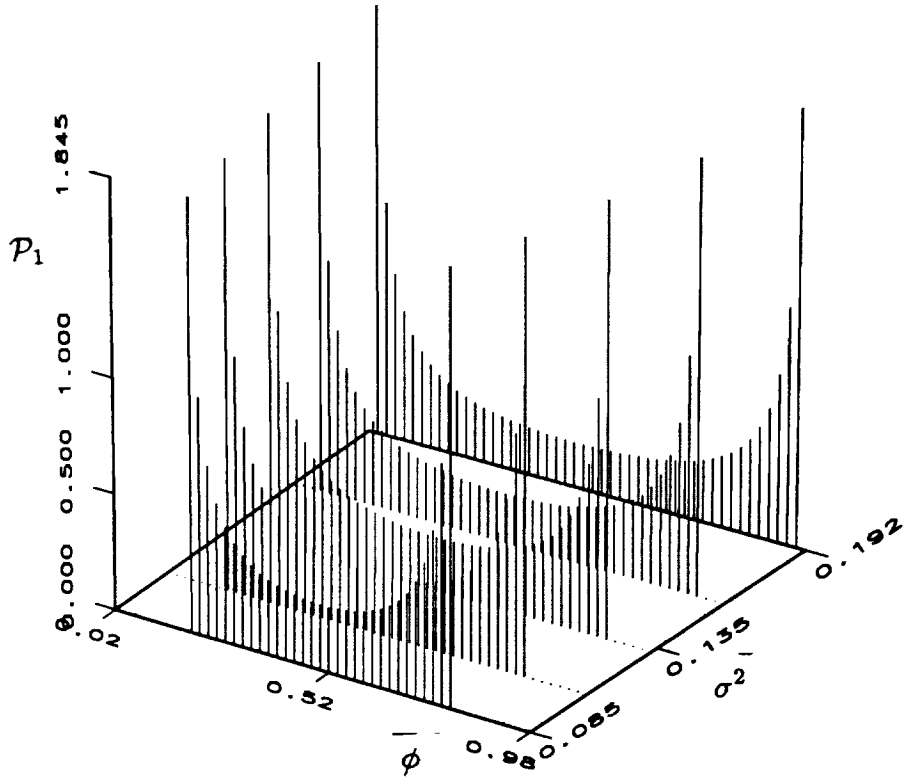

FIGURE 8 The Beta density (Pearson Type II) for a domain with moving boundaries, and $\beta = 0.1$.

bounds as the mixing proceeds. For all three models, the PDF is always *defined* within a fixed range through its course of evolution. It is easy to show that both the conditional expected dissipation and the conditional expected diffusion are correctly predicted by all the models near the mean scalar value. For the erf^{-1}-Normal distribution, this is evident from Eqs. (33) and (41) and can be also shown by analyzing the behavior of Eq. (31) near the region $\phi \approx 0$, as the variance becomes small. Noting that

$$Lim_{(\phi \approx 0)} erf\left(\frac{\phi}{\phi_u}\right) \approx \frac{\sqrt{\pi}}{2}\frac{\phi}{\phi_u} \tag{44}$$

and, from Eq. (11)

$$Lim_{(\sigma^2 \to 0)} \frac{d\gamma}{dt} = \frac{-2\phi_u}{\sqrt{\pi\sigma^2}}\frac{d\sigma}{dt}, \tag{45}$$

it is easily concluded that

$$Lim_{(t \to \infty)} \varepsilon(\phi \approx 0, t) = -\sigma\frac{d\sigma}{dt}. \tag{46}$$

Following the same procedure, it is derived

$$Lim_{(t\to\infty)}D(\phi\approx 0,t)=-\frac{\epsilon}{\sigma^2}\phi. \tag{47}$$

Due to the similarity of the three closures, it is reasonable to expect similar behaviors for the other models as well. Equations (46)-(47) indicate a Gaussian-like distribution near the mean $\phi\approx 0$ (Eqs. (24,39)). This is in accord with the DNS data. However, at distances away from the mean value the predicted results do not correspond to that of a Gaussian field. Neither do these results agree well with DNS data. The deficiency of the models in predicting the DNS results is made clear by considering the bounds of the scalar field as the mixing proceeds. This is demonstrated in Fig. 7, showing the temporal decay/growth of the scalar maxima/minima obtained by DNS. This trend is consistent with physical intuition, but is not incorporated into any of the three models. In the AMC and the JET generated frequencies, due to the nature of the translation $Z(\phi_0,t)$ and the constraints imposed by Eq. (15), the scalar is always bounded within the same range. This problem is also encountered in the PF, in that Type I and II distribution families are always defined within the same fixed domain regardless of the magnitude of the variance.

With the examination of the PDF transport equation, it is shown that the physics of the problem requires the migration of the scalar bounds toward the mean value as the mixing proceeds. That is, the instantaneous values of the scalar minima and maxima change with mixing progression. To demonstrate this, again consider a symmetric field with a PDF, $P_1(\phi,t)$, defined within the *time-dependent* domain of zero mean, $\phi\varepsilon[\phi_{\min}(t)=-\phi_{\max}(t),\phi_{\max}(t)]$. At all the stages of the evolution, the PDF must satisfy the physical requirements

$$\int_{\phi_{\max}(t)}^{\phi_{\max}(t)}P_1(\phi,t)d\phi=1,$$

$$<\phi>=\int_{\phi_{\min}(t)}^{\phi_{\max}(t)}\phi P_1(\phi,t)d\phi=0,$$

$$\sigma^2(t)=\int_{\phi_{\min}(t)}^{\phi_{\max}(t)}\phi^2P_1(\phi,t)d\phi, \tag{48}$$

The first of Eq. (48) requires

$$\frac{d}{dt}\int_{\phi_{\min}(t)}^{\phi_{\max}(t)}P_1(\phi,t)d\phi=0 \tag{49}$$

Evaluating this integral via Leibnitz's rule, and making use of Eqs. (3)-(7), it is shown that

$$P_1(\phi_{\max}(t),t)\frac{d\phi_{\max}}{dt}=-P_1(\phi_{\min}(t),t)\frac{d\phi_{\min}}{dt}=\left\{\frac{\partial}{\partial\phi}[\varepsilon(\phi,t)P_1(\phi,t)]\right\}_{\phi=\phi_u}$$

$$P_1(\phi_{\max}(t),t)\left[\frac{d\phi_{\max}}{dt}-D(\phi_{\max}(t),t)\right]=P_1(\phi_{\min}(t),t)\left[\frac{d\phi_{\min}}{dt}-D(\phi_{\min}(t),t)\right]=0,$$

$$\phi_{\max}(0)=\phi_u,\phi_{\min}(0)=\phi_t=-\phi_u. \tag{50}$$

Following the same procedure for the second of Eq. (48), yields the obvious requirement

$$\int_{\phi_{\min}(t)}^{\phi_{\max}(t)} D(\phi,t)P_1(\phi,t)d\phi = 0. \tag{51}$$

The third part of Eq. (48) yields Eq. (12), and

$$P_1(\phi_{\max}(t),t)\varepsilon(\phi_{\max}(t),t) = P_1(\phi_{\min}(t),t)\varepsilon(\phi_{\min}(t),t) = 0,$$

$$P_1(\phi_{\max}(t),t)\left[\frac{d\phi_{\max}}{dt} - D(\phi_{\max}(t),t)\right] =$$

$$-P_1(\phi_{\min}(t),t)\left[\frac{d\phi_{\min}}{dt} - D(\phi_{\min}(t),t)\right] = 0. \tag{52}$$

The remaining parts of Eq. (48) yield higher order statistical information pertaining to the inner integrated evolution of the conditional expected dissipation and diffusion, and their relation with the higher central moments. With an additional assumption of a nonzero PDF within the region of its definition, that is by defining $\phi_{\max}(t)$ and $\phi_{\min}(t)$ as the extreme locations with nonzero PDF, a combination of Eqs. (50) and (52) yields

$$\varepsilon(\phi_{\max}(t),t) = \varepsilon(\phi_{\min}(t),t) = 0,$$

$$\frac{d\phi_{\max}}{dt} = \frac{\partial\varepsilon}{\partial\phi}|\phi_{\max} = D(\phi_{\max}(t),t),$$

$$\frac{d\phi_{\min}}{dt} = \frac{\partial\varepsilon}{\partial\phi}|\phi_{\min} = D(\phi_{\min}(t),t),$$

$$\phi_{\max}(0) = \phi_u, \phi_{\min}(0) = \phi_\ell. \tag{53}$$

Equation (53) indicates that with fixed boundaries, the conditional dissipation would adopt a zero slope at the boundaries and the conditional diffusion would also be zero there. However, Fig. 7 indicates that in a physical situation the boundaries are not fixed and move inwards as the mixing proceeds. It is interesting to note that this problem is not observed in the numerical results obtained by the C/D type closures. That is, while the C/D closures are not capable of predicting the PDF evolution in accord with DNS data, they do have the mechanism for shrinking the bounds of the composition space. Obviously, in the context of single-point description without the knowledge of the dissipation field, it is not possible to determine *a priori* the temporal bounds of the scalar field. Therefore, the closures can be modified only by making further assumptions in describing this transport. For a general case, the JET frequencies can be generated by the original form proposed by Johnson (1949a)

$$\phi(\phi_0,t) = \lambda(t)z\left(\frac{\phi_0}{\gamma(t)}\right) + \varrho(t), \tag{54}$$

where the additional parameters $\lambda(t)$ and $\varrho(t)$ provide the extra degrees of freedom in order to account for the variations of the instantaneous boundaries of the composition domain. For the PF, the problem can be overcome, for example, by considering a "four-parameter Beta distribution"

$$P_1(\phi,t) = \frac{1}{[\phi_{\max}(t) - \phi_{\min}(t)]B(\beta_1,\beta_2)}\left(\frac{\phi - \phi_{\min}(t)}{\phi_{\max}(t) - \phi_{\min}(t)}\right)^{\beta_1 - 1}$$

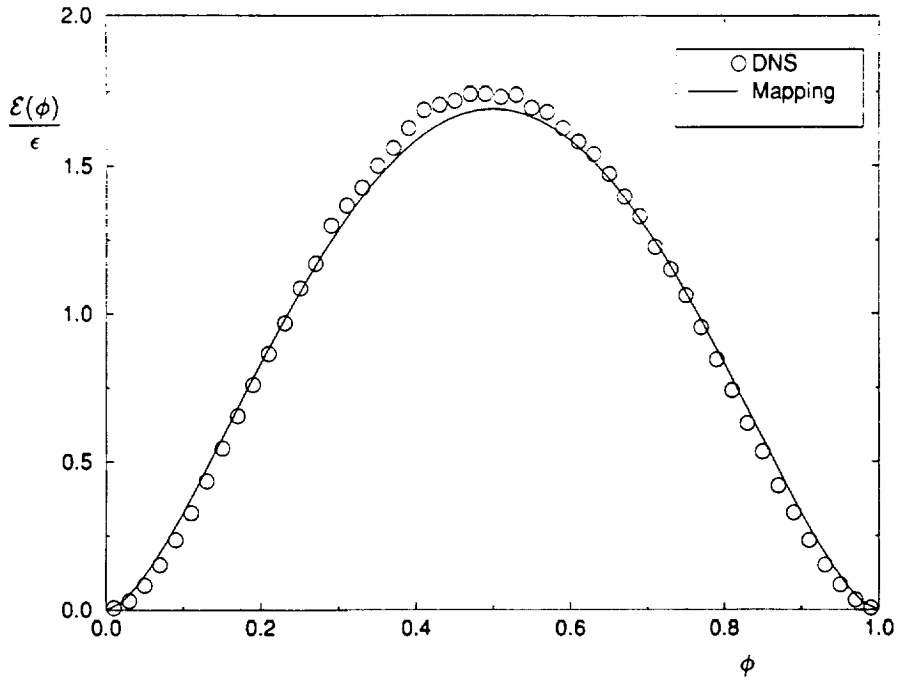

FIGURE 9a The comparison of the conditional expected scalar dissipation normalized with the total dissipation with DNS data as predicted by the AMC with the scalar bounds determined from the DNS results. (a) $\sigma^2 = 0.079$.

$$\left(1 - \frac{\phi - \phi_{\min}(t)}{\phi_{\max}(t) - \phi_{\min}(t)}\right)^{\beta_2 - 1}, \phi_{\min}(g) \leq \phi \leq \phi_{\max}(t), \tag{55}$$

with the extra two parameters being $\phi_{\min}(t)$ and $\phi_{\max}(t)$. For a symmetric PDF in the range $[0, 1] \equiv [\phi_{\min}(t = 0) = \phi_\ell, \phi_{\max}(t = 0) = \phi_u$; therefore, the variance decay can be influenced by increasing β, and/or by decreasing the scalar range $\Delta\phi(t) = \phi_{\max}(t) - \phi_{\min}(t)$. The former recovers the well-known two-parameter Beta distribution (Pearson Type II), while the latter is approximately equivalent to the LMSE closure (O'Brien, 1980). This latter case is presented in Fig. 8 showing a symmetric Beta density with $\beta(t) =$ fixed $= 0.1$. Note that as the mixing proceeds, the variance decays but the PDF preserves its initial approximate double delta shape. In a physical problem, the situation is somewhere between these two limiting cases. The exact situation depends on the characteristics of a particular mixing problem.

The discussions above suggest that in order to predict the final stage of mixing correctly, the effects of mixing on the shrinkage of the domain must be taken into account. To demonstrate this point, the results shown in Fig. 7 can be incorporated into the mixing models to determine the evolution of the conditional expected dissipation and diffusion. This is done here only for the erf^{-1}-Normal, and the results of the conditional expected dissipation are shown in Fig. 9. In the calculations resulting in this figure, analytical solutions are not possible for the moving boundary case. This is demonstrated by the equivalent form of Eq. (29)

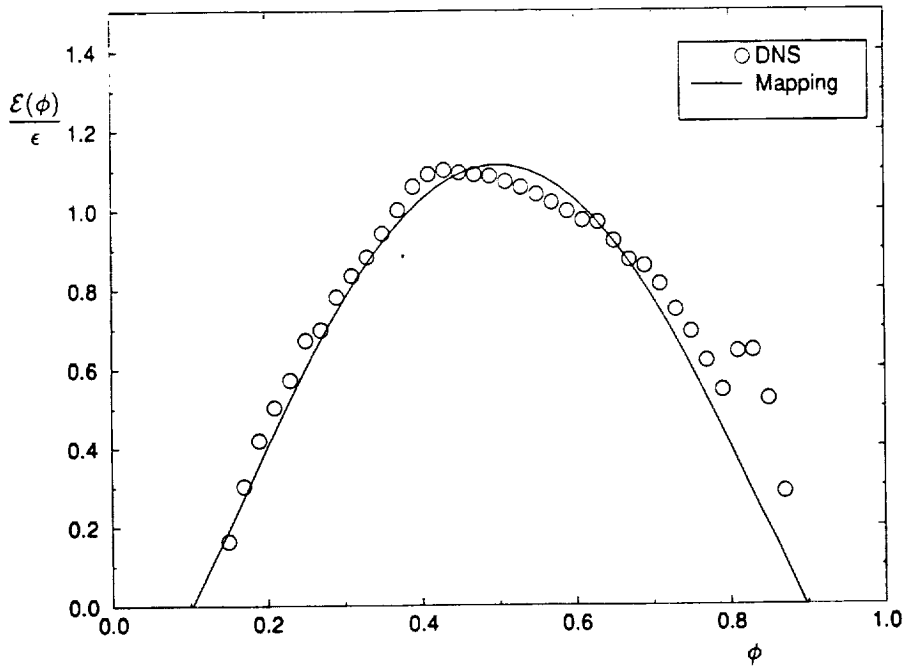

FIGURE 9b The comparison of the conditional expected scalar dissipation normalized with the total dissipation with DNS data as predicted by the AMC with the scalar bounds determined from the DNS results. (b) $\sigma^2 = 0.013$.

$$H(t) = \frac{-\phi_{\max}(t)\gamma}{\sqrt{2}\pi} \int_0^1 \frac{\exp\left\{-\left[erf^{-1}(\frac{\phi}{\phi_{\max}(t)})\right]^2 (1+\frac{z^2\gamma^2}{2})\right\}}{1+\frac{z^2\gamma^2}{2}} dz + \frac{1}{2}(\phi + \phi_{\max}(t)). \tag{56}$$

With this equation, therefore, the effect of the temporal variation of the PDF on the conditional dissipation is through the $\partial H/\partial t$ term in Eq. (28). This term has the form

$$\frac{dH}{dt} = \frac{-\sqrt{2}\phi_{\max}(t)\frac{d\gamma}{dt}}{\pi(2+\gamma^2)} \exp\left\{-(1+\frac{\gamma^2}{2})\left[erf^{-1}(\frac{\phi}{\phi_{\max}(t)})\right]^2\right\} + \frac{1}{2}\frac{d\phi_{\max}}{dt}$$
$$\left(1 - \frac{\phi}{\phi_{\max}(t)} \exp\left\{\left[erf^{-1}(\frac{\phi}{\phi_{\max}(t)})\right]^2\right\} + \right.$$
$$\left. \frac{2}{\sqrt{\pi}} \int_{-\infty}^{erf^{-1}(\frac{\phi}{\phi_{\max}(t)})} erf(\frac{\gamma z}{\sqrt{2}}) \exp(-z^2) dz \right). \tag{57}$$

The first term on RHS of Eq. (57) is the same as that in Eq. (30), and the effects of moving boundaries manifest themselves through the second term. This term cannot be evaluated analytically. However, Eqs. (56)-(57) show that due to the direct dependence on $\frac{d\phi_{\max}}{dt}$,

the conditional dissipation does not retain its original functional dependence, suggested by Eq. (33). Also, Fig. 9 shows that the effect of the moving boundaries is to force the conditional expected dissipation to zero at the current scalar maxima/minima. Therefore, the predicted results compare much better with DNS data than those presented in Fig. 4. Due to the similarity of the PDF's, it is expected that the other two closures would also behave in the similar fashion.

The influence of boundary encroachment is also sensed in the conditional expected diffusion field. For the erf^{-1}-Normal scalar PDF, the equivalent form of Eq. (41) is

$$D(\phi,t) = -\frac{2\phi_{\max}(t)}{\gamma\sqrt{\pi}}\frac{d\gamma}{dt}\exp\left\{-\left[erf^{-1}(\frac{\phi}{\phi_{\max}(t)})\right]^2\right\}$$

$$erf^{-1}\left(\frac{\phi}{\phi_{\max}(t)}\right) + \left(\frac{\phi}{\phi_{\max}(t)}\right)\frac{d\phi_{\max}}{dt}, \tag{58}$$

with an average dissipation of

$$\epsilon(t) = \frac{4\phi_{\max}^2(t)}{\pi(\gamma^2+2)\sqrt{\gamma^2+4}}\frac{d\gamma}{dt} - \frac{2\phi_{\max}(t)}{\pi}\arctan\left(\frac{2}{\gamma\sqrt{\gamma^2+4}}\right)\frac{d\phi_{\max}}{dt}. \tag{59}$$

Equations (58)-(59) show the influence of the boundary movement through the last term on the RHS of both these equations. With these additional terms, the normalized form similar to Eq. (41) is not very useful, and Eqs. (58)-(59) are evaluated numerically.

The equivalent of Eq. (58) for the Logit-Normal and the Beta density are, respectively,

$$D(\phi,t) = \frac{(\phi_{\max}^2-\phi^2)}{\phi_{\max}\gamma}\frac{d\gamma}{dt}\tanh^{-1}\left(\frac{\phi}{\phi_{\max}(t)}\right) + \left(\frac{\phi}{\phi_{\max}(t)}\right)\frac{d\phi_{\max}}{dt}, \tag{60}$$

$$D(\phi,t) = -\frac{1}{P_1(\phi,t)}\frac{\partial}{\partial t}\left(I_{\left\{\frac{\phi-\phi_{\min}}{\phi_{\max}-\phi_{\min}}\right\}}(\beta,\beta)\right) \tag{61}$$

An interesting characteristic displayed by Eqs. (58) and (60) is the influence of the terms containing the temporal derivative of $\phi_{\max}(t)$. Note that at the boundaries, *i.e.* $\phi = \phi_{\max}(t)$, the first term on the RHS of these equations vanish, but the last term prohibit the conditional expected diffusion from going to zero. This is in accordance with the DNS data as shown in Fig. 6. In order to demonstrate this more clearly, results are presented in Fig. 10 of the conditional expected diffusion predicted by the erf^{-1}-Normal, with the input of the variance and the scalar bounds from DNS. A comparison between this figure and Fig. 6 show the influence of the boundary movement, and a better agreement between the model predictions and the DNS data. This agreement is more pronounced at scalar values away from the mean. Near the mean value, the influence of the boundary migration is slight, as also indicated by Eqs. (58) and (59).

8 DISCUSSIONS AND APPLICATIONS

In the previous section, a rather detailed discussion was presented of the problem of scalar mixing from an initially symmetric binary state. These discussions were primarily intended to provide a means of assessing the differences between the currently available tools in probability modeling of the scalar mixing problem. This problem is of significant interest, considering the extent of previous works focused on its analysis (Pope, 1976;

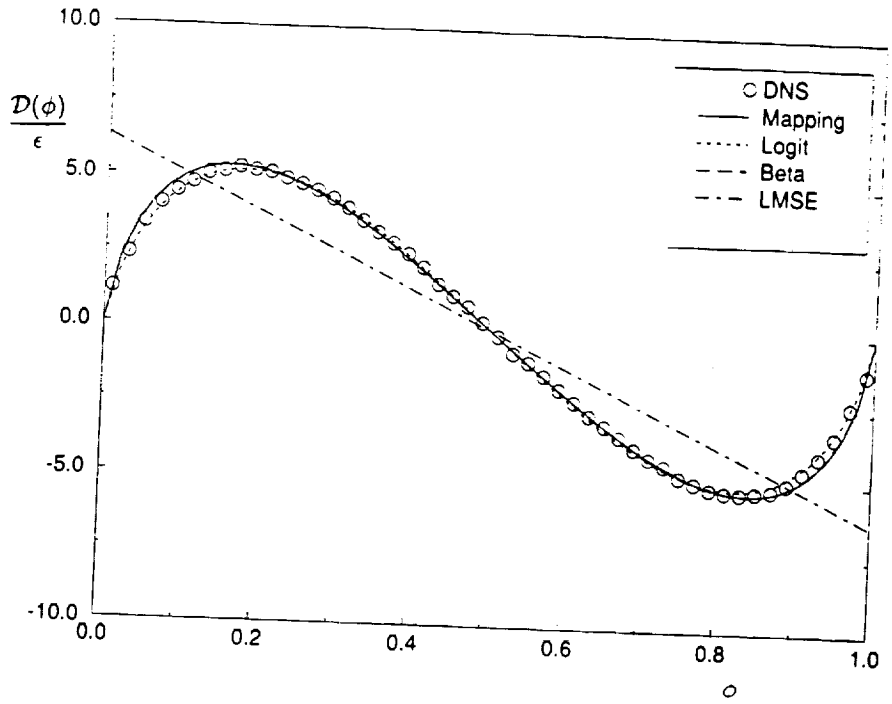

FIGURE 10a The comparison of the conditional expected scalar diffusion normalized with the total dissipation with DNS data as predicted by the AMC and the LMSE closures with the scalar bounds determined from the DNS results. (a) $\sigma^2 = 0.079$.

Pope, 1979; Pope, 1982; O'Brien, 1980; Dopazo, 1973; Kosaly and Givi, 1987; Pope, 1991; Gao, 1991; O'Brien and Jiang, 1991; Nomura and Elgobashi, 1992). The results obtained here are particularly useful in highlighting some of the deficiencies of these closures, and in suggesting future research towards overcoming these drawbacks. There are, however, many other physical problems that are not subject to the restricting conditions imposed in these analyses. In this section, therefore, some discussions are presented as to the practical implications of these models, together with some speculations on their extensions for future applications.

Perhaps one of the most important practical applications of the closures considered here is the treatment of reactive flow phenomena. In fact, the most important advantage of scalar PDF methods is due to their applicability in the modeling of turbulent combustion (Pope, 1979; Pope, 1985; Pope, 1990; Kollmann, 1990; O'Brien, 1980). The results generated here can be used directly in the modeling of *mixing controlled* homogeneous chemically reacting systems. Namely, in examining the compositional structure of a reacting system under chemical equilibrium, or in determining the limiting rate of reactant conversion in a simple chemistry of the prototype Fuel + Air $\rightarrow$ Products. The determination of this rate has been the subject of extensive investigations over the past forty years (see Hawthorne *et al.* (1949); Toor (1962); Williams (1985)). It is now well-established that in a mixing controlled binary irreversible reaction of this type, the statistics of the reacting fields can be related to those of an appropriately defined conserved scalar (such as ϕ) (Bilger, 1980; Toor, 1975; Williams, 1985). Therefore, the frequencies generated herein can be utilized for estimating the statistics of the reacting field with an infinitely fast chemistry model in a homogeneous flow with an

initially segregated reactants under stoichiometric conditions. Albeit very restricting, this problem is of great practical importance for modeling and design of batch mixers and plug flow reactors in which these conditions prevail (Toor, 1975; Brodkey, 1981; Dutta and Tarbell, 1989). Madnia *et al.* (1991b); Madnia *et al.* (1992) have shown that with the erf^{-1}-Normal (AMC) and the Beta density models, this rate can be predicted by simple analytical means. For the Logit-Normal density, a complete analytical solution cannot be obtained and determination of the statistics requires numerical integration of the PDF. The results generated by these closures agree with DNS data better than those obtained by means of the C/D closures (McMurtry and Givi, 1989), or other models previously available in the chemical engineering literature (Dutta and Tarbell, 1989) (see Givi (1989) for a review). Also, the results provided by the AMC (Frankel *et al.*, 1992a) are shown to compare well with experimental data on plug flow reactors if the additional information pertaining to the evolution of the scalar length scale is accurately provided.

The most obvious issues in regard to the applications of these models are associated with their extension for the treatment of (1) non-symmetric binary scalar mixing, (2) non-binary scalar mixing, (3) multiple scalar mixing, and (4) non-homogeneous mixing. The first problem constitutes a more general form of the binary mixing problem and is also important for the analysis of non-stoichiometric reacting systems. The second problem is appropriate for the analysis of other mixing systems in which the initial conditions are not of a two-feed configuration. The third problem is of interest in reacting systems in which the transport of a passive scalar (like ϕ) is not sufficient for a complete analysis. For example, any reacting system under non-equilibrium conditions. Finally, the importance of the fourth problem is obvious in view of the fact that the flow within most practical mixing devices cannot be assumed homogeneous.

In regard to the first issue, all of the three closures considered here can be used for the probability modeling of scalar mixing within a *fixed* scalar domain. The use of the AMC is straightforward, but the mathematical procedure is somewhat complex (Madnia *et al.*, 1992). The Pearson frequencies can be generated easily for non-symmetric problems. In this case, the Pearson Type I provides a reasonably accurate representation of the scalar field regardless of the degree of asymmetry of the PDF (Frankel *et al.*, 1992b; Madnia *et al.*, 1992). The use of the JET in this regard is most difficult, since closed form analytical expressions are not available for the variance of the scalar by which the PDF can be characterized (Johnson, 1949a). In treating these problems, therefore, the first two models can be more readily employed and subsequently used for the treatment of mixing controlled reacting systems under non-stoichiometric conditions. In fact, as demonstrated by Madnia *et al.* (1992) the solution of the non-symmetric form of the AMC and the Beta density provide a very good means of predicting the limiting rate of reactant conversion in homogeneous reacting flows. However, it should be indicated that with both models the problem associated with the scalar bounds still exists and must be dealt with as discussed in Section 7.

In addressing the second issue, it is obvious that the AMC is more appropriate than the other closures for simulating the mixing problem from an initially "arbitrary" state. The extension of JET and PF for treating multi- (higher than bi-) modal distributions have been reported in statistics literature. However, as the degree of modality of the PDF increases the procedure becomes more complex and not suitable for practical applications. Fortunately, in most mixing problems in simple flows, *i.e.* homogeneous turbulence and turbulent shear flows, the PDF exhibits strong bimodal features (Madnia *et al.*, 1992; Frankel *et al.*, 1992b). In those cases, the use of the Beta density can be justified. In fact, in non-homogeneous flows it is easier to use this density, at least until further developments of the AMC for practical applications (see Frankel *et al.* (1992b); Gaffney *et al.* (1992)).

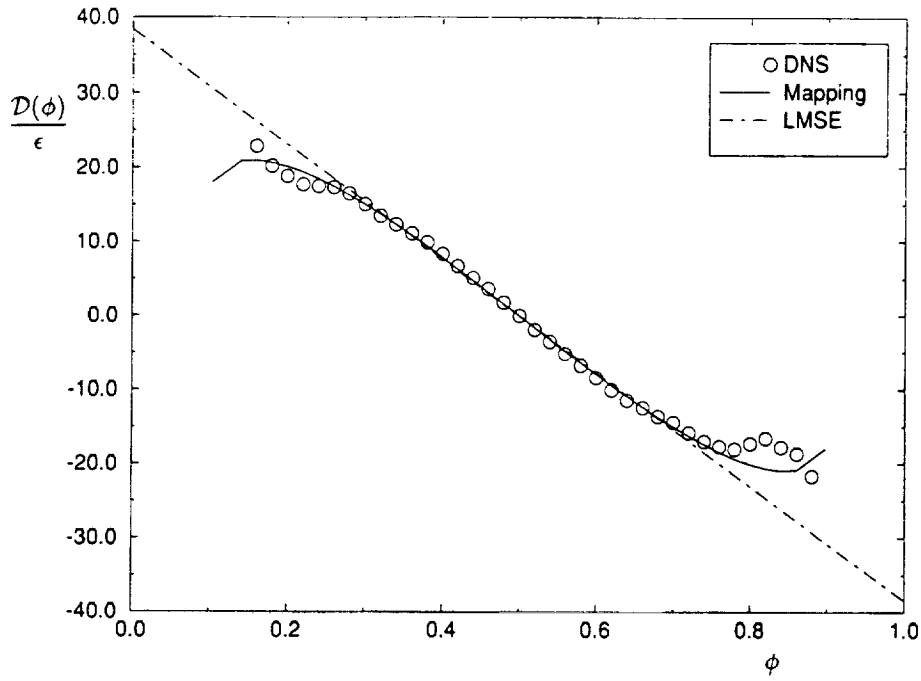

FIGURE 10b The comparison of the conditional expected scalar diffusion normalized with the total dissipation with DNS data as predicted by the AMC and the LMSE closures with the scalar bounds determined from the DNS results. (b) $\sigma^2 = 0.013$.

The extension of all of the three models in describing multi-scalar mixing is possible. The problem naturally falls within the realm of the *multivariate* statistical analyses. In these analyses, the implementation of the AMC is relatively straightforward since it provides a transport equation for the joint PDF's of the scalar variable in a multivariable sense (Pope, 1991). However, it is not presently clear how to devise an efficient computational procedure, typically based on Monte Carlo methods (Pope, 1981), for the numerical treatment of these equations. Some work in this regard is currently under way (Valiño and Gao, 1991). The extension of assumed distributions based on the Beta density for treating multi-scalars is more straightforward but less trivial to justify. The most obvious means is to implement the multivariate form of the PF. The direct analog of the Beta density is the *Dirichlet* frequency (Johnson, 1987; Narumi, 1923; Johnson and Kotz, 1972). The application of this density in modeling of multiple species reactions has been discussed by Girimaji (1991a); Girimaji (1991b); Gaffney *et al.* (1992). However, the use of the Dirichlet frequency cannot be justified for modeling of reacting flows in a general sense (Frankel, 1992). Finally the extension of the JET in generating multivariate frequencies has been reported in statistics literature since the subsequent work of Johnson (1949b). As one may suspect, the procedure is more complex, and the same reservations as those associated with the Dirichlet distributions apply.

All of the models considered here can be extended for the analysis of non-homogeneous mixing (and reacting) systems. Obviously, in most cases, the problem requires numerical integration of the appropriate conservation equations. For instance, the AMC can be invoked in the *mixing* step of a fractional stepping procedure, similar to that of typical Monte Carlo procedures (Pope, 1981). The PF densities (*e.g.* Beta or Dirichlet) and JET

generated frequencies require modelled transport equations for the first two moments and cross moments of the scalar field. These equations, "hopefully", include the essential information pertaining to the spatial inhomogeneity of the flow. Naturally, the PDF is not generally symmetric, and must be determined from the knowledge of the parameters $\beta_1, \beta_2, \gamma, \lambda, \varrho$, and the local $\phi_{\max}(t), \phi_{\min}(t)$ values. With this information, all the higher order statistics of the scalar field can be determined. In regard to this last issue, it must be indicated that the Beta density has been extensively used for the modeling of non-homogeneous reacting systems (*e.g.* Rhodes (1975); Jones and Priddin (1978); Lockwood and Moneib (1980); Janicka and Peters (1982); Peters (1984); Frankel *et al.* (1992b); Gaffney *et al.* (1992); for recent reviews, see Givi (1989); Priddin (1991)). Due to their special mathematical properties, the Beta and/or the Dirichlet frequencies yield relatively simple analytical solutions for the higher order statistics of the reacting fields. From this point of view, the use of the PF is more practical than the AMC since the solution procedure does not require the numerical treatment of the PDF transport equation. This point has been discussed in detail by Girimaji (1991b). However, as indicated above, the use of the Dirichlet frequency cannot be justified for modeling of unpremixed reacting flow in a general sense. Also, there is no way of implementing this density directly for modeling of non-equilibrium flames, involving strong correlation of the temperature and the species mass fractions. Even with the assumption of statistical independence of the reacting species and the temperature, the question of the local scalar range imposes a severe restriction on the validity of this approximation. For example, it is demonstrated by Gaffney *et al.* (1992) that in the modeling of a reacting turbulent shear flow, depending on the *a priori* choice of the magnitudes of the local scalar bounds the predicted results can be altered significantly. Obviously, this problem is not eliminated with the usage of JET frequencies in either a univariate or multivariate sense.

9 CONCLUDING REMARKS

It is shown that the family of frequencies generated by the Johnson-Edgeworth Translation (JET) provides a reasonable means for statistical modeling of binary symmetric scalar mixing in homogeneous turbulence. It is also shown that the results predicted by one of the members of this family is identical to the solution generated by the Amplitude Mapping Closure (AMC) of Kraichnan. This similarity is useful in two regards: (1) establishing a mathematical reasoning for the similarity of the probability frequency of the Pearson Family (PF) and that of the AMC for the description of the problem, and (2) suggesting the possible use of other members of the JET frequencies in approaches in which the Probability Density Function (PDF) is assumed *a priori*. The PDF's generated by all these models are shown to compare well with each other and also with the results obtained by Direct Numerical Simulations (DNS). However, none of the models are capable of accurately predicting the conditional expected dissipation and the conditional expected diffusion of the scalar field. This problem is associated with the incapability of the models to account for the migration of the scalar bounds as mixing proceeds.

ACKNOWLEDGEMENTS

We are indebted to Dr. Gordon Erlebacher for the use of his computer codes. We also appreciate the efforts of Ms. Debbie Young for assisting us with the literature search. This work is sponsored by the Office of Naval Research under Grant N00014-90-J-1403, by NASA Langley Research Center under Grant NAG-1-1122, and by the National Science Foundation under Grant CTS-9253488. The computational resources are provided by NSF through NCSA at the University of Illinois, and by the NAS program at NASA Ames Research Center. Correspondence should be directed to P. Givi.

REFERENCES

Abramowitz, M. and Stegun, I. A. (1972). *Handbook of Mathematical Functions and Formulas, Graphs, and Mathematical Tables.* Government Printing Office, Washington, D.C.

Bilger, R. W. (1980). Turbulent flows with nonpremixed reactants. In Libby, P. A. and Williams, F. A., editors, *Turbulent Reacting Flows,* chapter 3, pages 65-113. Springer-Verlag, Heidelberg.

Brodkey, R. S. (1981). Fundamental of turbulent motion. *Chem. Eng. Comm.* **8,** 1-23.

Casella, G. and Berger, R. L. (1990). *Statistical Inference.* Brooks/Cole Publishing Company, Belmont, CA.

Chen, H., Chen, S., and Kraichnan, R. H. (1989). Probability distribution of a stochastically advected scalar field. *Phys. Rev. Lett.* **63,** 2657-2660.

Curl, R. L. (1963). Dispersed phase mixing: I. Theory and effects in simple reactors. *AIChE J.* **9,** 175-181.

Dopazo, C. (1973), *Non-Isothermal Turbulent Reactive Flows: Stochastic Approaches.* Ph.D. Thesis, Department of Mechanical Engineering, State University of New York at Stony Brook, Stony Brook, NY.

Dutta, A. and Tarbell, J. M. (1989). Closure models for turbulent reacting flows. *AIChE J.* **35,** 2013-2027.

Edgeworth, F. Y. (1907). On the representation of statistical frequency by a series. *Journal of the Royal Statistical Society, Series A.* **70,** 102-106.

Erlebacher, G., Hussaini, M. Y., Speziale, C. G., and Zang, T. A. (1987). Toward the large eddy simulation of compressible turbulent flows. ICASE Report 87-20, NASA Langley Research Center, Hampton, VA. Also available as *NASA CR 178273.*

Erlebacher, G., Hussaini, M. Y., Speziale, C. G., and Zang, T. A. (1990). Toward the large eddy simulation of compressible turbulent flows. ICASE Report 90-76, NASA Langley Research Center, Hampton, VA. Also available as *NASA CR 187460.*

Erlebacher, G., Hussaini, M.Y., Kreiss, H. O., and Sarkar, S. (1990). The analysis and simulation of compressible turbulence. *Theoret. Comput. Fluid Dynamics* **2,** 73-95.

Eswaran, V. and Pope, S. B. (1988). Direct numerical simulations of the turbulent mixing of a passive scalar. *Phys. Fluids* **31,** 506-520.

Frankel, S. H., Jiang, T.-L., and Givi, P. (1992). Modeling of isotropic reacting turbulence by a hybrid mapping-EDQNM closure. *AIChE J.* **38,** 535-543.

Frankel, S. H., Madnia, C. K., and Givi, P. (1992). Modeling of the reactant conversion rate in a turbulent shear flow. *Chem. Eng. Comm.* **113,** 197-209.

Frankel, S. H. (1992). Ph.D. Thesis, Department of Mechanical and Aerospace Engineering, State University of New York at Buffalo, Buffalo, NY. in preparation.

Gaffney, R. L., White, J. A., Girimaji, S. S., and Drummond, J. P. (1992). Modeling of turbulent/chemistry interactions using assumed pdf methods. AIAA paper AIAA-92-3638.

Gao, F. (1991). Mapping closure and non-Gaussianity of the scalar probability density functions in isotropic turbulence. *Phys. Fluids A* **3,** 2438-2444.

Girimaji, S. S. (1991a). Assumed β-pdf model for turbulent mixing: Validation and extension to multiple scalar mixing. *Combust. Sci. and Tech.* **78,** 177-196.

Girimaji, S. S. (1991b). A simple recipe for modeling reaction-rates in flows with turbulent-combustion. AIAA paper AIAA-91-1792.

Girimaji, S. S. (1992). Towards understanding turbulent scalar mixing. NASA CR 4446.

Givi, P. and McMurtry, P. A. (1988). Non-premixed reaction in homogeneous turbulence: Direct numerical simulations. *AIChE J.* **34,** 1039-1042.

Givi, P. (1989). Model free simulations of turbulent reactive flows. *Prog. Energy Combust. Sci.* **15,** 1-107.

Hawthorne, W. R., Wedell, D. S., and Hottel, H. C. (1949). Mixing and combustion in turbulent gas jets. In *3rd Symp. on Combustion, Flames and Explosion Phenomena,* pages 266-288. The Combustion Institute, Pittsburgh, PA.

Hussaini, M. Y., Speziale, C. G., and Zang, T. A. (1990). The potential and limitations of direct and large eddy simulations. In Lumley, J. L., editor, *Whither Turbulence? Turbulence at the Crossroads,* volume 357 of *Lecture Notes in Physics,* pages 354-368. Springer.

Janicka, J. and Peters, N. (1982). Prediction of turbulent jet diffusion flame lift-off using a pdf transport equation. In *Proceedings of 19th Symp. (Int.) on Combustion* pages 367-374. The Combustion Institute, Pittsburgh, PA.

Janicka, J., Kolbe, W., and Kollmann, W. (1979). Closure of the transport equation for the probability density function of turbulent scalar field. *J. Nonequil. Thermodyn.* **4,** 47-66.

Jiang, T.-L., Givi, P., and Gao, F. (1992). Binary and trinary scalar mixing by Fickian diffusion-some mapping closure results. *Phys. Fluids A* **4,** 1028-1035.

Johnson, N. L. and Kotz, S. (1972). *Distributions in Statistics: Continious Multivariate Distributions.* John Wiley and Sons, New York, NY.

Johnson, N. L. (1949a). Systems of frequency curves generated by methods of translation. *Biometrika* **36,** 149-176.

Johnson, N. L. (1949b). Bivariate distributions based on simple translation systems. *Biometrika* **36,** 297-304.

Johnson, M. E. (1987). *Multivariate Statistical Simulation.* John Wiley and Sons, New York, NY.

Jones, W. P. and Priddin, C. H. (1978). Predictions of the flowfield and local gas composition in gas turbine combustors. In *17th Symp. (Int.) on Combustion*, pages 399-409. The Combustion Institute, Pittsburgh, PA.

Kollmann, W. (1990). The pdf approach to turbulent flow. *Theoret. Comput. Fluid Dynamics* **1**, 249-285.

Kosaly, G. and Givi, P. (1987). Modeling of turbulent molecular mixing. *Combust. Flame* **70**, 101-118.

Kosaly, G. (1986). Theoretical remarks on a phenomenological model of turbulent mixing. *Combust. Sci. and Tech.* **49**, 227-234.

Kraichnan, R. H. (1989). Closures for probability distributions. *Bull. Amer. Phys. Soc.* **34**, 2298.

Liñan, A. (1974). The asymptotic structure of counterflow diffusion flames for large activation energies. *Acta Astronautica* **1**, 1007-1039.

Lockwood, F. C. and Moneib, H. A. (1980). Fluctuating temperature measurement in a heated round free jet. *Combust. Sci. and Tech.* **22**, 63-81.

Madnia, C. K. and Givi, P. (1992). On DNS and LES of homogeneous reacting turbulence. In Galperin, B. and Orszag, S. A., editors, *Large Eddy Simulations of Complex Engineering and Geophysical Flows*. Cambridge University Press, Cambridge, U.K. in press.

Madnia, C. K., Frankel, S. H., and Givi, P. (1991b). Mathematical modeling of the reactant conversion rate by single-point pdf methods. In *Proc. Fall Technical Meeting of the Combustion Institute, Eastern Section*, Ithaca, NY.

Madnia, C. K., Frankel, S. H., and Givi, P. (1992). Reactant conversion in homogeneous turbulence: Mathematical modeling, computational validations and practical applications. *Theoret. Comput. Fluid Dynamics*. In press.

McMurtry, P. A. and Givi, P. (1989). Direct numerical simulations of mixing and reaction in a nonpremixed homogeneous turbulent flow. *Combust. Flame* **77**, 171-185.

Miyawaki, O., Tsujikawa, H., and Uraguchi, Y. (1974). Turbulent mixing in multi-nozzle injector tubular mixers. *J. Chem. Eng. Japan* **7**, 52-74.

Narumi, S. (1923). On the general form of bivariate frequency distributions which are mathematically possible when regression and variation are subjected to limiting conditions, I. *Biometrika* **15**, 77-88.

Nomura, K. K. and Elgobashi, S. E. (1992). Mixing characteristics of an inhomogeneous scalar in isotropic and homogeneous sheared turbulence. *Phys. Fluids A* **4**, 606-625.

Norris, A. T. and Pope, S. B. (1991). Turbulent mixing model based on ordered pairing. *Combust. Flame* **83**, 27.

O'Brien, E. E. and Jiang, T.-L. (1991). The conditional dissipation rate of an initially binary scalar in homogeneous turbulence. *Phys. Fluids A* **3**, 3121-3123.

O'Brien, E. E. (1980). The probability density function (PDF) approach to reacting turbulent flows. In Libby, P. A. and Williams, F. A., editors, *Turbulent Reacting Flows*, chapter 5, pages 185-218. Springer-Verlag, Heidelberg.

Passot, T. and Pouquet, A. (1987). Numerical simulation of compressible homogeneous flows in the turbulent regime. *J. Fluid Mech.* **181**, 441-466.

Pearson, K. (1895). Contributions to the mathematical theory of evolution: II. skew variations in homogeneous material. *Philos. Trans. of the Royal Soc. of London, Series A.* **186**, 343-414.

Peters, N. (1984). Laminar diffusion flamelet models in non-premixed turbulent combustion. *Prog. Energy Combust. Sci.* **10**, 319-339.

Pope, S. B. (1976). The probability approach to modelling of turbulent reacting flows. *Combust. Flame* **27**, 299-312.

Pope, S. B. (1979). The statistical theory of turbulent flames. *Phil. Trans. Royal Soc. London* **291**, 529-568.

Pope, S. B. (1981). A Monte Carlo method for the pdf equations of turbulent reactive flow. *Combust. Sci. and Tech.* **25**, 159-174.

Pope, S. B. (1982). An improved turbulent mixing model. *Combust. Sci. and Tech.* **28**, 131-145.

Pope, S. B. (1985). PDF methods for turbulent reacting flows. *Prog. Energy Combust. Sci.* **11**, 119-192.

Pope, S. B. (1990). Computations of turbulent combustion: Progress and challenges. In *Proceedings of 23rd Symp. (Int.) on Combustion*, pages 591-612. The Combustion Institute, Pittsburgh, PA.

Pope, S. B. (1991). Mapping closures for turbulent mixing and reaction. *Theoret. Comput. Fluid Dynamics* **2**, 255-270.

Priddin, C. H. (1991). Turbulent combustion modelling-A review. In Johansson, A. V. and Alfredsson, P. H., editors, *Advances in Turbulence 3*, pages 279-299. Springer-Verlag, Berlin.

Rhodes, P. R. (1975). A probability distribution function for turbulent flows. In Murthy, S. N. B., editor, *Turbulent Mixing in Non-Reactive and Reactive Mixing*, pages 235-241. Plenum Press, New York, NY.

Spalding, S. B. (1961). Theory of mixing and chemical reaction in the opposed-jet diffusion flame. *Journal of the American Rocket Society* **31**, 763-771.

Toor, H. L. (1962). Mass transfer in dilute turbulent and nonturbulent systems with rapid irreversible reactions and equal diffusivities. *AIChE J.* **8**, 70-78.

Toor, H. L. (1975). The non-premixed reaction: $A + B \rightarrow Products$. In Brodkey, R. S., editor, *Turbulence in Mixing Operations*, pages 123-166. Academic Press, New York, NY.

Valiño, L. and Gao, F. (1991). Monte Carlo implementation of the mapping closure for turbulent reacting flows. In *Fluid Dynamics Division Meeting of the American Physical Society*, Phoenix, Arizona.

Williams, F. A. (1985). *Combustion Theory*. The Benjamin/Cummings Publishing Company, Menlo Park, CA, 2nd edition.

4 Appendix II

This work summarizes all our efforts to-date in LES of reacting turbulent flows. The primary conclusion drawn from this work is that the procedure used in k transport equation should be also followed for the g-transport equation. We are presently in the process of undertaking this task.

Large Eddy Simulation of Turbulent Reacting Flow

S. H. Frankel, V. Adumitroaie, C. K. Madnia, and P. Givi
Department of Mechanical and Aerospace Engineering
State University of New York at Buffalo
Buffalo, NY 14260

Key Words

Large Eddy Simulation, Direct Numerical Simulation, Turbulent Reacting Flows, Subgrid Scale Modeling, Probability Density Function.

Abstract

A priori and *a posteriori* analyses of homogeneous and non-homogeneous flows are conducted in order to assess the validity of assumed Probability Density Function (PDF) models as potential subgrid scale (SGS) closures for Large Eddy Simulations (LES) of turbulent reacting flows. Specifically, *a priori* analysis of homogeneous and non-homogeneous turbulent flow is conducted, for both equilibrium and non-equilibrium chemistry, to investigate the potential of the Pearson Family PDF's (Beta and Dirichlet) as SGS models. Also LES of a two-dimensional turbulent reacting shear layer are conducted using a hybrid one-equation Smagorinsky/PDF SGS closure model. The traditional Smagorinsky closure, augmented by the solution of the subgrid turbulent kinetic energy (TKE) equation, is employed to account for the hydrodynamic fluctuations and an assumed PDF is employed for treatment of the scalar fluctuations. An isothermal reaction of the type $A + B \rightarrow Products$ is considered. For this reaction, the assumed PDF approach requires the local mean scalar values and the local subgrid covariance. This covariance is obtained by solving an additional modeled transport equation. This approach results in simple algebraic closures for the chemical source terms appearing in both the species continuity equations as well as in the species covariance equation. The simulations are performed by using a hybrid spectral/finite-difference numerical algorithm. Results are compared to those obtained via Direct Numerical Simulations (DNS) of the same flow in order to assess the validity of our hybrid S/PDF closure.

1 Introduction

Large Eddy Simulations (LES) lie somewhere between Direct Numerical Simulations (DNS) and Reynolds Averaged Navier-Stokes (RANS) computations. In DNS all relevant scales are resolved and no attempt is made at modeling the statistical behavior of the flowfield (Givi, 1989). In RANS calculations, all scales are modeled and moments above a certain level (usually second) are truncated (Launder and Spalding, 1972). In LES the large, energy-containing scales of motion are treated directly, while the effect of the small scales is modeled. Thus scales below a certain level are truncated and modeled. LES is currently viewed as a research tool, but because of the savings in computational resources over DNS, it has the potential to be used for engineering applications.

Over the past 30 years, since the early work of Smagorinsky (1963), there has been relatively little effort, compared to that received for Reynolds Averaged Navier-Stokes (RANS) calculations, to make full use of the LES approach for engineering applications. The most prominent model has been the Smagorinsky eddy viscosity model which relates the unknown subgrid scale Reynolds stresses to the large scale rate of strain. The eddy viscosity performs the predominant role of mimicking the dissipative behavior of the unresolved small scales. One-equation models, which provide the subgrid scale turbulent kinetic energy as the velocity scale for the eddy viscosity, have shown improvement over algebraic models for coarse grid simulations and for modeling higher order moments (Lilly, 1967; Schumann, 1975; Horiuti, 1985). In transitional flows where the assumption of a balance between production and dissipation may not always be valid, higher order models allow more freedom for the subgrid scale eddies to adjust to local flow conditions (Rogallo and Moin, 1984).

LES of mixing layers have been conducted by Mansour *et al.* (1978), Cain *et al.* (1981), Lesieur *et al.* (1988), Maruyama (1988), and more recently by Ragab *et al.* (1992). With regards to applying LES to chemically reacting turbulent flows the literature is even more scarce. Schumann (1989) seems to have been one of the first to conduct LES of reacting flows. However, his assumption to simply neglect the subgrid scale (SGS) contributions from the chemical reactions is questionable. The importance of the scalar fluctuation correlations in turbulent reactive flows has been well recognized (Libby and Williams, 1980). The success of PDF methods for the treatment of chemically reacting flows has been associated with the closed form of the chemical source term (Pope, 1985; 1990; Givi, 1989). These methods have been used extensively for the modeling of turbulent reacting shear flows in a variety of different RANS applications (Lockwood and Naguib, 1975; Bockhorn, 1987; Frankel *et al.*,

1990). Recently it has been demonstrated that the Beta density provides reasonable means for predicting the statistical behavior of a conserved scalar in both homogeneous and non-homogeneous flows (Madnia and Givi, 1992; Madnia *et al.*, 1991; Frankel *et al.*, 1991,1992). Girimaji (1991) suggests the use of a Beta density for modeling of turbulence/chemistry interactions in multivariate species fields. Gaffney *et al.* (1992) and Baurle *et al.* (1992) have used the joint Beta PDF in RANS calculations with complex kinetic mechanisms. The idea to hybridize the DNS approach with PDF methods for treatment of reacting flows is a natural extension of the current technique and is warranted in view of predicted computer capabilities for the foreseeable future.

In this work, we first consider a *priori* analysis of a homogeneous reacting flow in order to assess the extent of validity of the Pearson type PDF's as a SGS model. Then, we propose a hybrid SGS model in order to conduct LES of turbulent reacting flows. In both cases, a chemical reaction of the type $A + B \rightarrow Products$ is considered. The model consists of the traditional Smagorinsky closure for the hydrodynamics with the turbulent kinetic energy providing the velocity scale and an assumed PDF approach for treatment of the chemical reaction rate terms. This technique requires the solution of an additional transport equation for the subgrid scale turbulent kinetic energy and the species covariance. Results are compared to those obtained without the PDF chemistry model as well as those obtained directly by DNS.

2 Hydrodynamic Formulation

The incompressible Navier-Stokes equations are,

$$\frac{\partial u_i}{\partial x_i} = 0 \tag{1}$$

$$\frac{\partial u_i}{\partial t} + \frac{\partial (u_i u_j)}{\partial x_j} = -\frac{1}{\rho}\frac{\partial p}{\partial x_i} + \nu \frac{\partial^2 u_i}{\partial x_j \partial x_j} \tag{2}$$

Typically one defines a filter in order to delineate the resolved or large scale field from the subgrid scale motions,

$$\overline{u} = \int G(\mathbf{r} - \mathbf{r}') u(\mathbf{r}')\, d\mathbf{r}' \tag{3}$$

where G is a filter function with characteristic length Δ. There are two main approaches towards this filtering process. They are the prefiltering approach and the grid averaging

approach. In this work we choose to employ the latter for its ease of implementation. Thus all flow variables are considered to be grid averaged variables and as such can be decomposed into subgrid scale fluctuations from the large scale field,

$$u_i' = u_i - \overline{u_i} \tag{4}$$

Applying the filter to the governing equations,

$$\frac{\partial \overline{u_i}}{\partial x_i} = 0 \tag{5}$$

$$\frac{\partial \overline{u_i}}{\partial t} + \frac{\partial (\overline{u_i u_j})}{\partial x_j} = -\frac{1}{\rho}\frac{\partial \overline{p}}{\partial x_i} + \nu \frac{\partial^2 \overline{u_i}}{\partial x_j \partial x_j} \tag{6}$$

The nonlinear term, $\overline{u_i u_j}$, looks like

$$\overline{u_i u_j} = (\overline{u_i' + \overline{u_i}})(\overline{u_j' + \overline{u_j}}) = \overline{u_i' u_j'} + \overline{u_i' \overline{u_j}} + \overline{\overline{u_i} u_j'} + \overline{\overline{u_i}\,\overline{u_j}} \tag{7}$$

The last term depends on large scale components and is computable in LES. The subgrid scale Reynolds' stresses are defined as,

$$R_{ij} = \overline{u_i' u_j'} + \overline{u_i' \overline{u_j}} + \overline{\overline{u_i} u_j'} \tag{8}$$

This forms the focus of hydrodynamic SGS modeling. Typically one decomposes the SGS stress into the sum of a trace-free tensor and a diagonal tensor,

$$R_{ij} = (R_{ij} - \frac{1}{3}\delta_{ij} R_{kk}) + \frac{1}{3}\delta_{ij} R_{kk} = \tau_{ij} + \frac{1}{3}\delta_{ij} R_{kk} \tag{9}$$

Substitute this into the equations,

$$\frac{\partial \overline{u_i}}{\partial t} + \frac{\partial (\overline{\overline{u_i}\,\overline{u_j}})}{\partial x_j} = -\frac{1}{\rho}\frac{\partial \overline{p}}{\partial x_i} - \frac{\partial \tau_{ij}}{\partial x_j} - \frac{\partial (\frac{1}{3}\delta_{ij} R_{kk})}{\partial x_j} + \nu \frac{\partial^2 \overline{u_i}}{\partial x_j \partial x_j} \tag{10}$$

or defining,

$$\overline{P} = \frac{\overline{p}}{\rho} + \frac{1}{3} R_{kk} \tag{11}$$

and employing the Smagorinsky eddy viscosity model for closure of the Reynolds' stress, we have:

$$\tau_{ij} = 2\nu_T S_{ij} = \nu_T \left(\frac{\partial \overline{u}_i}{\partial x_j} + \frac{\partial \overline{u}_j}{\partial x_i} \right) \tag{12}$$

In the original Smagorinsky model the eddy viscosity, ν_T, was related to the large scale strain rate. A suggestion made by Kwak *et al.* (1979) and discussed by Mansour (1981) is to relate the eddy viscosity to the trace of the resolved vorticity field. This is done in the hope of dealing with turbulent/non-turbulent interfaces more effectively, because the vorticity is zero in regions of irrotational flow, whereas the strain rate may not be. This model, while adequate for closure of the first order large scale transport equations, was found insufficient to achieve closure of the second order SGS species covariance equation. Therefore, the decision was made to go to a one-equation hydrodynamics closure model, specifically we solved the transport equation for the SGS turbulent kinetic energy, $k = \frac{1}{2}(\overline{u_i' u_i'})$. The eddy viscosity is of the form,

$$\nu_T = C_k \Delta \sqrt{k} \tag{13}$$

where C_k is a model constant chosen as 0.01, and Δ is the filter width chosen so as to enable comparison to the same physical space as in the DNS calculations. Then our modeled momentum equation becomes,

$$\frac{\partial \overline{u_i}}{\partial t} + \frac{\partial (\overline{\overline{u_i}\,\overline{u_j}})}{\partial x_j} = -\frac{1}{\rho}\frac{\partial \overline{P}}{\partial x_i} + \frac{\partial}{\partial x_j}\left((\nu + \nu_T)\frac{\partial \overline{u_i}}{\partial x_j}\right) + \frac{\partial \nu_T}{\partial x_j}\frac{\partial \overline{u_j}}{\partial x_i \partial x_j} \tag{14}$$

The form of the modeled TKE equation is shown below,

$$\frac{Dk}{Dt} = \frac{\partial}{\partial x_i}\left((\nu + \frac{\nu_T}{\sigma_k})\frac{\partial k}{\partial x_i}\right) + P_k - C_D \frac{k^{\frac{3}{2}}}{\Delta} \tag{15}$$

where P_k is the production term given by,

$$P_k = \nu_T \left(\frac{\partial \overline{u_j}}{\partial x_i} + \frac{\partial \overline{u_i}}{\partial x_j}\right)\frac{\partial \overline{u_j}}{\partial x_i} \tag{16}$$

This term can be rewritten in terms of the large scale strain rate, $S_{ij} = \frac{1}{2}\left(\frac{\partial \overline{u_j}}{\partial x_i} + \frac{\partial \overline{u_i}}{\partial x_j}\right)$, as $P_k = 2\nu_T S_{ij} S_{ij}$. The form of this term arises from extending Bousinesque's relation for the laminar stress tensor to the turbulent stress tensor. This relation postulates that the the unknown subgrid stress tensor is proportional to the large scale strain rate, the proportionality being an eddy viscosity. We found that this traditional modeling resulted in too small a production of TKE at the mid- and far- field regions of the flow domain. This will be shown in the results section, but this problem necessitated an unorthodox modeling approach for the production term in the TKE. Thus, we found out that if we modeled the production term using the square of the rotation tensor we get a much improved solution

for the TKE over more than two thirds of the flow domain. This model is based on two observations: (1) the regions of large turbulence kinetic energy are observed to coincide with regions of strong vorticity, and (2) one can show that the modification of the Smagorinsky model which is based on the vorticity rather than the large scale strain rate, as proposed by Mansour *et al.* to deal with regions of turbulent/ non-turbulent flow, can be shown to result from a production equals dissipation argument with the production term modeled on the rotation tensor.

As mentioned the Smagorinsky model is based on the stress being proportional to the rate of strain as in a laminar flow. Lund *et al* (1991) points out that for turbulence transport this relation may need to be augmented. He suggests that rotation should be included in a model for turbulence transport. He then proposes a subgrid-scale stress model which is based not only on the strain rate but on the rotation rate and products of the strain and rotation rate tensors. Recently, Taulbee (1992) developed an improved algebraic Reynolds stress model. His expression for the Reynolds stress is linear in the rate of strain but contains higher-order terms involving combinations of the rotation and strain tensors. Taulbee showed that the improved algebraic model gives better predictions that the previous algebraic Reynolds stress models for the simple flows he considered.

The turbulence Prandtl number, σ_k, is taken as unity and C_D is a model constant chosen as 0.5. We shall now consider closure of the thermochemical equations.

3 Thermochemical Formulation

We consider a two-species reaction of the type $A + B \rightarrow Products$ in an isothermal, incompressible flow. The species A mass fraction, Y_A, conservation equation, with $\mathcal{D}$ constant, is,

$$\frac{\partial Y_A}{\partial t} + \frac{\partial u_i Y_A}{\partial x_i} = \mathcal{D}\frac{\partial^2 Y_A}{\partial x_i \partial x_i} + \dot{\omega}_A \tag{17}$$

and a similar equation for species B. Filtering the above equation,

$$\frac{\partial \overline{Y_A}}{\partial t} + \frac{\partial \overline{u_i Y_A}}{\partial x_i} = \mathcal{D}\frac{\partial^2 \overline{Y_A}}{\partial x_i \partial x_i} + \overline{\dot{\omega}_A} \tag{18}$$

Let,

$$Y_A = \overline{Y_A} + Y_A' \ , \ \ u_i = \overline{u_i} + u_i' \tag{19}$$

then,

$$\frac{\partial \overline{Y_A}}{\partial t} + \frac{\partial(\overline{\overline{u_i}\,\overline{Y_A}} + \overline{\overline{u_i}Y_A'} + \overline{u_i'\overline{Y_A}} + \overline{u_i'Y_A'})}{\partial x_i} = \mathcal{D}\frac{\partial^2 \overline{Y_A}}{\partial x_i \partial x_i} + \overline{\dot{\omega}_A} \tag{20}$$

where $\overline{\overline{u_i}\,\overline{Y_A}}$ is computable from the resolved field and,

$$\overline{\overline{u_i}Y_A'} + \overline{u_i'\overline{Y_A}} + \overline{u_i'A'} = \mathcal{D}_T\frac{\partial \overline{Y_A}}{\partial x_i} \tag{21}$$

So then,

$$\frac{\partial \overline{Y_A}}{\partial t} + \frac{\partial \overline{\overline{u_i}\,\overline{Y_A}}}{\partial x_i} = \frac{\partial}{\partial x_i}\left((\mathcal{D} + \mathcal{D}_T)\frac{\partial \overline{Y_A}}{\partial x_i}\right) + \overline{\dot{\omega}_A} \tag{22}$$

Here $\mathcal{D}_T = \nu_T/Sc_T$ where we choose $Sc_T = 1.0$.

4 Chemical Source Formulation

The chemical source term appearing in the species continuity equation is of the form

$$\dot{\omega}_A = -k_f Y_A Y_B \tag{23}$$

where k_f is the rate constant and is quantified by the Damköhler number, Da, is defined as:

$$Da = \frac{k_f Y_{A\infty}}{\Delta U/\lambda} \tag{24}$$

where $Y_{A\infty}$ is the freestream species concentration, ΔU is the freestream velocity difference and λ is the vorticity thickness. The filtered non-dimensionalized source term is,

$$\overline{\dot{\omega}_A} = -Da(\overline{Y_A}\,\overline{Y_B} + \overline{Y_A'Y_B'}) \tag{25}$$

An alternative approach is to replace the spatial average with a probability average, that is,

$$\overline{\dot{\omega}_A} = -Da \int \dot{\omega}_A \mathcal{P}_{AB}(\psi', \psi'')\, d\psi'\, d\psi'' \tag{26}$$

where ψ' and ψ'' are the sample space variables for species A and B. Thus if we knew the form of the joint PDF of species A and B we would be able to determine the space filtered chemical source term exactly. Based on our experiences as indicated in the previous section, here we employ a member of the Pearson family of distributions, namely the Dirichlet distribution,

for the joint PDF of A and B. We note that this assumption implies a univariate Beta density for the marginal species distributions.

The Dirichlet or joint Beta distribution for the two species A and B is defined as follows,

$$\mathcal{P}_{AB}(\psi', \psi'') = \frac{\Gamma(p_1 + p_2 + p_3)}{\Gamma(p_1)\Gamma(p_2)\Gamma(p_3)} (\psi')^{p_1 - 1} (\psi'')^{p_2 - 1} (1 - \psi' - \psi'')^{p_3 - 1} \tag{27}$$

where,

$$\psi' \geq 0 \ , \ \psi'' \geq 0 \ , \ \psi' + \psi'' \leq 1 \ , \ p_1, p_2, p_3 > 0 \tag{28}$$

The parameters p_1, p_2, p_3 are determined from the knowledge of any three of the following five quantities: $\overline{Y_A}$, $\overline{Y_B}$, subgrid scale species A variance, $\overline{Y_A'^2}$, subgrid scale species B variance, $\overline{Y_B'^2}$, or the covariance of the two species, $\overline{Y_A' Y_B'}$. The chemical source term should depend on all of the above turbochemical quantities. We shall discuss this later. If we select the two species mean values along with the species covariance we can determine the three parameters. They are coupled through:

$$p_1 = -\overline{Y_A} S \tag{29}$$

$$p_2 = -\overline{Y_B} S \tag{30}$$

$$p_3 = (\overline{Y_A} + \overline{Y_B} - 1) S \tag{31}$$

where,

$$S = 1 + \overline{Y_A}\ \overline{Y_B} / \overline{Y_A' Y_B'} \tag{32}$$

With this assumed form of the joint PDF, one can simply integrate the chemical source term in order to obtain its large scale component. This results in closed form expression for the source term,

$$\overline{\dot{\omega}_A} = -Da \frac{p_1 p_2}{(a+1)a} \tag{33}$$

where $a = p_1 + p_2 + p_3$. Substituting the definitions from Equations (26-29) into Equation (30) it can be seen that the source term is consistent with Equation (22). This serves to highlight the difference between mean chemistry and accounting for the subgrid fluctuations. The values of $\overline{Y_A}$ and $\overline{Y_B}$ are computable from their respective transport equations. In order to ascertain the subgrid species covariance $\overline{Y_A' Y_B'}$ we must solve an additional transport equation. This equation can be derived in a straighforward manner and its modeling is well

known in turbulence literature (Pope, 1979):

$$\frac{D\overline{Y_A'Y_B'}}{Dt} = \frac{\partial}{\partial x_i}\left((\mathcal{D}+\mathcal{D}_T)\frac{\partial\overline{Y_A'Y_B'}}{\partial x_i}\right) + C_1\mathcal{D}_T\left(\frac{\partial\overline{Y_A}}{\partial x_i}\frac{\partial\overline{Y_B}}{\partial x_i}\right) - C_2\overline{Y_A'Y_B'}\,\frac{k^{\frac{1}{2}}}{\Delta} + \overline{\dot{\omega}_A Y_B'} + \overline{\dot{\omega}_B Y_A'} \quad (34)$$

where C_1 and C_2 are adjustable constants.

The chemical source terms in this equation can be likewise modeled using the assumed PDF. After integration their form becomes,

$$\overline{\dot{\omega}_B Y_A'} = -Da\left(\frac{(p_1+1)p_1p_2}{(a+2)(a+1)a} - \overline{Y_A}\frac{p_1p_2}{(a+1)a}\right) \quad (35)$$

$$\overline{\dot{\omega}_A Y_B'} = -Da\left(\frac{(p_2+1)p_1p_2}{(a+2)(a+1)a} - \overline{Y_B}\frac{p_1p_2}{(a+1)a}\right) \quad (36)$$

The TKE and the subgrid scalar covariance are initialized with their respective time zero filtered DNS quantities for comparison purposes. Thus the hybrid Smagorinsky/PDF subgrid scale closure is complete.

5 Numerical Formulation and Problem Description

In order to solve the set of Equations (10,19,32), boundary and initial conditions are needed. In the homogeneous flow case the 2D simulations are performed with a pseudospectral collocation alogorithm utilizing 256^2 collocation points. The simulations are similar to those described in Madnia *et al.* (1992) and the reader is refered to this for more details. In the shear flow configuration free-slip boundary conditions are employed for the cross-stream direction. A zero-gradient outflow boundary condition on the velocity and species fields is employed. The concentration fields are initialized with an error function distribution. The initial conditions for the mean streamwise velocity are by a hyperbolic tangent velocity profile, and the mean cross-stream velocity component is set equal to zero. In order to develop the vorticity rollup and pairing, which are known features of such flows, a small perturbation in the form of the most unstable mode and its subharmonics, calculated from linear stability analysis, is added to this mean profile. The presence of the fundamental mode in the shear layer produces a single vortex rollup, while the superimposed subharmonic perturbation is responsible for the second rollup in the form of the merging of two vortices. These phenomena have significant effects on the chemical reactions that occur within the layer.

The assumption of even periodicity of the flow in the y direction allows us to use pseudospectral Fourier sine/cosine expansions. However, in the streamwise direction an overall second-order finite difference scheme is used with a quadratic upwind differencing for the convection term. This eliminates the spurious oscillations associated with the dispersive error of the second-order scheme. The pressure is decoupled from the momentum equation by solving the appropriate Poisson equation. Time advancement is accomplished with the second-order Adams-Bashforth technique.

The computational domain was selected to be a region bounded by $(0 < x < 32\delta)$ and $(-8\delta < y < 8\delta)$ where δ is the vorticity thickness. For the LES runs there are 64 equally spaced finite difference grid points in the streamwise direction and 32 Fourier modes in the transverse direction. For DNS comparison runs the resolution is improved to 512×256 and for *apriori* analysis subsequently filtered to 64×32.

A number of non-dimensional parameters characterize the flow. They are the Reynolds number, $Re = \Delta U \delta / \nu$, based on the initial shear layer thickness, the mean velocity difference across the layer and the kinematic viscosity, the velocity ratio, $R = \Delta U / (U_1 + U_2)$, and the Peclet number, $Pe = \Delta U \delta / \mathcal{D}$. Moderate values of these parameters must be chosen due to the computational limitations of the current simulations. It is hoped that with the development of the SGS model herein and future advancements these artificial limits can be surpassed. For this preliminary study we choose $Re = Pe = 1000$ and $R = 0.5$. The resolution provided here is sufficient for these simulation parameters.

6 *A priori* Analysis

The Dirichlet distribution is used to model the statistics of the species field within the subgrids in LES of homogeneous turbulence. Since the behavior within the subgrid can be assumed isotropic with a good degree of accuracy (Ferziger, 1981), the use of these models with their demonstrated capabilities in homogeneous flows is well justified. For the Dirichlet model in equilibrium chemistry, the first two moments of an appropriately defined Shvab-Zeldovich variable can be obtained by a properly devised SGS closure (Antonopoulos-Domis, 1981). With the adoption of a Dirichlet density, all the higher order statistics of the reacting field can then be determined. In these cases, the mixture within the subgrid is usually non-stoichiometric, even if the initial sample within the subgrid is supplied with equivalence ratio of unity. In finite rate chemistry the Dirichlet distribution will be assumed for the joint PDF

of the two reacting species.

In order to examine the applicability of the Dirichlet density for subgrid modeling, we have performed a *priori* evaluation of the model. These evaluations are similar to those of previous assessments by Erlebacher *et al.* (1987). With the construction of the DNS database for a 2D homogeneous flow, the results are used to construct the PDF's of the scalar variables within the subgrid. In Figure 1 the contours of the subgrid product mass fraction predicted by the Dirichlet density model are compared with those generated directly via DNS. These results are taken from an arbitrary plane within the three-dimensional box. The comparisons shown in these figures reveal a good agreement between the model predictions and the DNS data. This agreement provides a justification for recommending the Dirichlet density as a reasonable closure to account for the statistical variations within the subgrid. Due to a rather small sample size within the subgrid, the comparison of higher order statistical quantities generated by the model with those of DNS suffers from statistical errors. Also, the implementation of the model requires accurate input of the first two moments of the Shvab-Zeldovich variable.

It has been shown previously that the Dirichlet PDF performs well in RANS modeling of non-homogenous flows in the limits of frozen and equilibrium chemistry (Frankel *et al.*, 1992). With this assumed form we can obtain analytical relations for all the moments of the two species (Madnia *et al.*, 1992). We first consider the case for $Da = 0$. To make comparison with DNS results, the Dirichlet PDF is parameterized by the species mean values and the covariance. With this choice, in Figure 2 we display the *a priori* predictions and the DNS computations. Here we can see that the assumed PDF does very well in predicting the statistical behavior of the scalar values. For finite rate chemistry, consider Figure 3 for $Da = 5$. Specifically, we consider the third order moments $\overline{Y_A'^2 Y_B'}$ and $\overline{Y_A' Y_B'^2}$, which are needed in the solution to the covariance transport equation. Figure 4 shows the third order moments at the same Damköhler number for the case where the PDF is parameterized by the two means and the sum of the variances. This choice of parameters has been utilized by Narayan and Girimaji (1992), and requires solution of a transport equation for the sum of the variances, or the so called scalar energy. The differences in the statistical predictions between this choice and the selection of the covariance is not sufficient to warrant one choice over the other. Since the covariance appears naturally in the filtered source term we chose to use that version in this work.

For our non-homogeneous shear flow we compare predictions obtained by employing the

Dirichlet distribution for equilibrium chemistry with the filtered DNS results. In Figure 5 we show the results for the instantaneous product thickness as a function of streamwise distance. The plots confirms that the Dirichlet distribution does a reasonable job of predicting the subgrid statistics in the limit of fast chemistry. The issue of the models validity for the case of finite-rate chemistry is taken up in the following section.

7 Reacting Shear Flows

In this section a number of simulation results are presented in order to make comparisons and assess the validity of the proposed SGS closure. We begin with a nonreacting flow case in order to ascertain whether our hydrodynamic subgrid model and our modeled species covariance transport equation are performing satisfactorily. This will consist of comparisons between two sets of simulations, LES conducted on a 64x32 grid and a DNS conducted on a 512x256 grid, subsequently filtered to a 64x32 grid. Next, we will consider reacting flows in which the performance of our hybrid Smagorinsky/PDF closure will be assessed. In order to see the effect of the PDF closure we shall also compare to results obtained using the Smagorinsky closure while neglecting the effect of subgrid scale fluctuations on the chemistry. These will be denoted as using the *mean* closure. Contour plots, transverse profiles and integral thickness plots of various flow-field related quantities will aid us in our model assessments.

In order to assess whether the one-equation Smagorinsky model is performing adequately we present LES results for a nonreacting case. The filter width was chosen so as to contain the same physical space as the DNS results in order to make an accurate comparison. In Figure 6 we show transverse profiles of the streamwise velocity component at five downstream locations at a particular time during the simulation. The large scale velocity field is predicted well in the LES results. For flow visualization purposes contour plots of species A are shown in Figure 7. The effect of the subgrid scale model is to smear out the small scale features of the species field within the large scale coherent structures as evidenced in the plot.

In Figure 8 we show contour plots of the subgrid scale TKE obtained from the (a) solution of the modeled transport equation and the (b) filtered DNS results. The reasonable agreement can be more clearly seen in Figure 9, which shows transverse profiles at select downstream locations. Good agreement is obtained at four out of the five downstream locations. At the last downstream location the TKE equation severly underpredicts the turbulence level. This

may be due to deficiencies in modeling the Reynolds stress in terms of the rotation tensor alone. Inclusion of other terms such as the strain rate and/or products of the strain and rotation tensors may be necessary to improve the TKE predictions. This will be discussed further in the next section.

Figure 10 shows contour plots of the subgrid scale species covariance obtained from the modeled transport equation and the filtered DNS for the non-reacting flow case. This plot serves to highlight the deficiences with the modeling of the scalar flux via gradient transport.

For the reacting flow cases considered here the Damköhler number is selected as $Da = 10$. This value is fixed for all the simulations. In Figure 11, contour plots of the product species from the LES and DNS are presented. From these figures we can see the LES and DNS results show similar large scale structures. Figure 12 shows product thickness distribution from the filtered DNS and the LES results obtained with and without the PDF closure. Here we can see that inclusion of the subgrid fluctuations gives results that predict the correct trend are closer to those of the filtered DNS. We note that the *mean* chemistry results show a gross overprediction of the extent of reaction when compared to the filtered DNS results. This highlights the importance of accounting for the subgrid species fluctuations in such flows.

Figure 13 depicts contour plots of the results for the subgrid species covariance obtained from the filtered DNS as well as the modeled transport equation. This demonstrates the problem of accurately predicting the covariance. Figure 14 shows this in a more quantitative manner by displaying the average unmixedness versus streamwise distance. This poor agreement is in part due to the third order moments which are closed using the assumed Dirichlet distribution. As demonstrated in the *a priori* analysis section this distribution has difficulties with predicting the higher order moments well. The discrepancies in the covariance solution are also observed in the non-reacting case as well, indicating that there may be other problems with this modeled equation. These solutions were not able to be improved by simply adjusting the model constants. One of the major problems we feel is that the modeling of the scalar flux in terms of the large scale scalar gradient is inadequate in the context of an LES. That is, the scalar flux may depend on other terms such as the strain and rotation tensors. This can be deduced by developing an algebraic model for the scalar flux in much the same way as has been done for the Reynolds stress. This issue will be further discussed in the next section.

8 Conclusions and Extensions

In this work, *a priori* and *a posteriori* of both homogeneous and non-homogeneous reacting flows are conducted in order to assess the validity of assumed PDF models as potential subgrid scale closures for LES of reacting flows. Specifically, *a priori* these studies revealed that if a Dirichlet distribution is assumed for the joint PDF of the two species, then for frozen and very fast chemistry chemistry the model performs reasonably well in predicting the statistical behavior of the scalar fields. For non-equilibrium chemistry, the PDF closure is not capable of modeling higher order moments accurately.

LES of reacting shear flow has also been conducted employing a hybrid one-equation Smagorinsky/PDF model for the statistical variations on the subgrid. Solutions for the subgrid turbulent kinetic energy and the species covariance have been obtained via solutions of modeled transport equations. The Dirichlet distribution has been employed to close the chemical source terms appearing in the thermochemical equations. The results demonstrate the effect of accounting for the subgrid scale species fluctuations on the product distribution within the shear layer. While the trends are encouraging they do highlight a number of areas where further work is required to improve the model.

First, a better model for the subgrid Reynolds stress is required to obtain more accurate predictions for the subgrid turbulence energy levels. This might involve accounting for some of the additional interactions between the strain and rotation tensors as discussed by Lund *et al.* and Taulbee. Along the same lines, modeling of the scalar flux via gradient transport in the context of a time-accurate LES calculation appears unable to give accurate solutions for second-order subgrid turbulence quantities, such as the species covariance. This modeling deficiency will manifest itself in any potential subgrid chemistry model requiring such statistical information. Algebraic scalar flux models along the lines of Taulbee's algebraic Reynolds stress model would perhaps reveal some of the important terms, other than the scalar gradient, which would better describe the scalar-turbulence interactions. Theses would probably involve the strain and rotation tensors, as well as the scalar gradient, in some appropriate form. Finally, the discrepancies between the assumed form for the joint PDF of species and the actual subgrid PDF will lead to errors, as seen, when predicting the higher-order moments which are needed to close the equations for the second-order subgrid statistics. One possible approach would be instead of assuming the form of the subgrid PDF to solve the appropriate PDF evolution equation for the species. At this stage this has not been looked at and here again some of the previous modeling assumptions may have to be

revised in the context of an LES. For more complex multi-species chemistry the Dirichlet distribution generalizes to n random variables very nicely while still providing analytic forms for all the joint statistics.

9 References

Antonopoulos-Domis, A., Large Eddy Simulations of a Passive Scalar in Isotropic Turbulence, *J. Fluid Mech.*, **104**, 55-79, (1981).

Baurle, R. A., Alexopoulos, G. A., Hassan, H. A., and Drummond, J. P., An Assumed Joint-Beta PDF Approach for Supersonic Turbulent Combustion, AIAA Paper No. 92-3844, (1992).

Bockhorn, H., The Effect of Multi-Dimensional PDFs on the Turbulent Reaction Rate in Turbulent Reacting Flows at Moderate Damköhler Numbers, *PhysicoChemical Hydrodynamics*, **9**, (3/4), 525-535, (1987).

Cain, A. B., Reynolds, W. C., and Ferziger, J. H., A Three-Dimensional Simulation of Transition and Early Turbulence in a Time-Developing Mixing Layer, Report No. TF-14, Thermosciences Division, Dept. of Mech. Eng., Stanford Univ., Stanford, Cal., August (1981).

Erlebacher, G., Hussaini, M. Y., Speziale, C. G., and Zang, T. A., Toward the Large Eddy Simulations of Compressible Turbulent Flows, *NASA CR 178273*, ICASE Report 87-20, NASA Langley Research Center, Hampton, VA. (1987).

Ferziger, J. H., Higher Level Simulations of Turbulent Flows, chapter in *Computational Methods for Turbulent, Transonic, and Viscous Flows*, Hemisphere Publishing Corporation, (1983).

Frankel, S. H., Hassan, H. A., and Drummond, J. P., A Hybrid Reynolds Averaged/PDF Closure Model for Supersonic Turbulent Combustion, AIAA Paper No. 90-1573, (1990).

Frankel, S. H., Madnia, C. K., and Givi, P., Modeling of the Unmixedness in Homogeneous Reacting Turbulence, *Chem. Eng. Comm.*, **104**, 117-125, (1991).

Frankel, S. H., Madnia, C. K., and Givi, P., Modeling of the Reactant Conversion Rate in a Turbulent Shear Flow, *Chem. Eng. Comm.*, **113**, 197-209, (1992).

Gaffney, R. L., White, J. A., Girimaji, S. S., and Drummond, J. P., Modeling Turbulent/Chemistry Interactions Using Assumed PDF Methods, AIAA Paper No. 92-3638, (1992).

Girimaji, S. S., Assumed Beta PDF Model for Turbulent Mixing: Validation and Extension to Multiple Scalar Mixing, *Combust. Sci. and Tech.*, **78**, 177-196, (1991).

Givi, P., Model Free Simulations of Turbulent Reactive Flows, *Prog. Energy Comb. Science*, **15**, No. 1, 1 (1989).

Horuiti, K., Large Eddy Simulation of Turbulent Channel Flow by One-Equation Modeling, *J. Phys. Soc. Jpn.*, **54**(8), 2855-2865, (1985).

Launder, B. E., and Spalding, D. B., *Lectures in Mathematical Models of Turbulence*, Academic Press, (1972).

Lesieur, M., Staquet, C., Le Roy, P., and Comte, P., The Mixing Layer and its Coherence Examined from the Point of View of Two-Dimensional Turbulence, J. Fluid Mech., Vol. 192, 511-534, (1988).

Libby, P. A., and Williams, F. A. (Eds.), *Turbulent Reacting Flows*, Springer, (1980).

Lilly, D. K., The Representation of Small-Scale Turbulence in Numerical Simulation Experiments, Proc. of the IBM Sci. Comp. Symposium on Env. Sci., IBM-Form No. 320-1951, 195-210, (1967).

Lockwood, F. C., and Naguib, A. S., The Prediction of the Fluctuations in the Properties of Free, Round-Jet, Turbulent Diffusion Flames, *Combust. and Flame*, **24**, 109-124, (1975).

Lund, T. S., and Novikov, E. A., Parameterization of Subgrid-Scale Stress by the Velocity Gradient Tensor, *Center for Turbulence Research Annual Research Briefs*, (1991).

Madnia, C. K., Frankel, S. H., and Givi, P., Direct Numerical Simulations of the Unmixedness in a Homogeneous Reacting Turbulent Flow, *Chem. Eng. Comm.*, **109**, 19-29, (1991a).

Madnia, C. K., and Givi, P., On DNS and LES of Homogeneous Reacting Turbulence, in Galperin, B. and Orszag, S. A., editors, *Large Eddy Simulations of Complex Engineering and Geophysical Flows*, Cambridge University Press, Cambridge, U.K. in press (1992).

Madnia, C. K., Frankel, S. H., and Givi, P., Reactant Conversion in Homogeneous Turbulence: Mathematical Modeling, Computational Validations and Practical Applications, *Theoret. Comput. Fluid Dynamics*, (1992).

Mansour, N. H., Ferziger, J. H., and Reynolds, W. C., Large Eddy Simulation of a Turbulent Mixing Layer, NASA Technical Report Number TF-11, April, (1978).

Maruyama, Y., A Numerical Simulation of a Plane Turbulent Shear Layer, Trans. Japan Soc. Aero. Space Sci., Vol. 31, No. 92, 79-93, (1988).

Narayan, J. R., and Girimaji, S. S., Turbulent Reacting Flow Computations Including Turbulent-Chemistry Interactions, AIAA Paper No. 92-0342, (1992).

Pope, S. B., The Statistical Theory of Turbulent Flames, *Phil. Trans. R. Soc. Lond.*, **A291**, 529, (1979).

Pope, S. B., PDF Methods for Turbulent Reacting Flows, *Prog. Energy Combust. Sci.*, **11**, 119-192, (1985).

Pope, S. B., Computations of Turbulent Combustion: Progress and Challenges, in *Proceedings of 23rd Symp. (Int) on Combustion*, 591-612, The Combustion Institute, Pittsburgh, PA, (1990).

Ragab, S. A., and Sheen, S., Large Eddy Simulation of a Mixing Layer, AIAA Paper No. 91-0233, (1991).

Ragab, S. A., Sheen, S., and Sreedhar, M., An Investigation of Finite-Difference Methods for Large Eddy Simulation of a Mixing Layer, AIAA Paper No. 92-0554, (1992).

Rogallo, R. S., and Moin, P., Numerical Simulation of Turbulent Flows, *Ann. Rev. Fluid Mech.*, **16**, 99-137, (1984).

Schumann, U., Subgrid Scale Model for Finite Difference Simulations of Turbulent Flows in Plane Channels and Annuli, *J. Comput. Phys.*, **18**, 376-404, (1975).

Schumann, U., Large Eddy Simulation of Turbulent Diffusion with Chemical Reactions in the Convective Boundary Layer, *Atmos. Env.*, **23**, (8), 1713-1727, (1989).

Smagorinsky, J., General Circulation Experiments with the Primitive Equations, I. The Basic Experiment, Monthly Weather Review, Vol. 91, 99-164, (1963).

Taulbee, D. B., An Improved Algebraic Reynolds Stress Model and corresponding Nonlinear Stress Model, *Phys. Fluids A*, **4**, (11), 2555, (1992).

Figure Captions

Figure 1. Contour plots of filtered product concentration.

Figure 2. Statistical moments vs. time for $Da = 0$ case.

Figure 3. Third order moments for the $Da = 5$ case parameterized by means and covariance.

Figure 4. Third order moments for the $Da = 5$ case parameterized by means and scalar energy.

Figure 5. Product thickness for equilbrium chemistry.

Figure 6. Transverse profiles of streamwise velocity at four downstream locations (a) 5δ, (b) 10δ, (c) 15δ, (d) 20δ.

Figure 7. Contour plots of species A for $Da = 0$ case (a) LES, (b) DNS.

Figure 8. Contour plots of subgrid scale turbulent kinetic energy (a) LES, (b) DNS.

Figure 9. Transverse profiles of subgrid scale turbulent kinetic energy at four downstream locations (a) 5δ, (b) 10δ, (c) 15δ, (d) 20δ, (e) 25δ.

Figure 10. Contour plots of subgrid scale species covariance for non-reacting case (a) LES, (b) DNS.

Figure 11. Contour plots of product species for $Da = 10$ case (a) LES, (b) DNS.

Figure 12. Product thickness for $Da = 10$ case.

Figure 13. Contour plots of subgrid scale species covariance for $Da = 10$ case (a) LES, (b) DNS.

Figure 14. Covariance thickness for $Da = 10$ case.

FIGURE 1

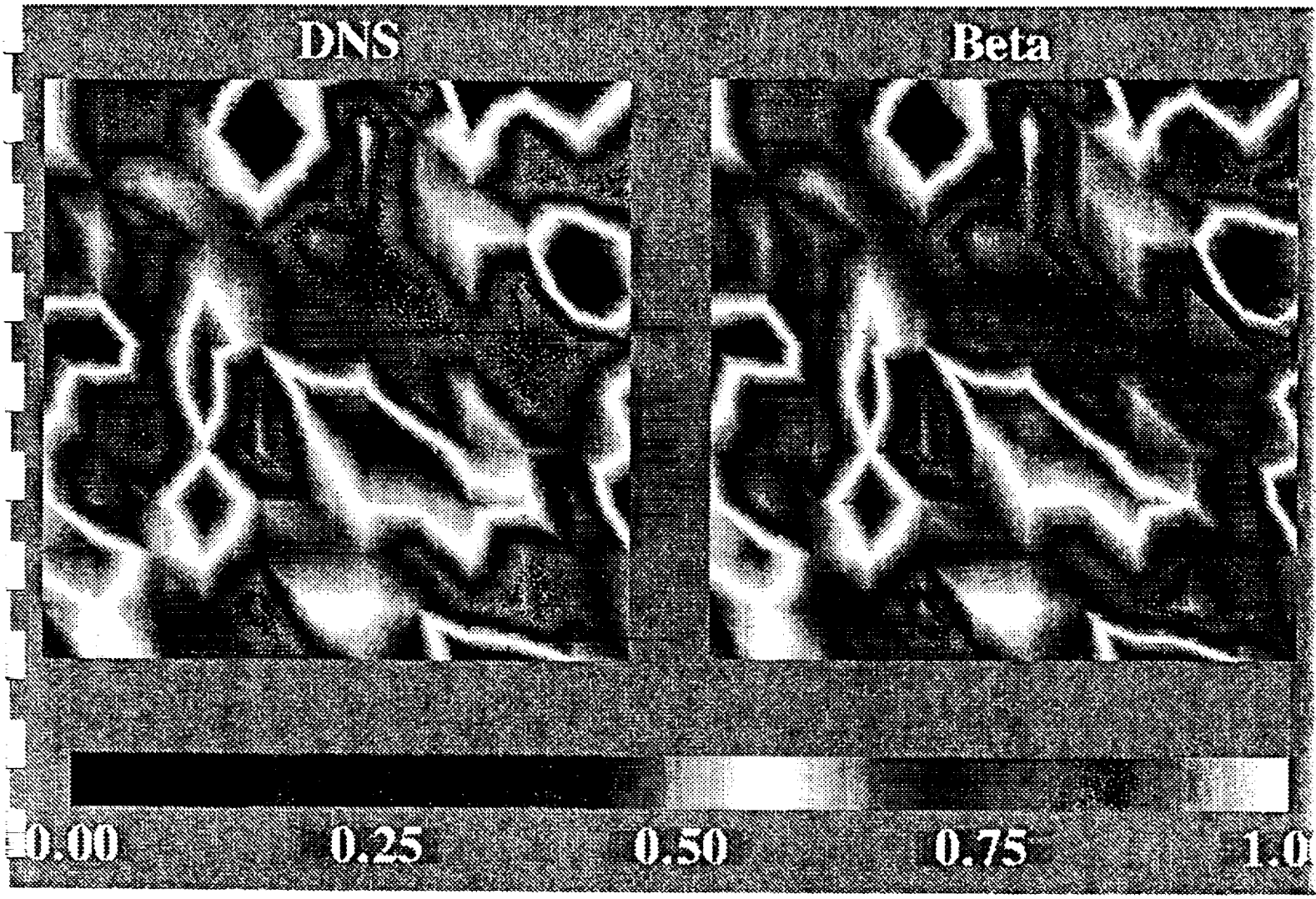

FIGURE 1.

$Da = 0$

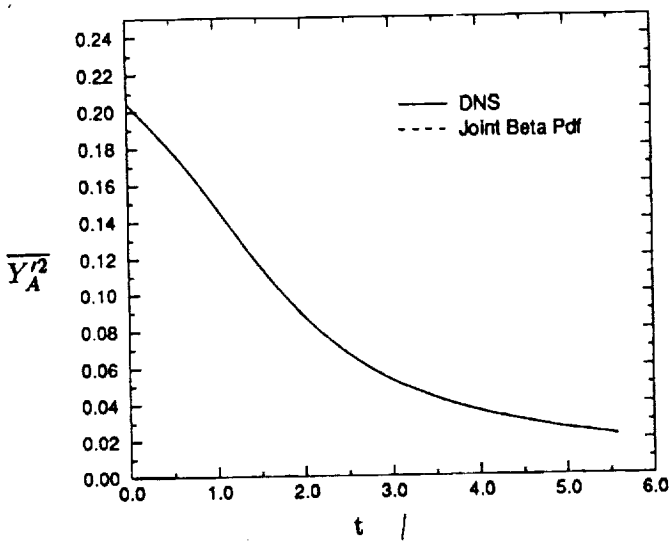
DNS
Joint Beta Pdf
$\overline{Y_A'^2}$
t

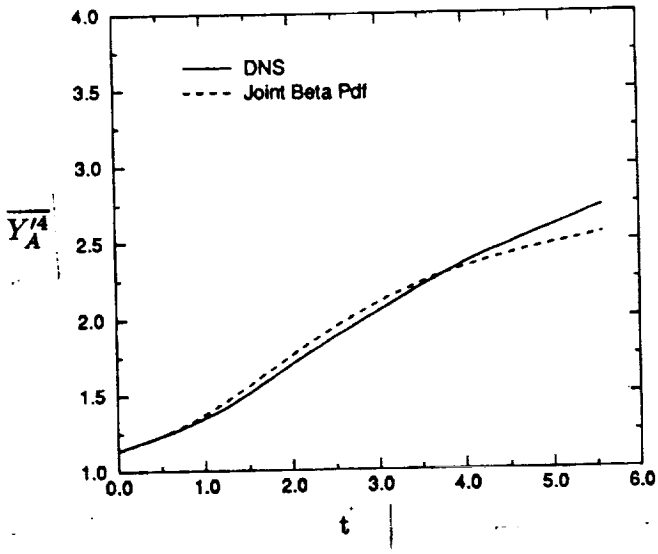
DNS
Joint Beta Pdf
$\overline{Y_A'^4}$
t

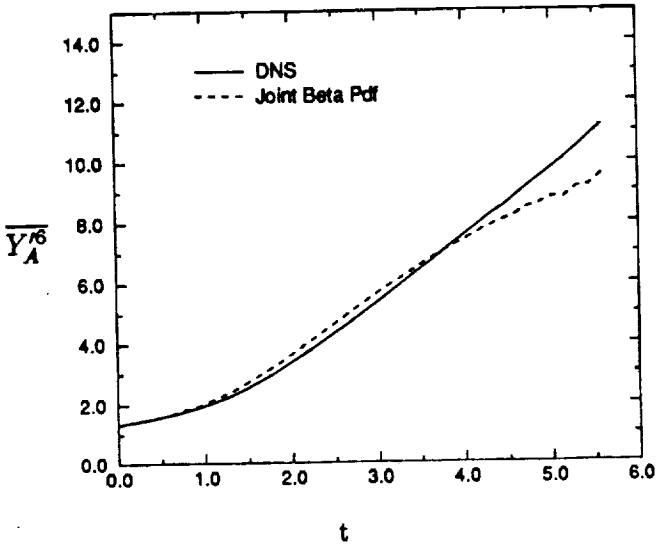
DNS
Joint Beta Pdf
$\overline{Y_A'^6}$
t

FIGURE 2

$Da = 5$

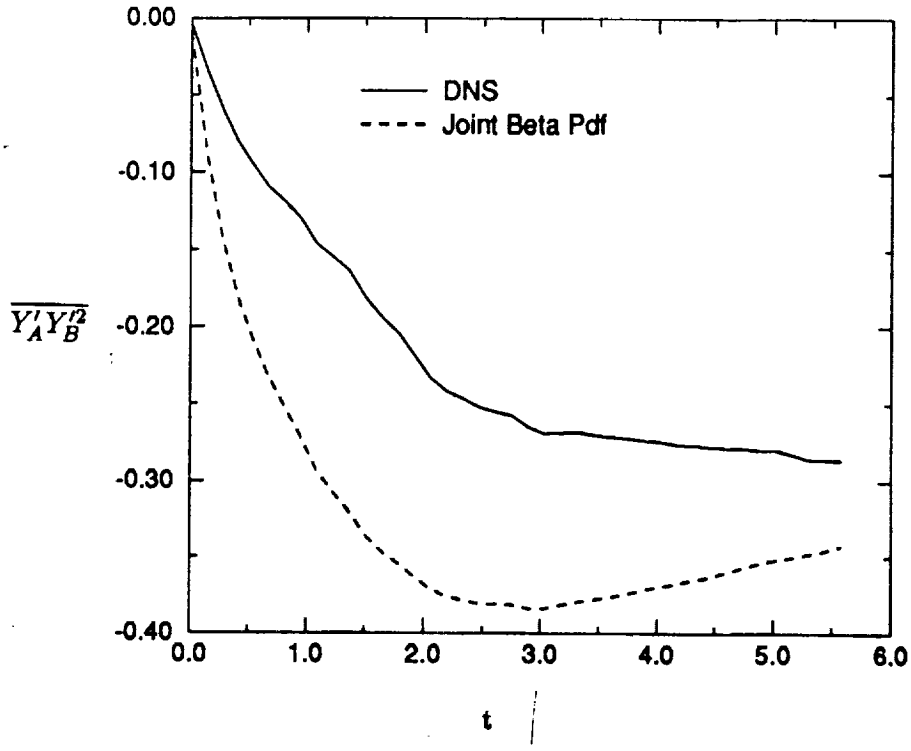
DNS
Joint Beta Pdf
$\overline{Y_A' Y_B'^2}$
0.00
-0.10
-0.20
-0.30
-0.40
0.0
1.0
2.0
3.0
4.0
5.0
6.0
t

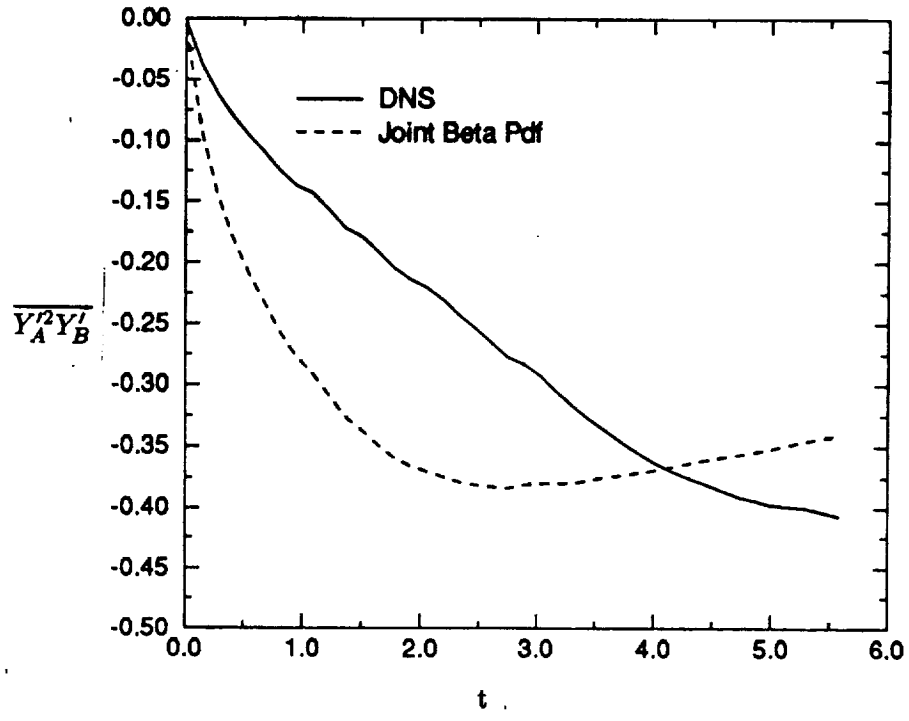
DNS
Joint Beta Pdf
$\overline{Y_A'^2 Y_B'}$
0.00
-0.05
-0.10
-0.15
-0.20
-0.25
-0.30
-0.35
-0.40
-0.45
-0.50
0.0
1.0
2.0
3.0
4.0
5.0
6.0
t

FIGURE 3

$Da = 5$

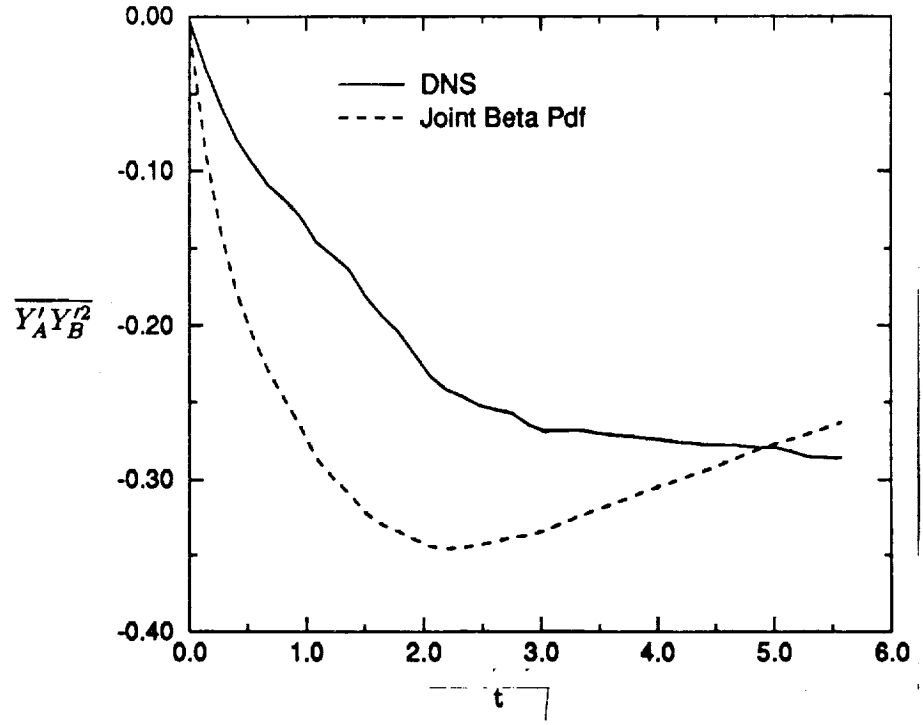
0.00
-0.10
-0.20
-0.30
-0.40
0.0
1.0
2.0
3.0
4.0
5.0
6.0
t
DNS
Joint Beta Pdf
$\overline{Y_A' Y_B'^2}$

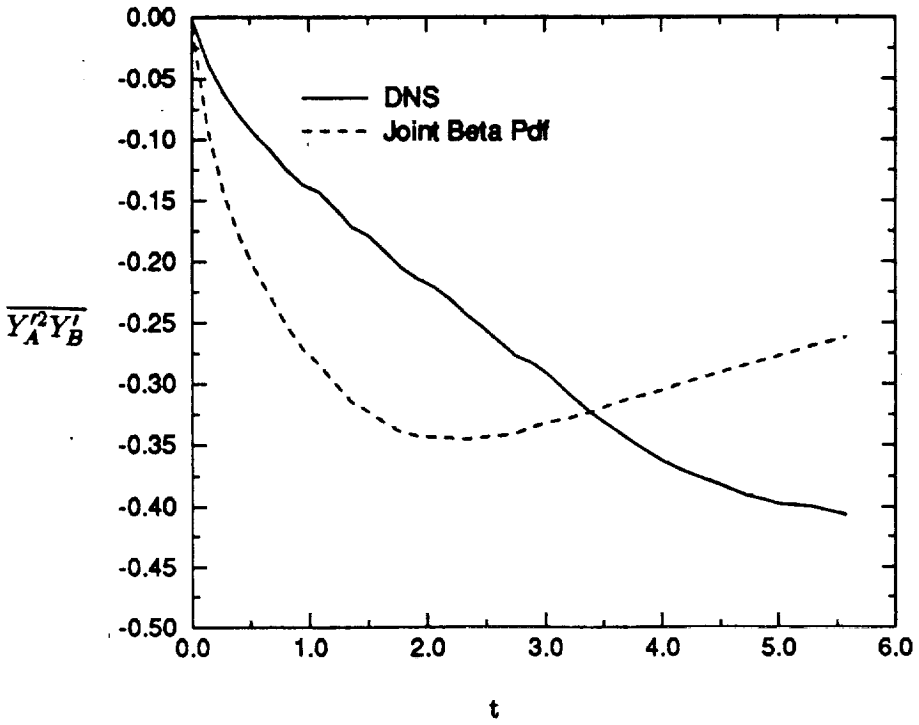
0.00
-0.05
-0.10
-0.15
-0.20
-0.25
-0.30
-0.35
-0.40
-0.45
-0.50
0.0
1.0
2.0
3.0
4.0
5.0
6.0
t
DNS
Joint Beta Pdf
$\overline{Y_A'^2 Y_B'}$

FIGURE 4.

Fig 5

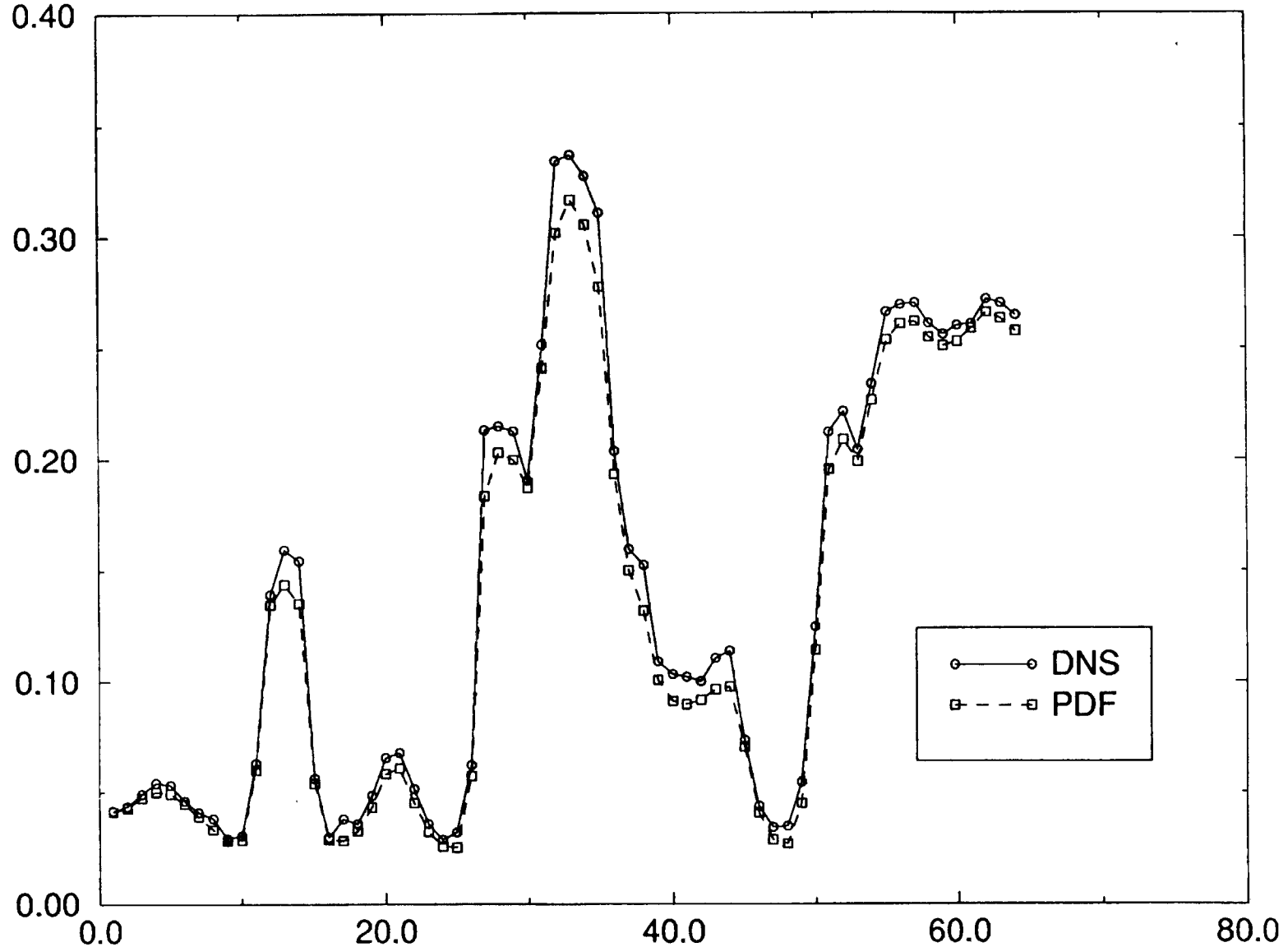

FIGURE 5

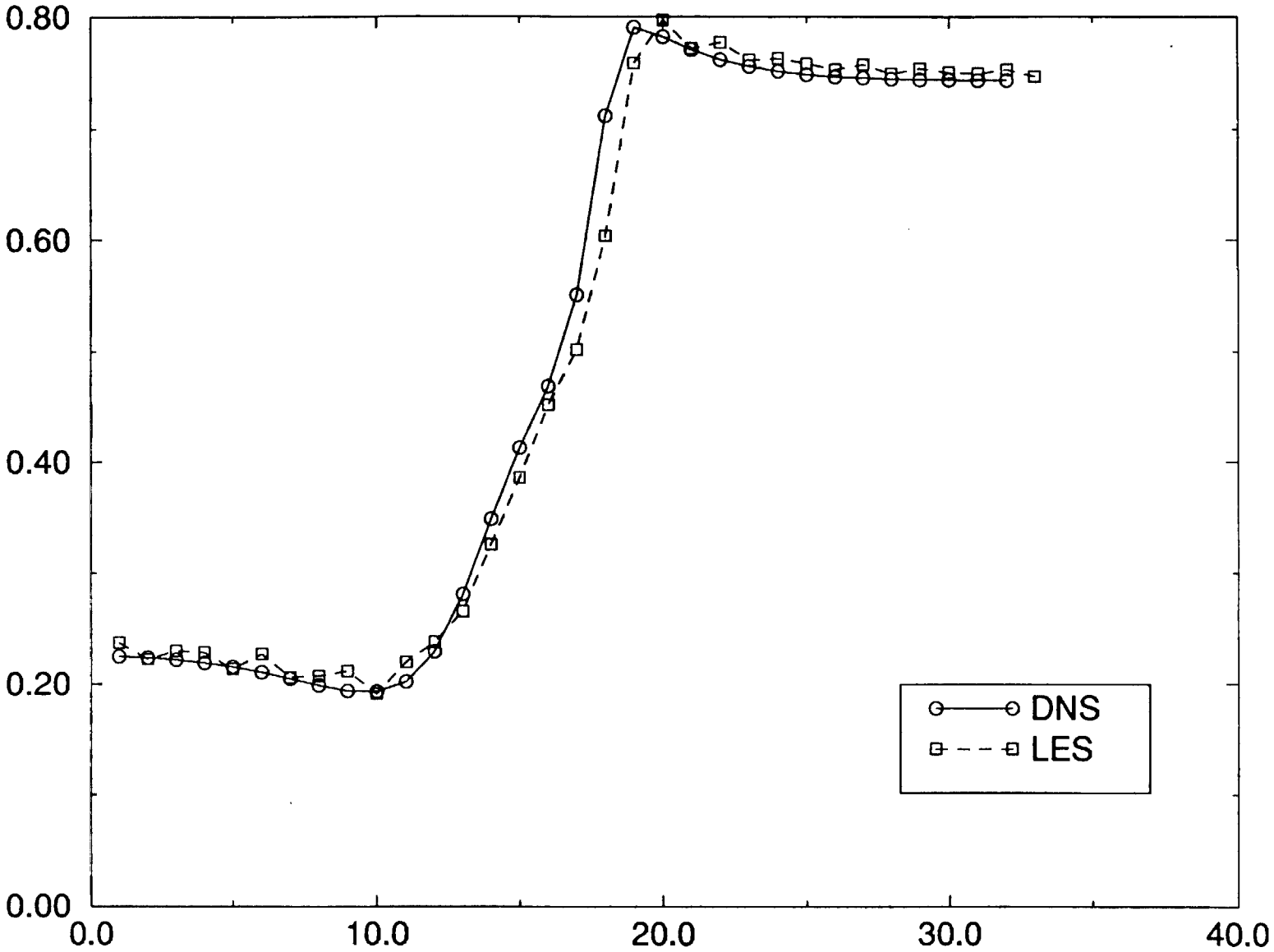

FIGURE 6(a)

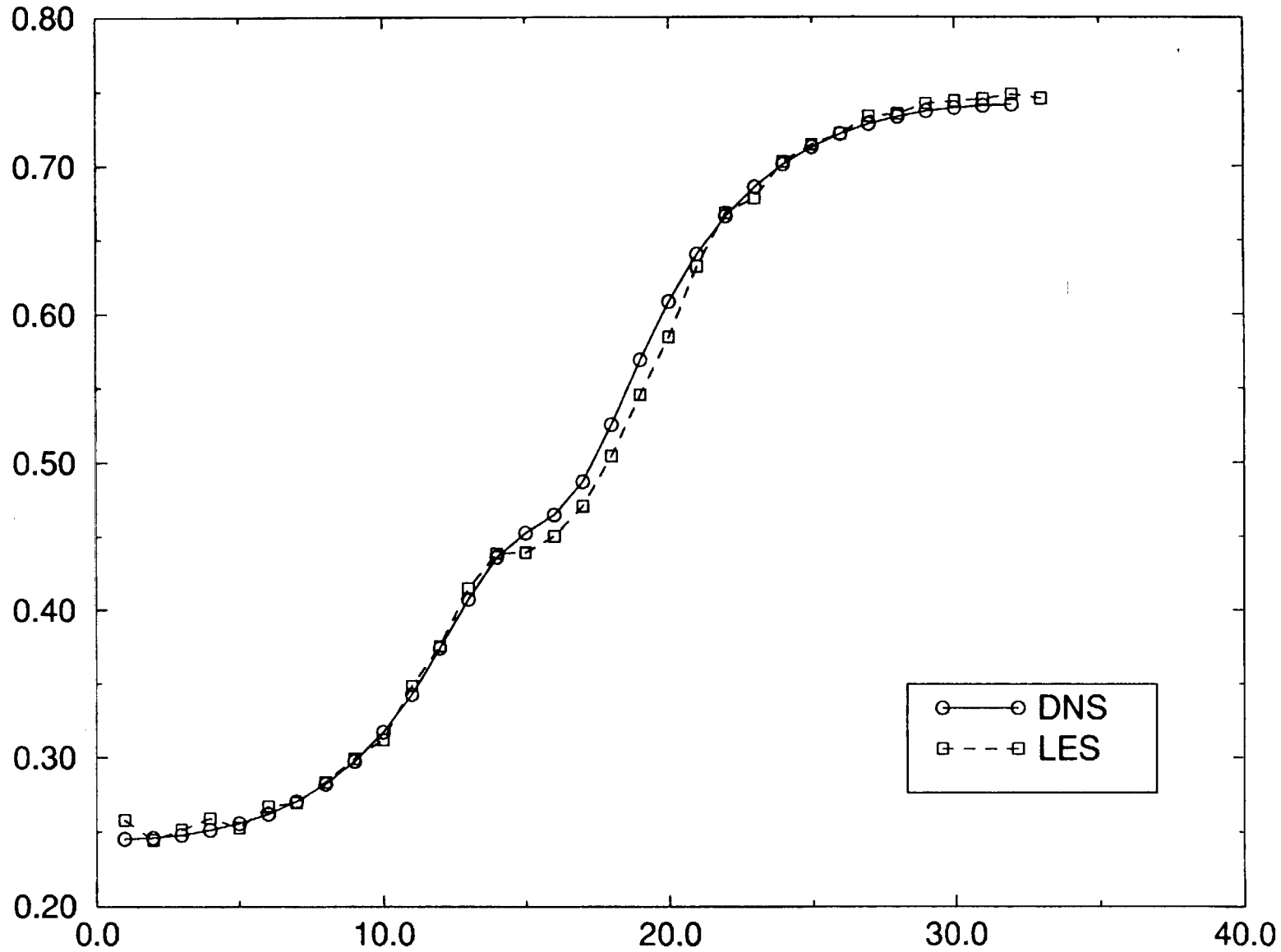

FIGURE 4(b)

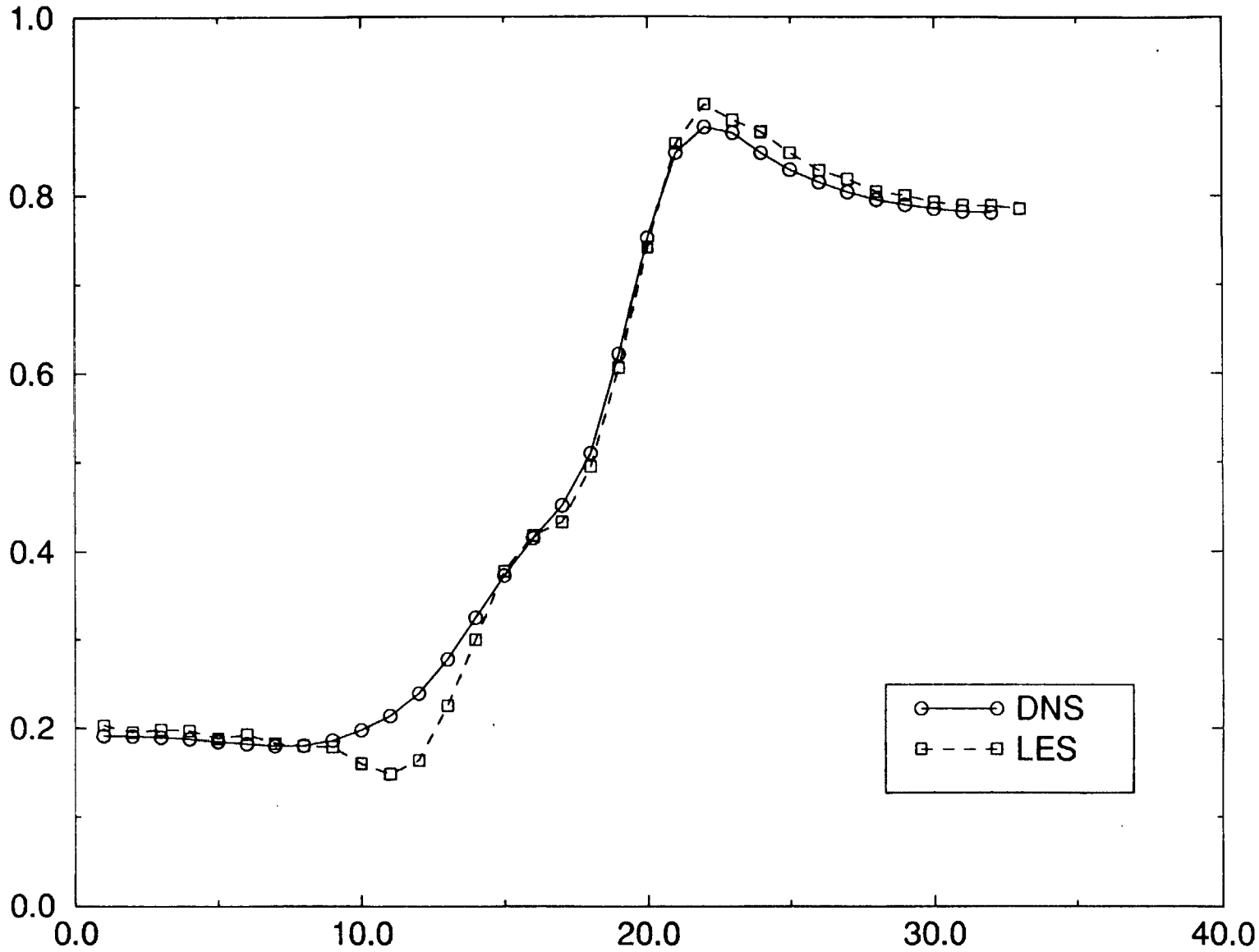

FIGURE 6(C)

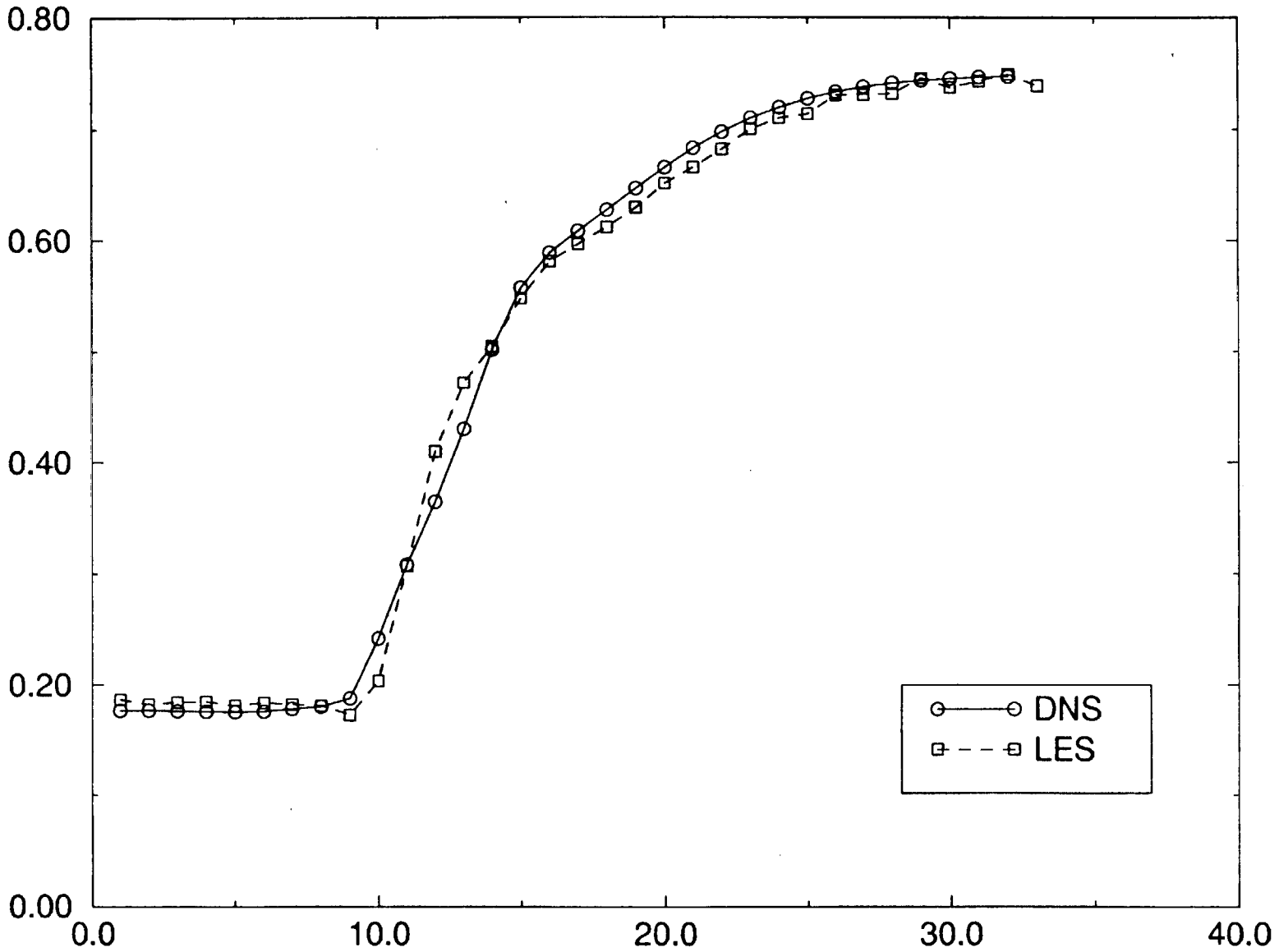

FIGURE 6d

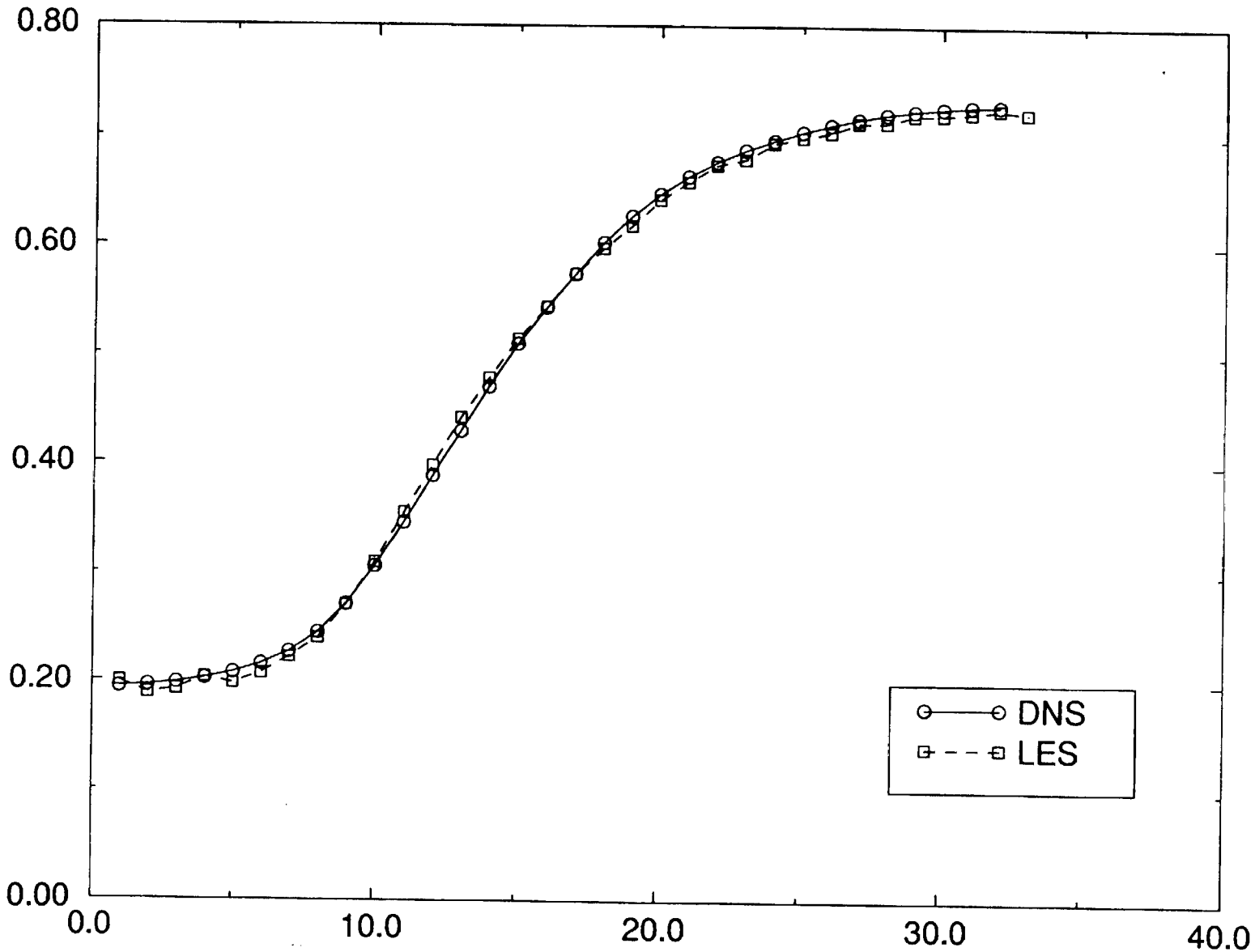

FIGURE 6(e)

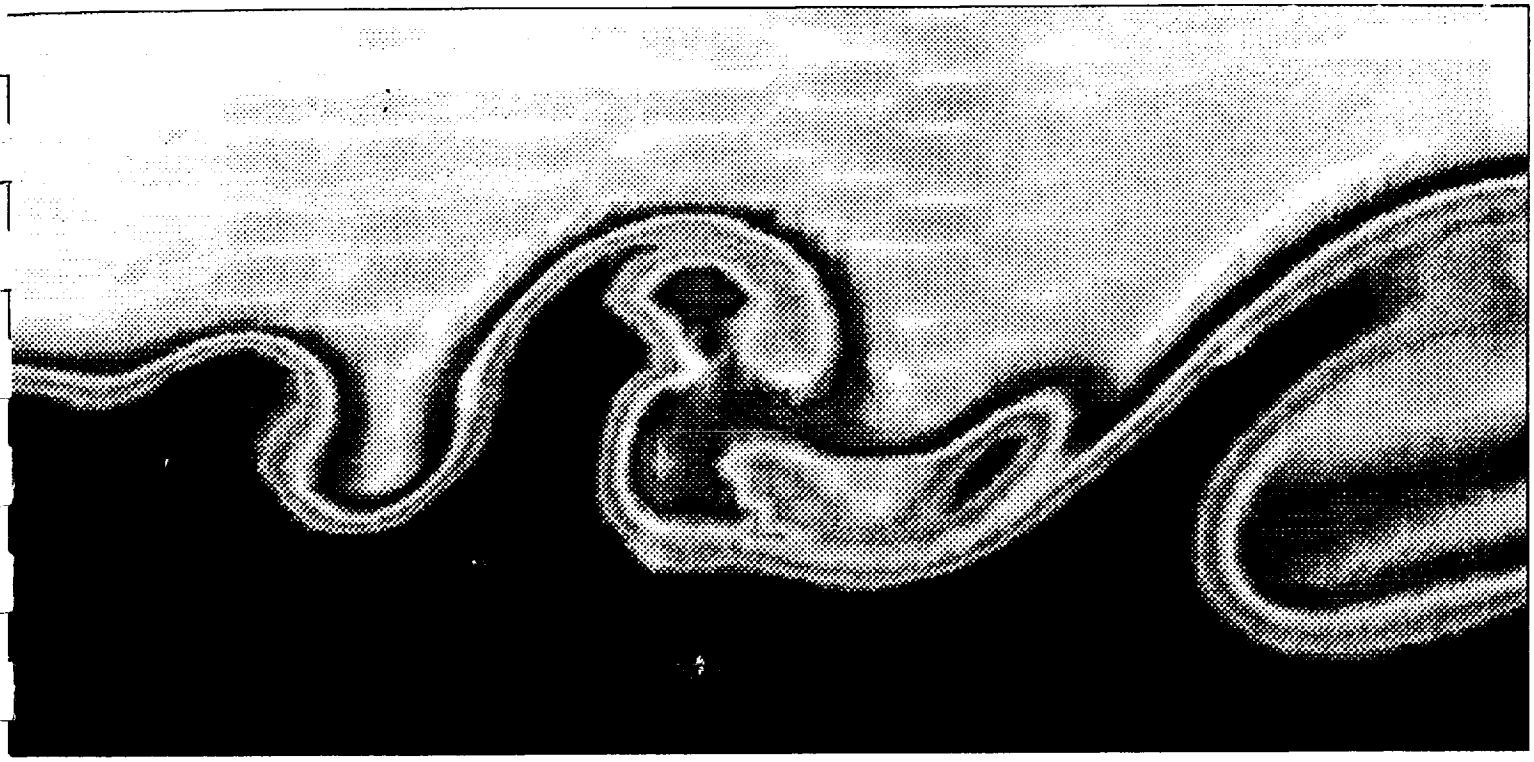

FIGURE 7(a)

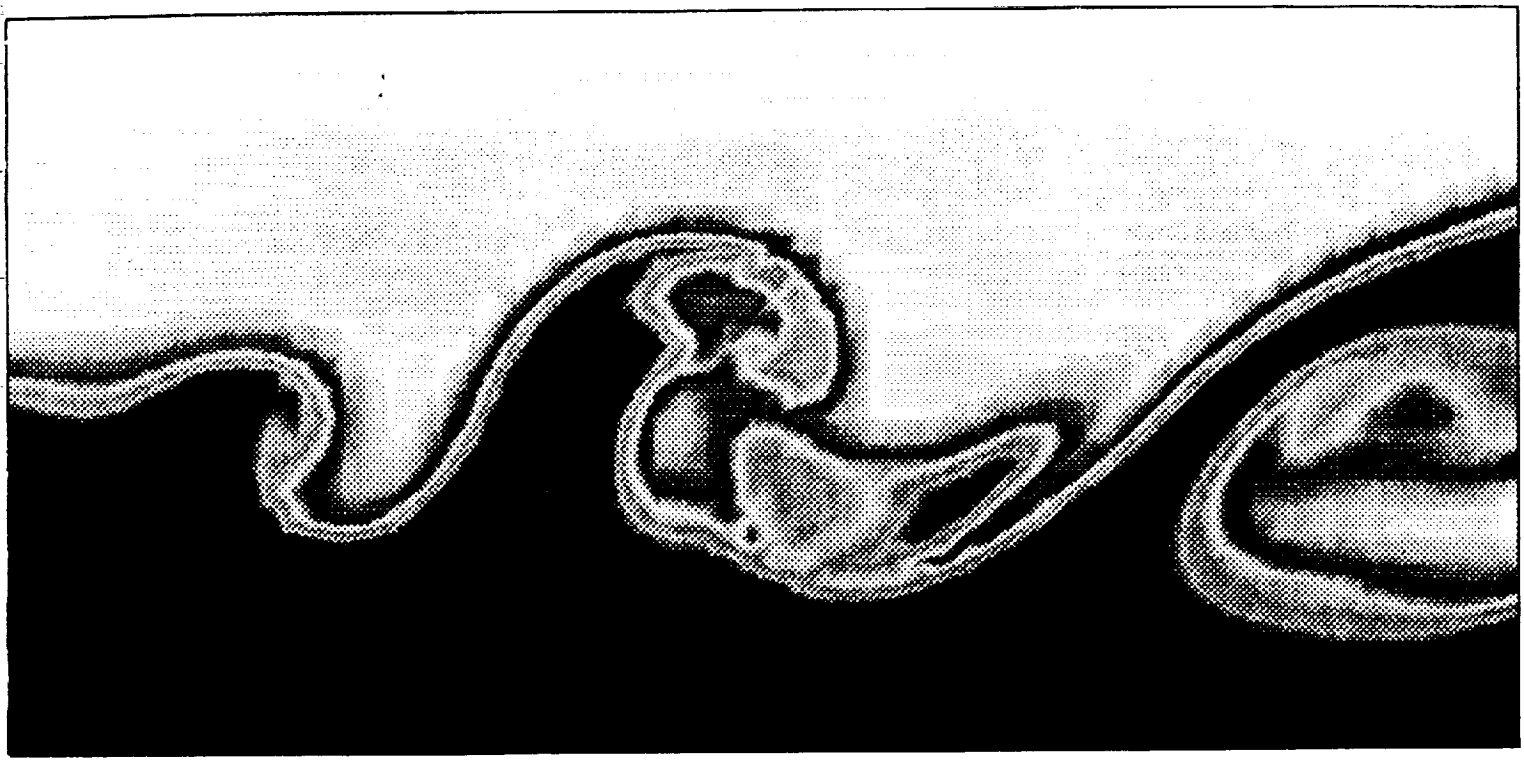

FIGURE 6 7(

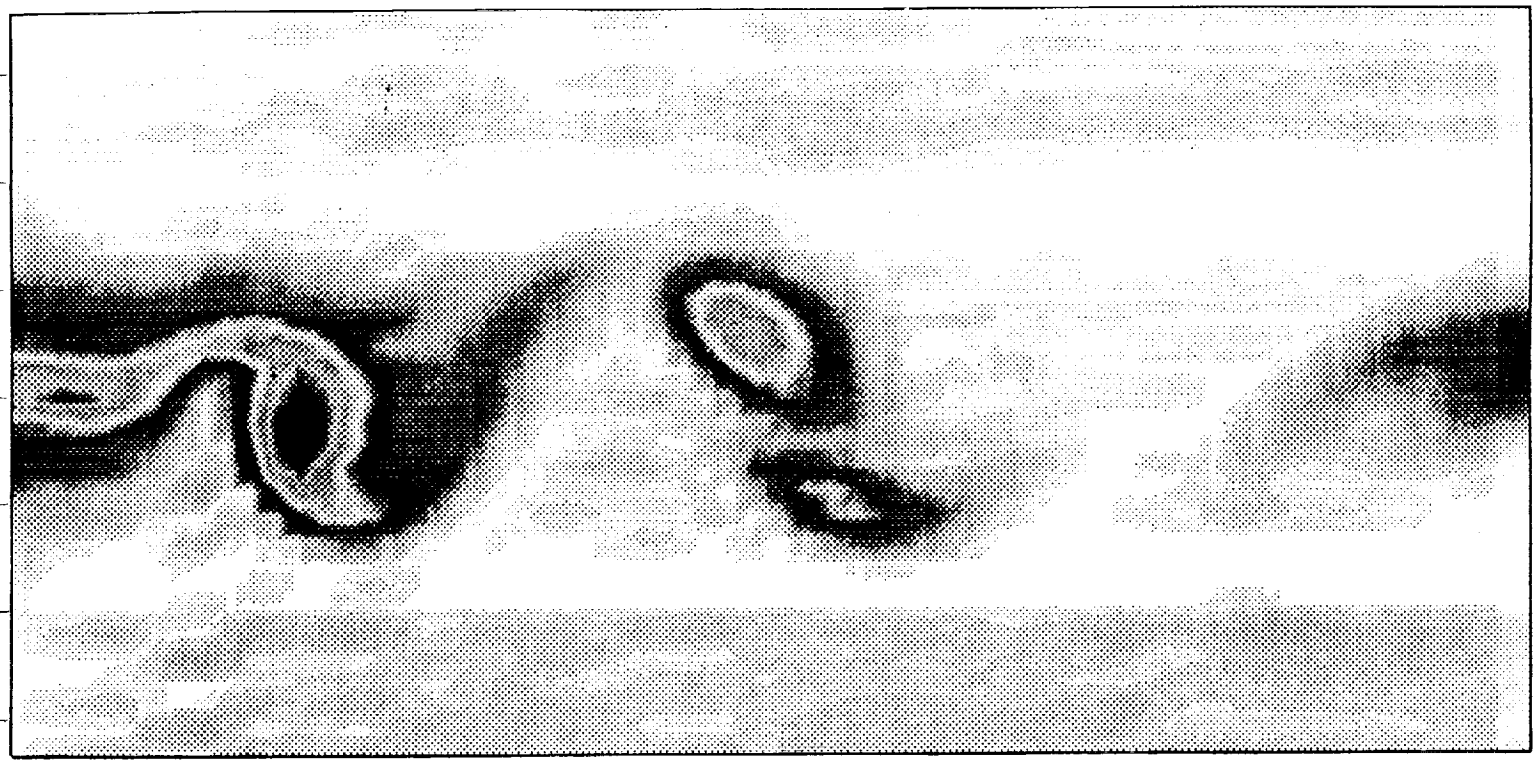

FIGURE 8(a)

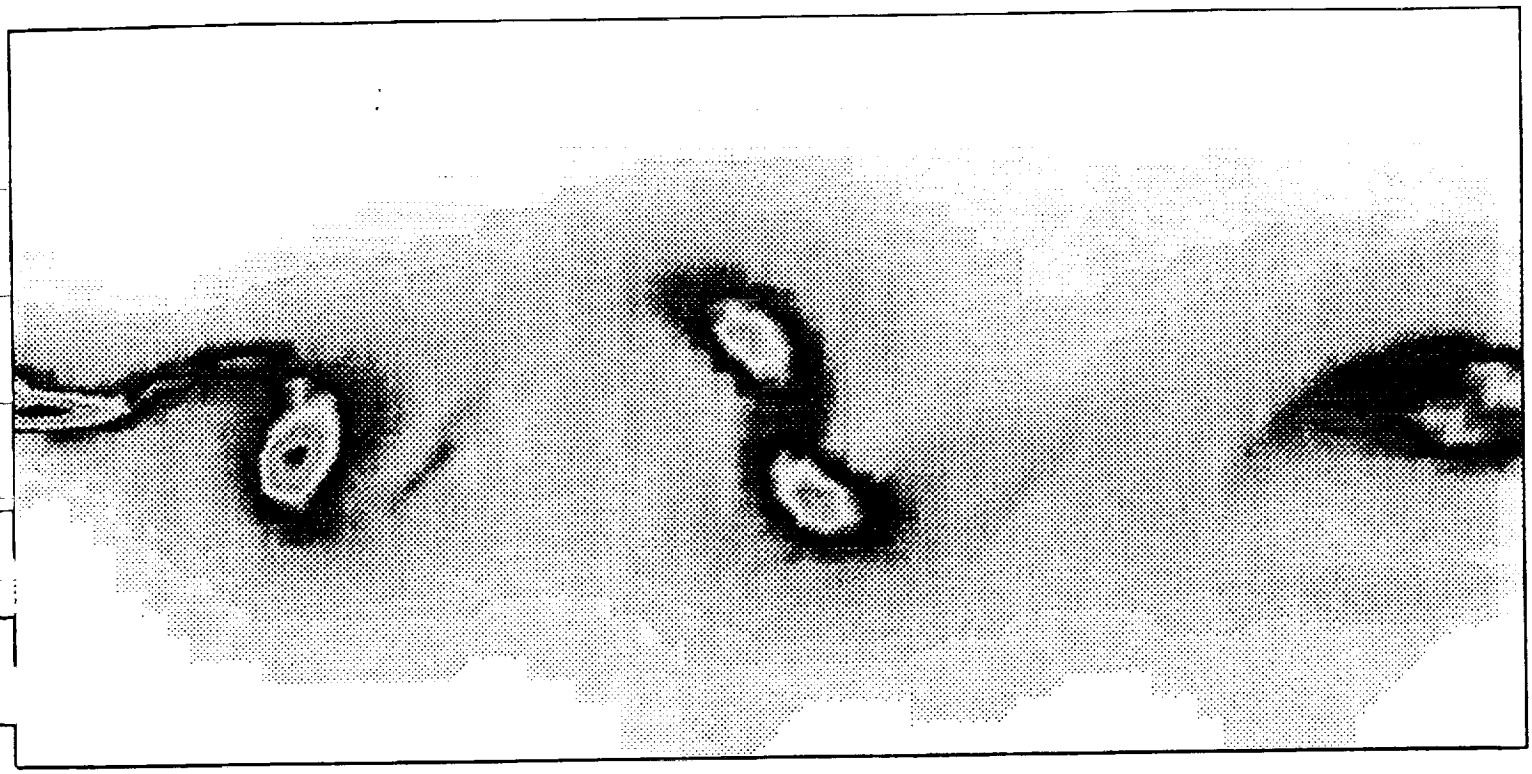

FIGURE 8(b)

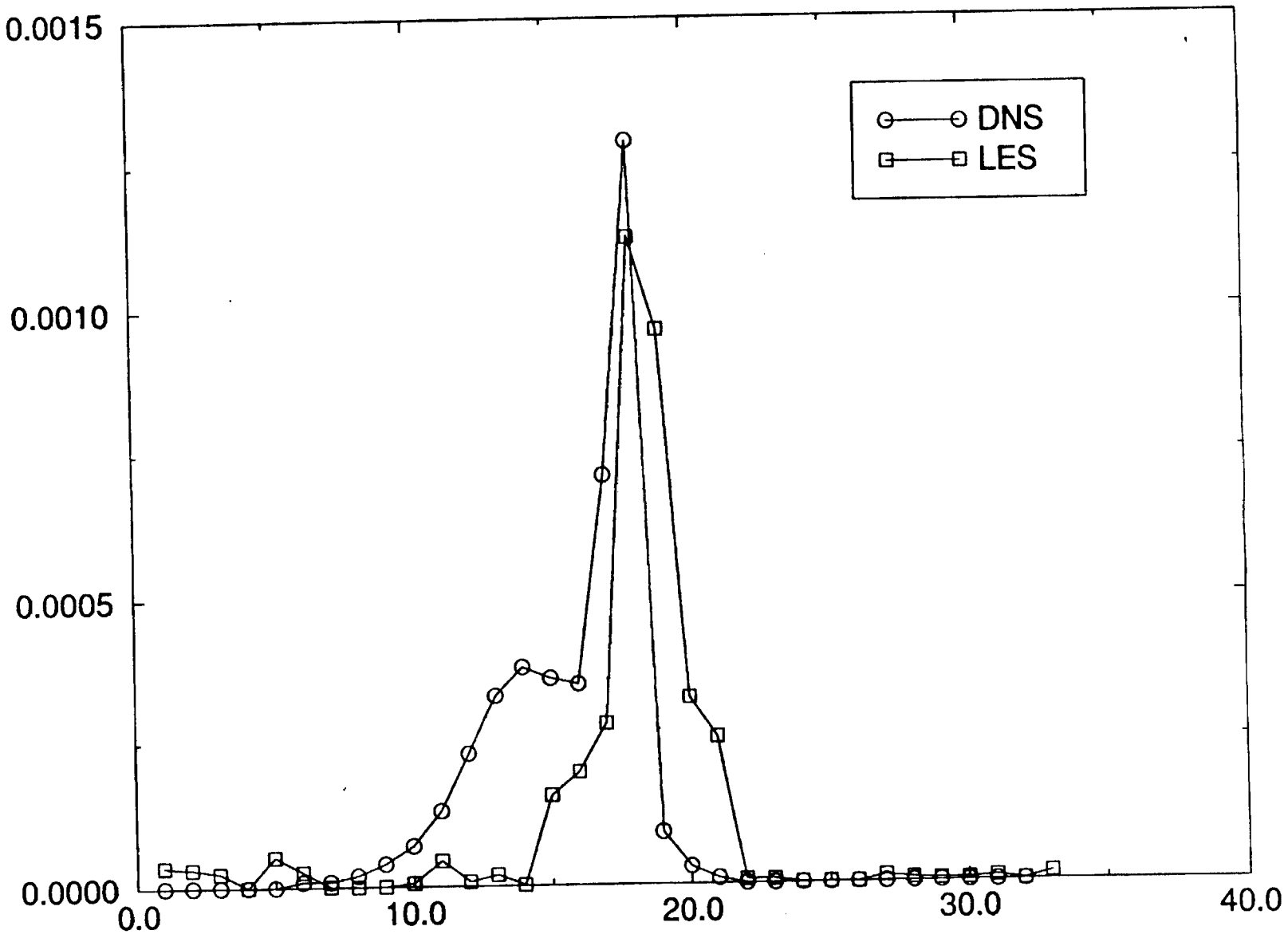
TKE: i=10, Co=0.1, Cd=0.5
0.0015
0.0010
0.0005
0.0000
0.0
10.0
20.0
30.0
40.0
DNS
LES

FIGURE 9(a)

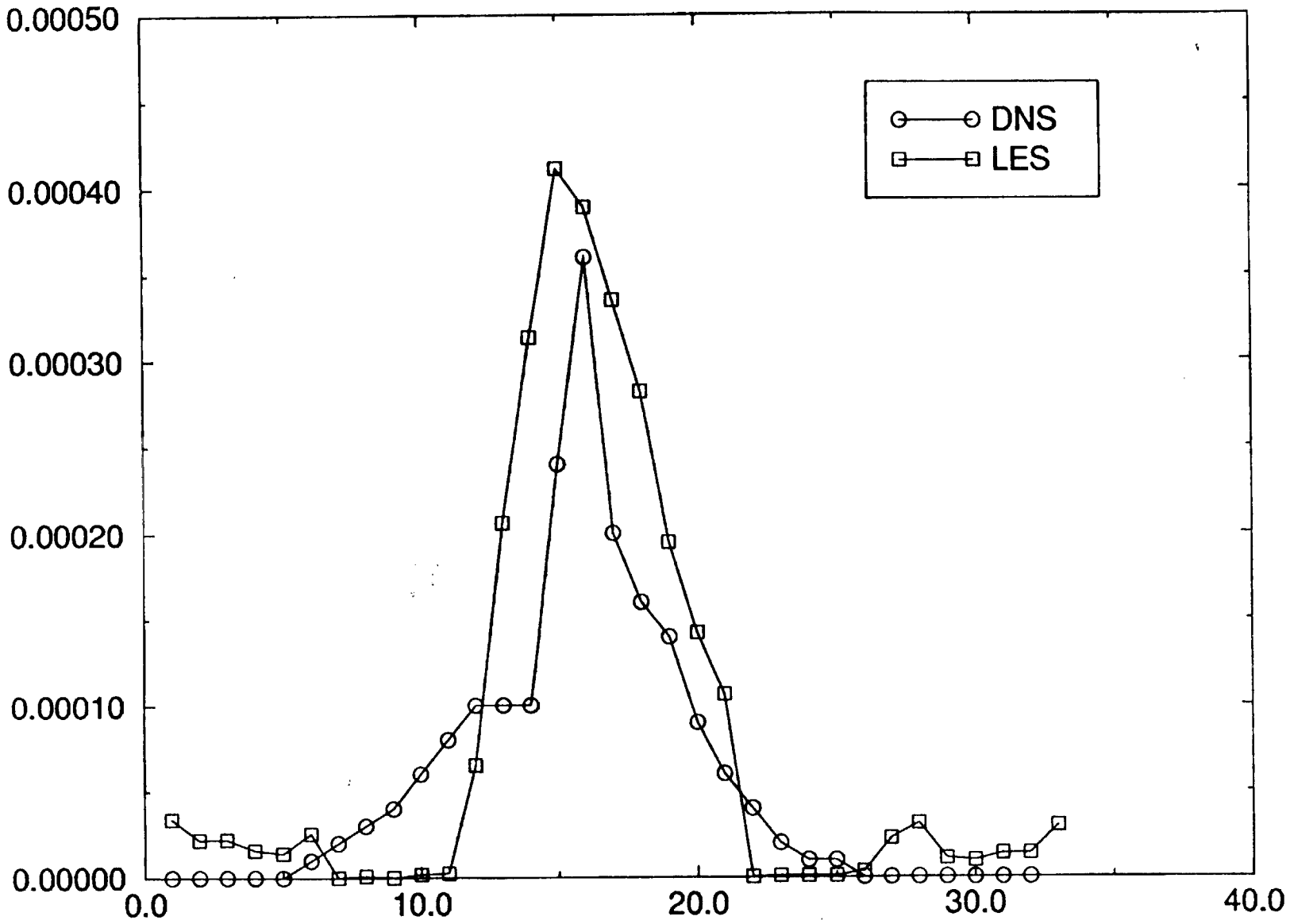
TKE: i=20, Co=0.1, Cd=0.5
0.00050
0.00040
0.00030
0.00020
0.00010
0.00000
0.0
10.0
20.0
30.0
40.0
DNS
LES

FIGURE 9(b)

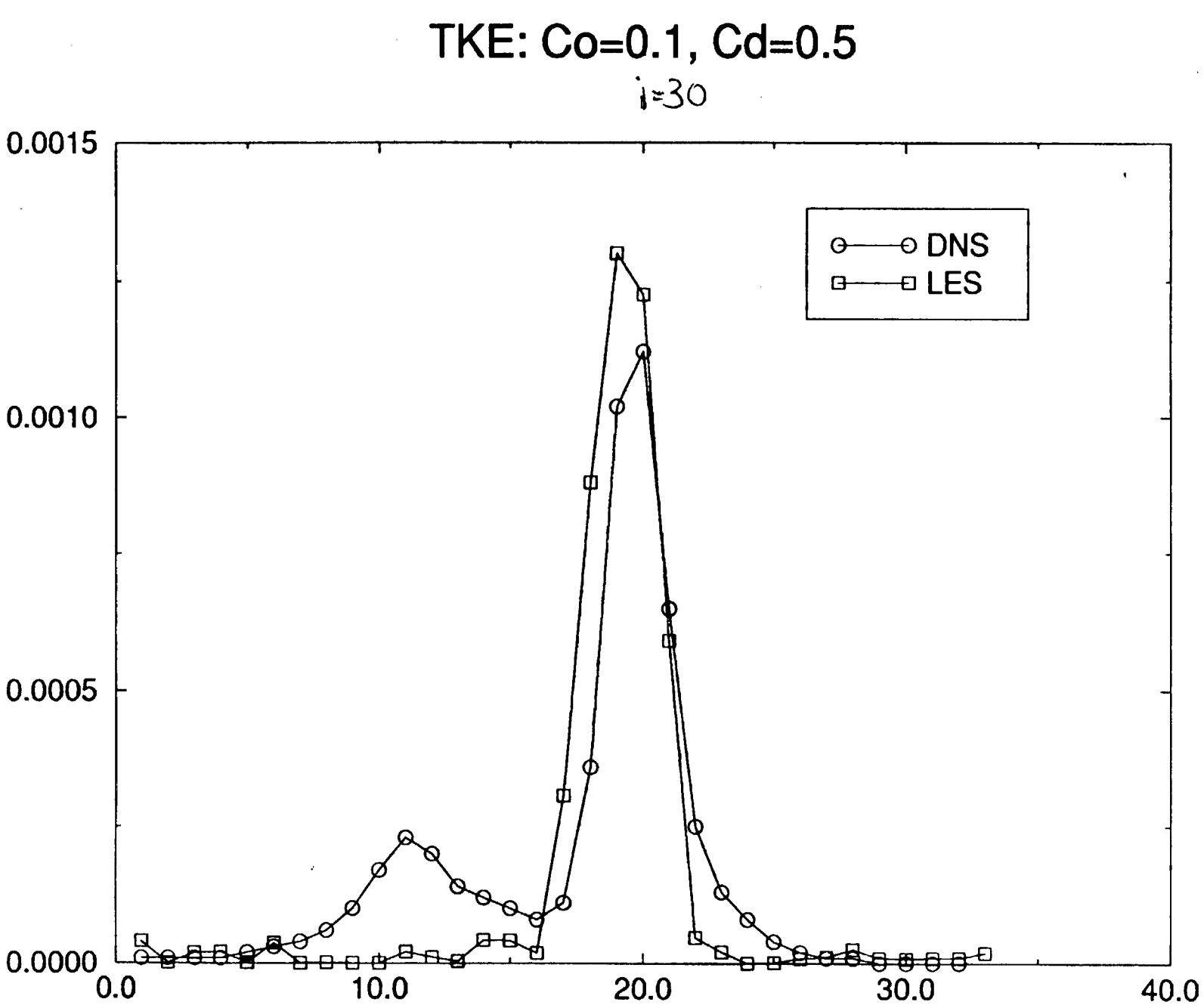
TKE: Co=0.1, Cd=0.5
i=30
0.0015
0.0010
0.0005
0.0000
0.0
10.0
20.0
30.0
40.0
DNS
LES

FIGURE 9(c)

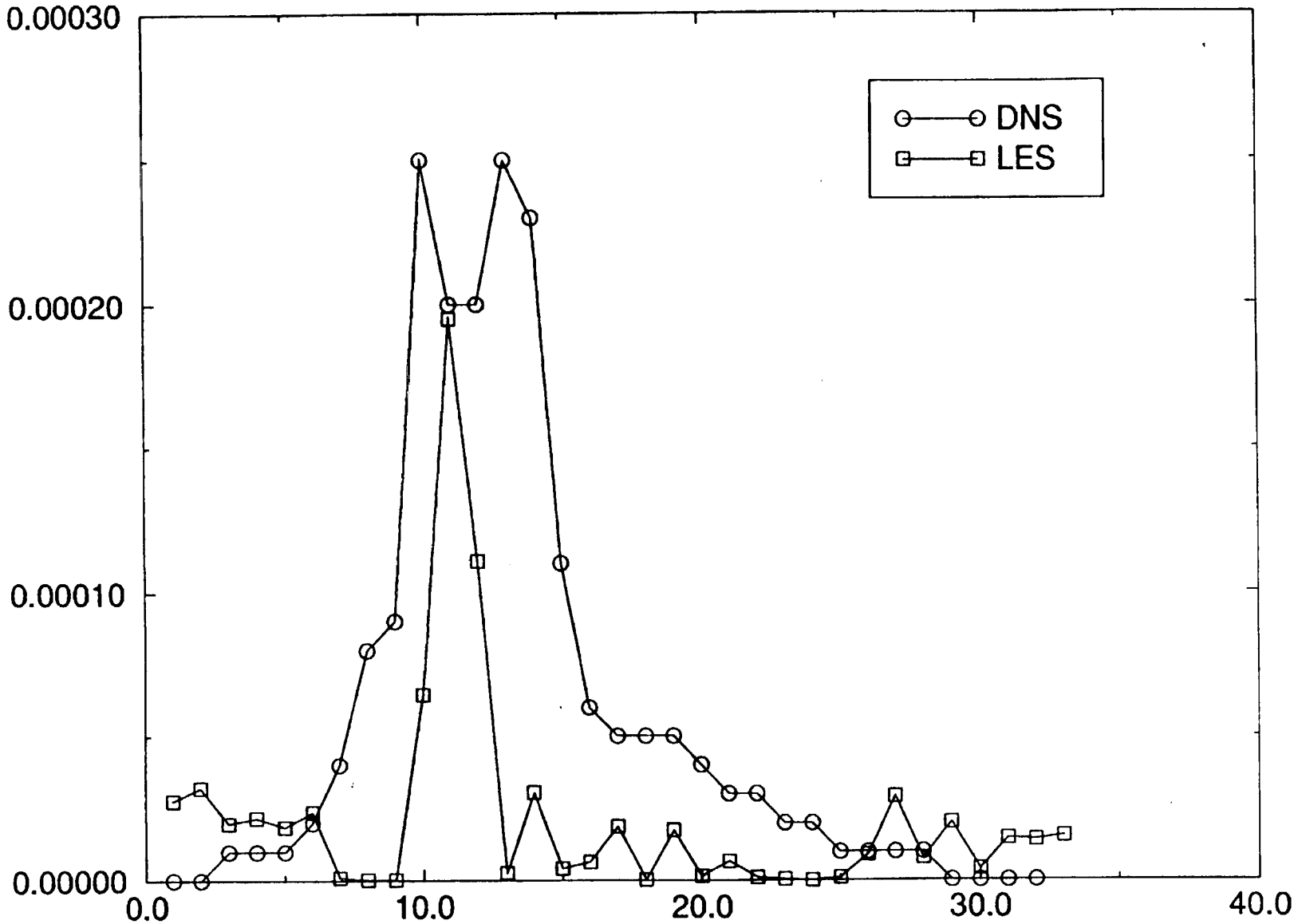
TKE: i=40, Co=0.1, Cd=0.5
0.00030
0.00020
0.00010
0.00000
0.0
10.0
20.0
30.0
40.0
DNS
LES

FIGURE 9(d)

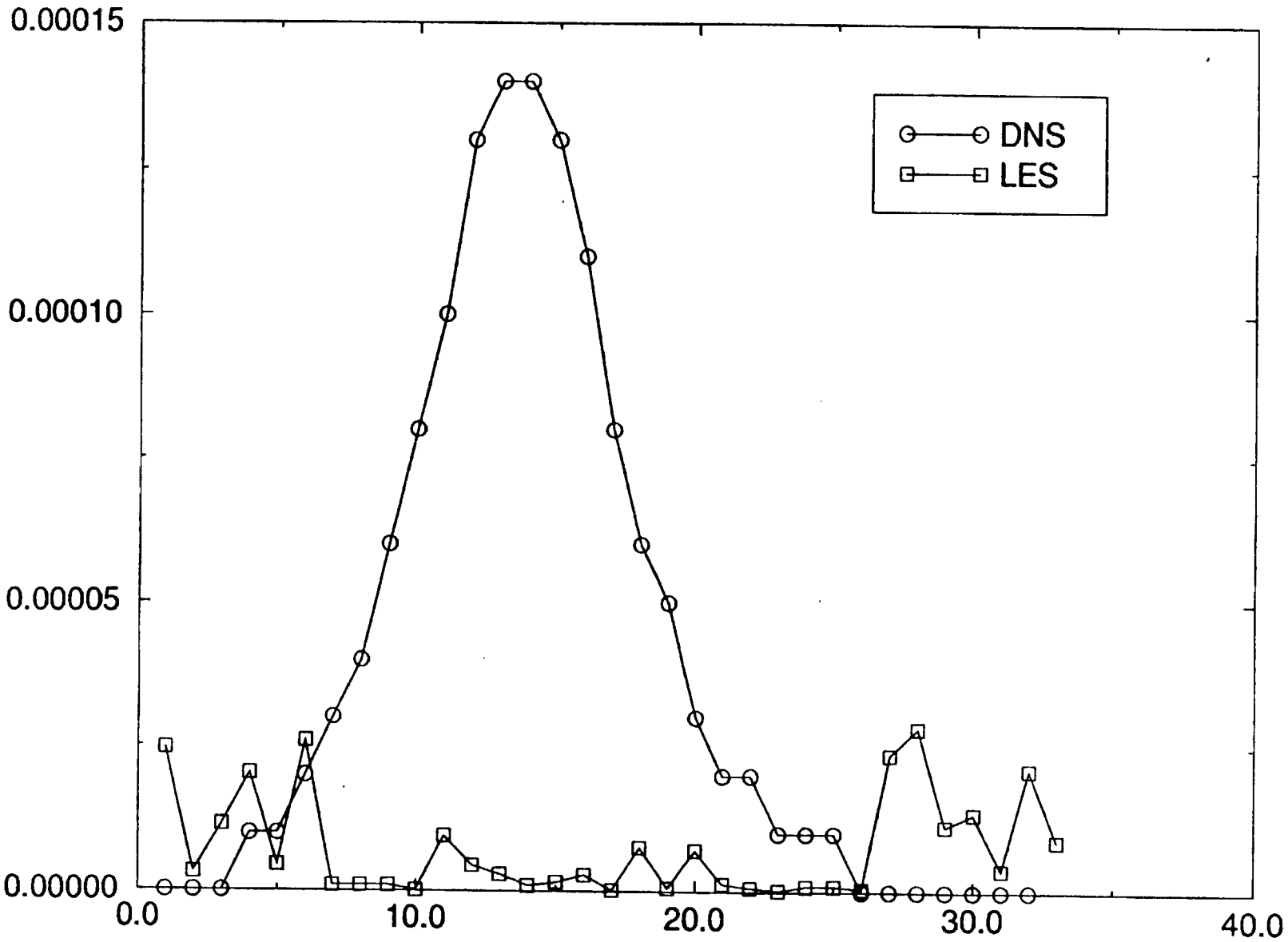
TKE: i=50, Co=0.1, Cd=0.5
0.00015
0.00010
0.00005
0.00000
0.0
10.0
20.0
30.0
40.0
DNS
LES

FIGURE 9(e)

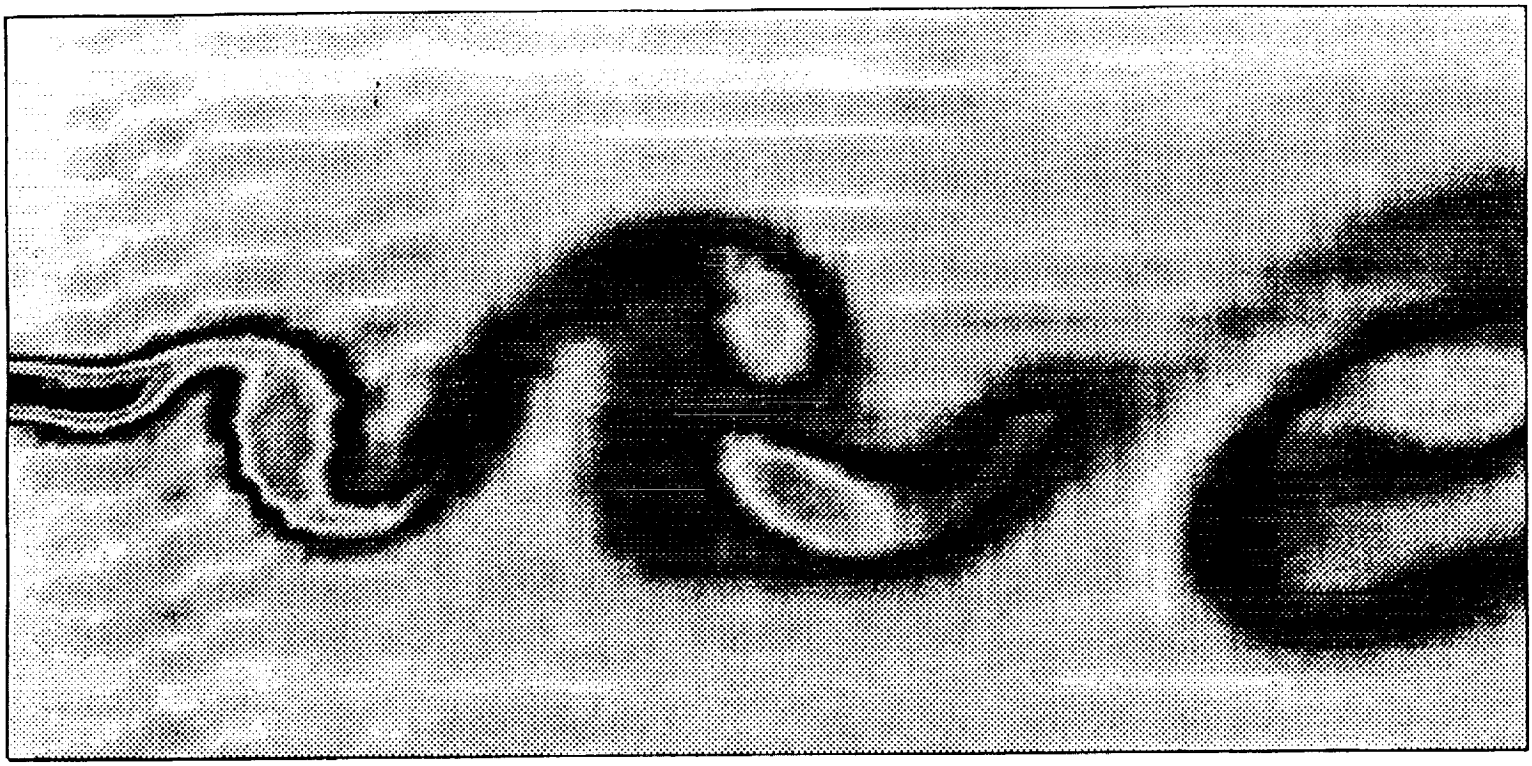

FIGURE 10(a)

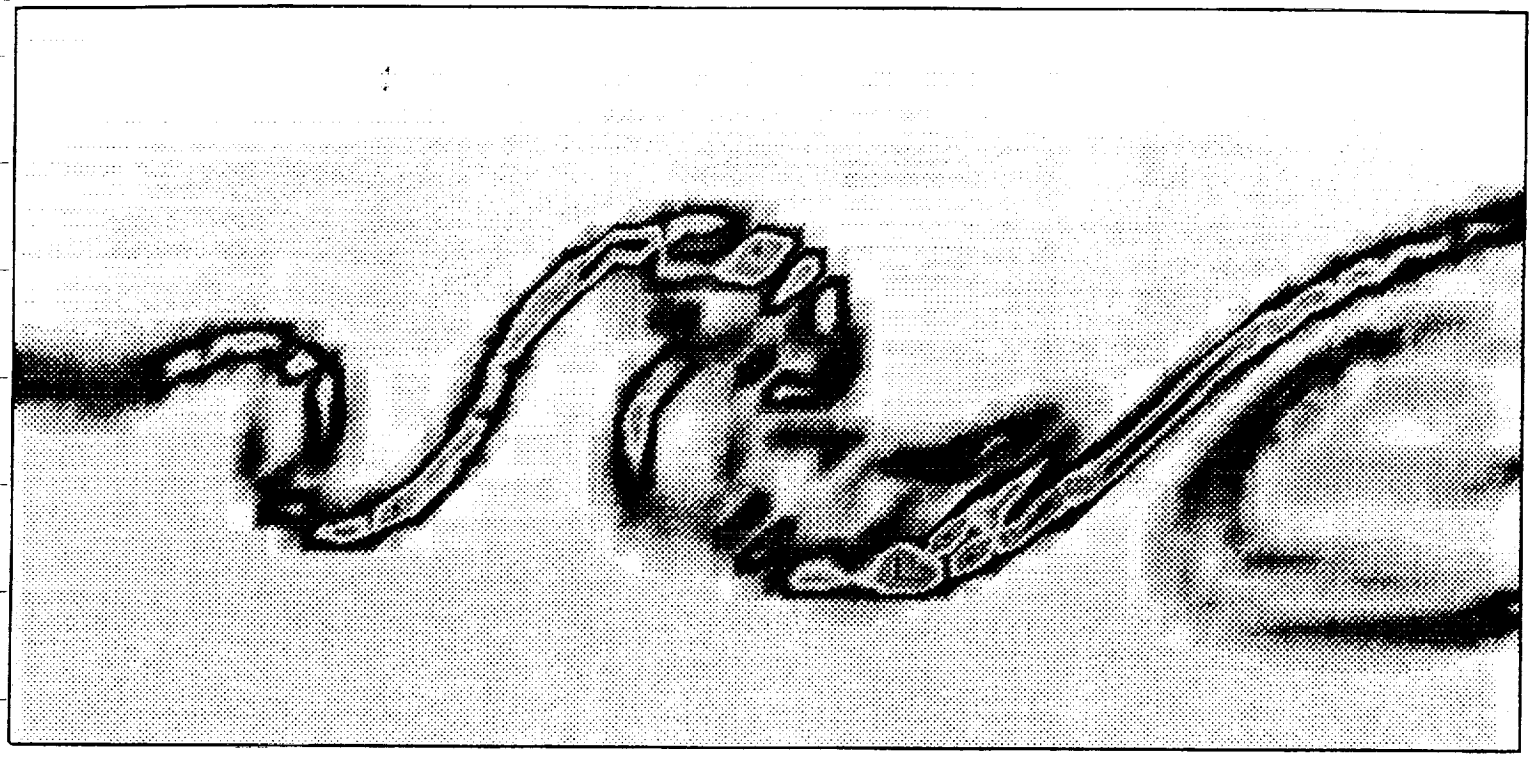

FIGURE 10(b)

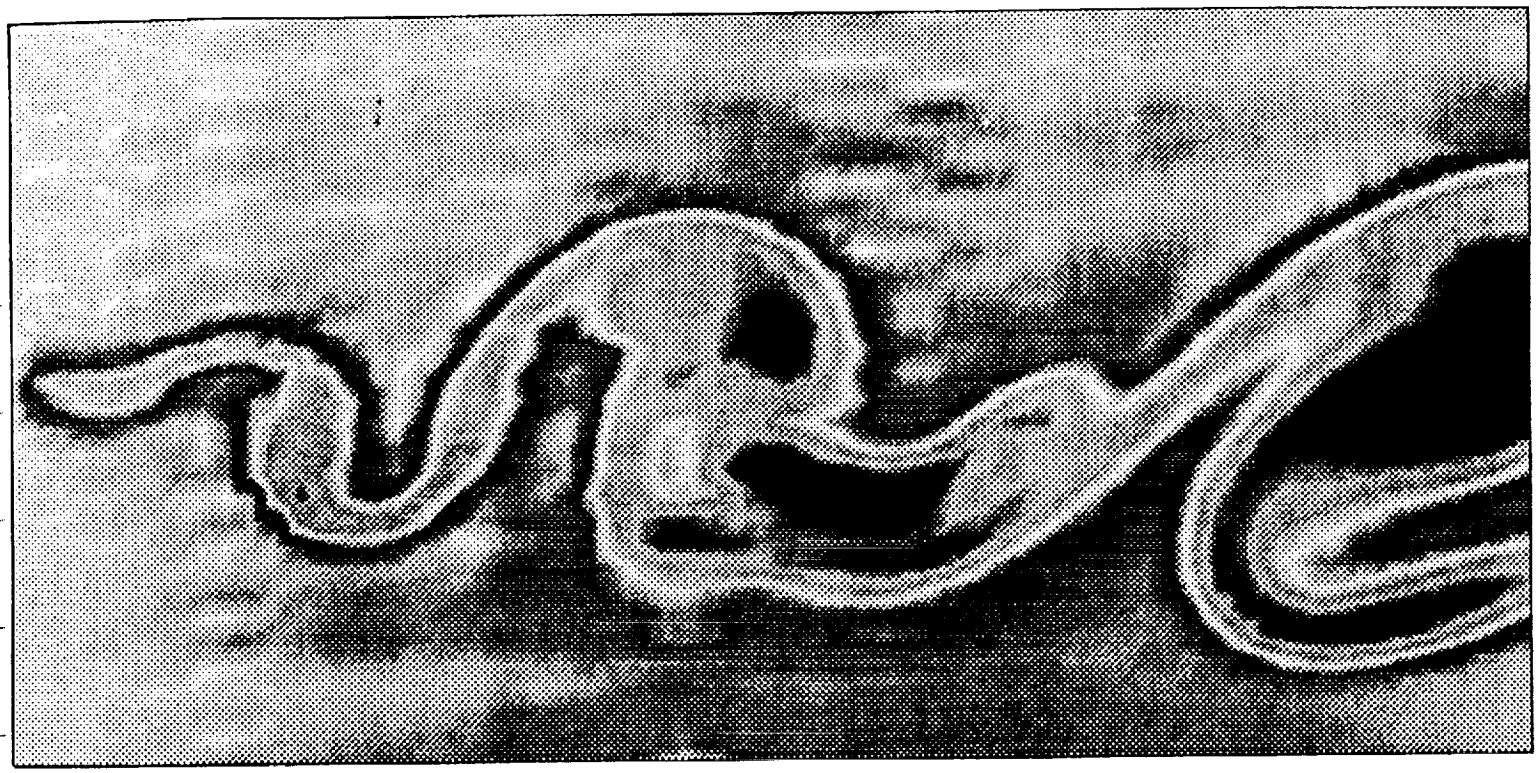

FIGURE 11(a)

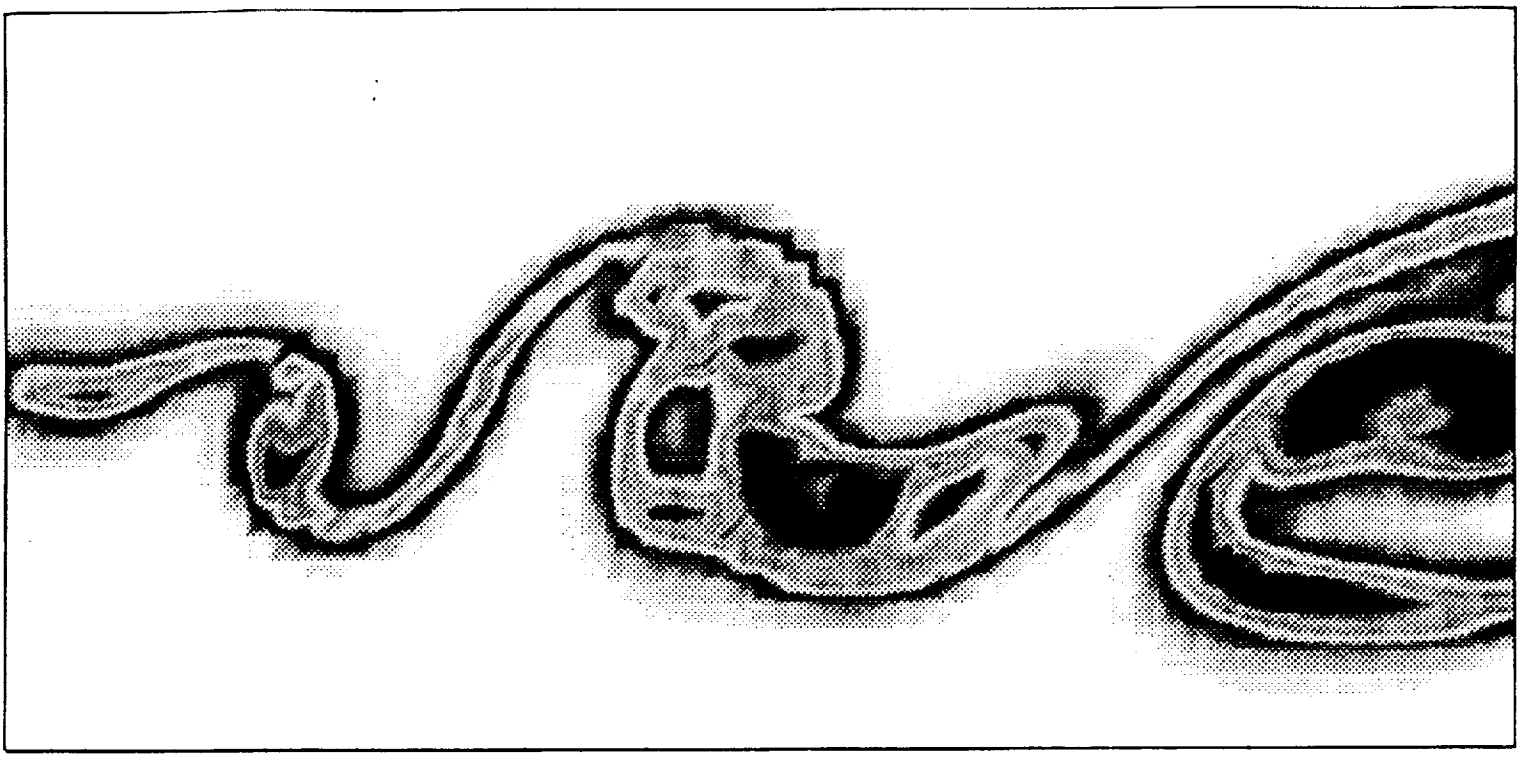

FIGURE 11(b)

Prod thickness vs x: Filtered DNS vs PDF and Mean for Da=10

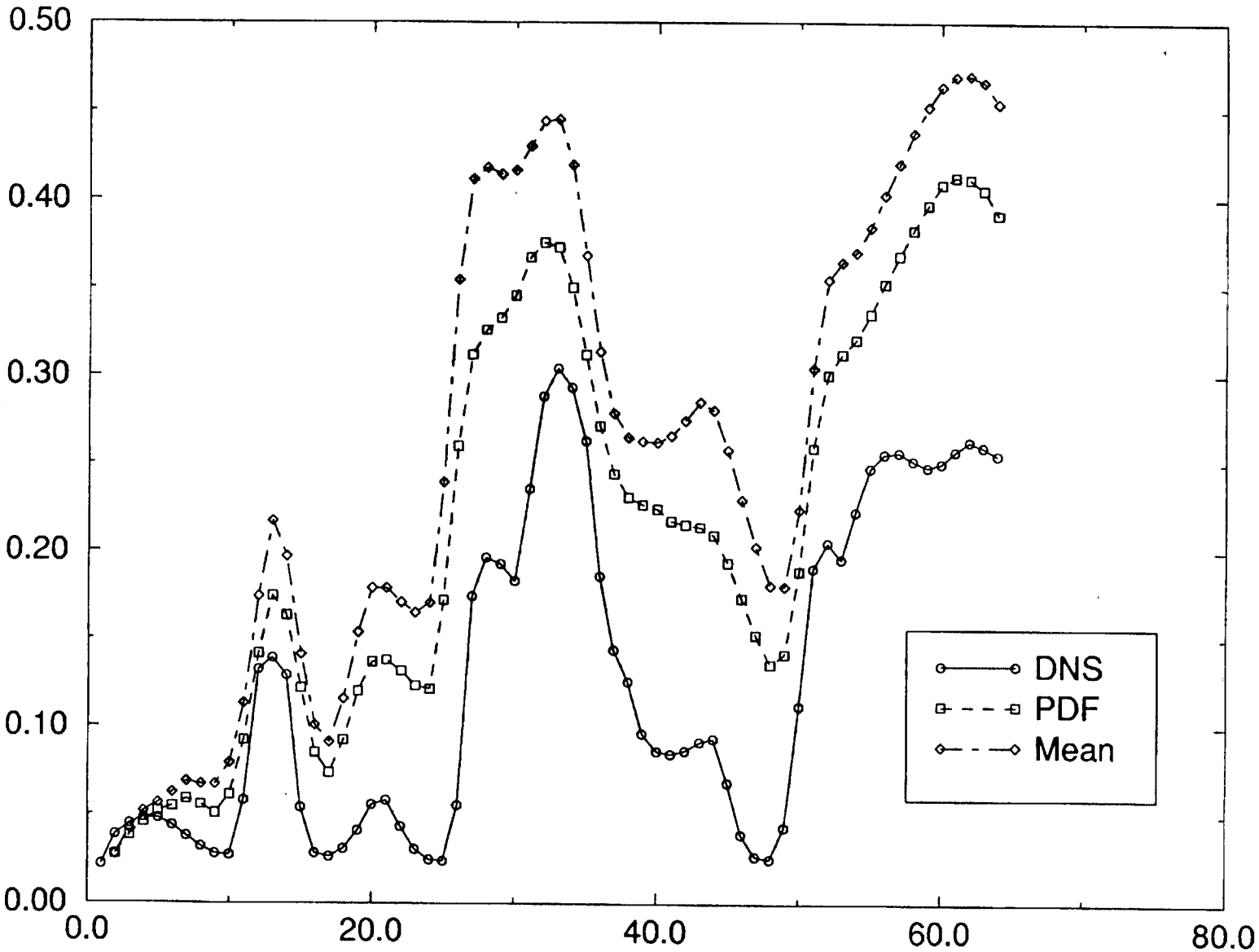

FIGURE 12

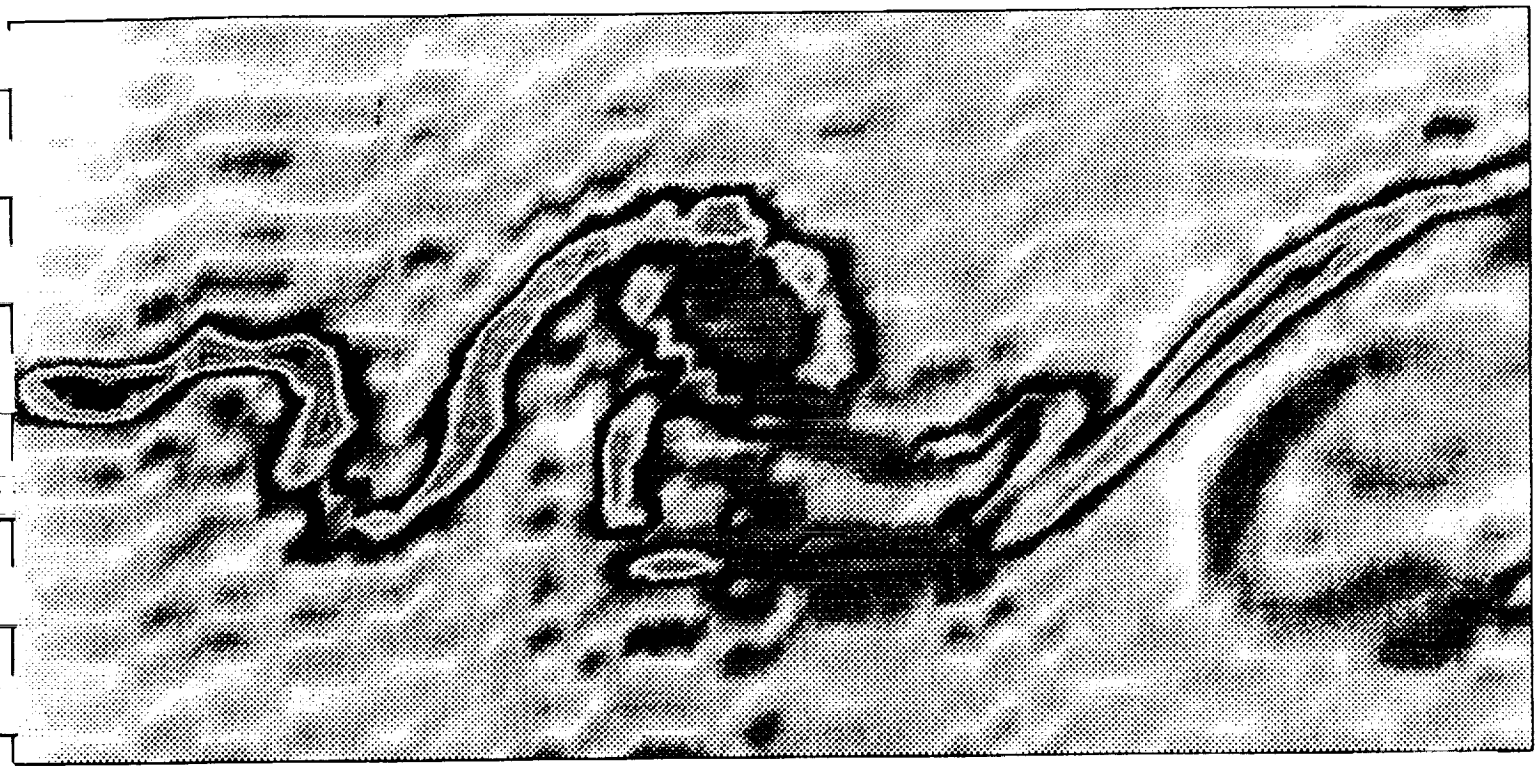

FIGURE 13 (a)

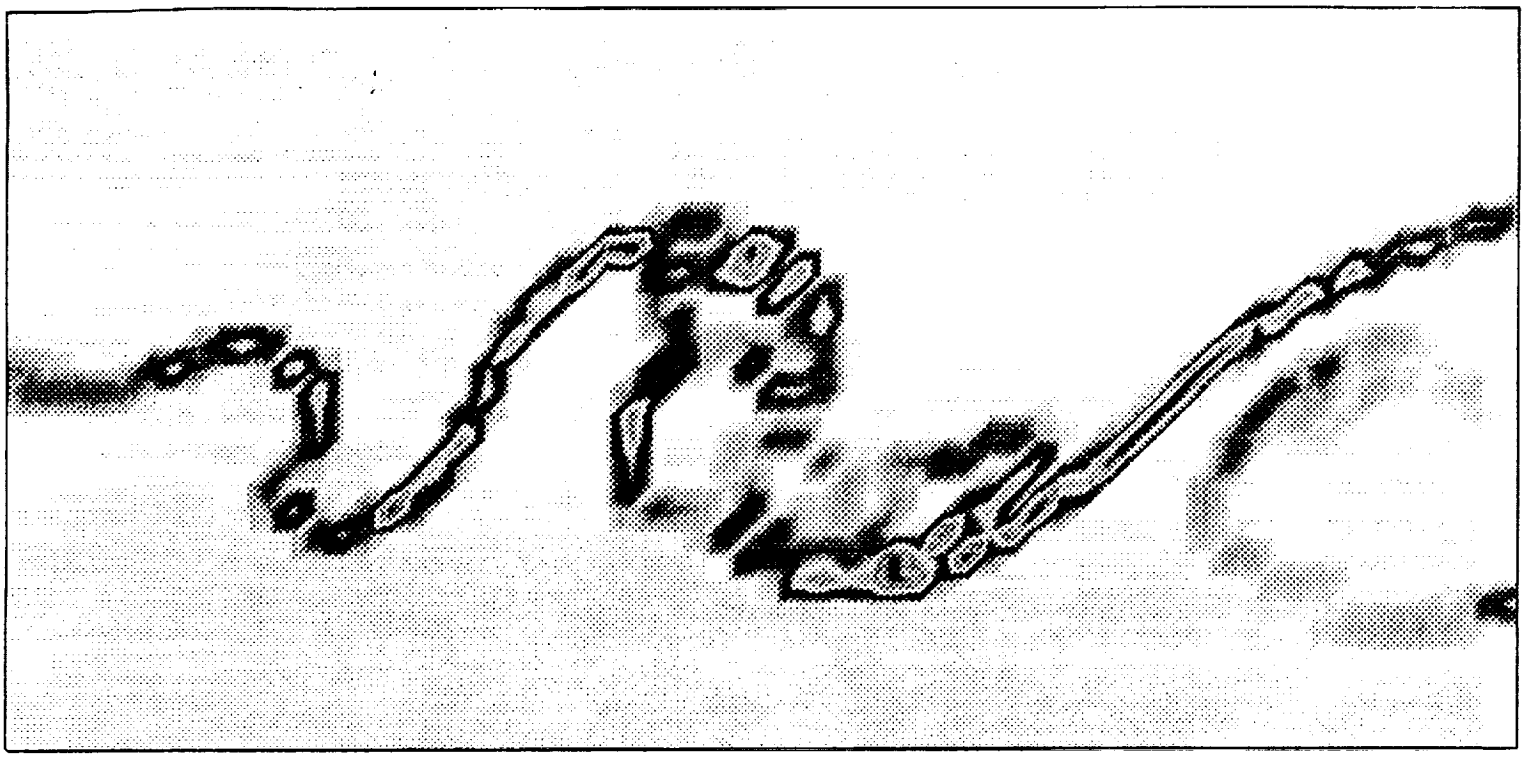

FIGURE 13 (b)

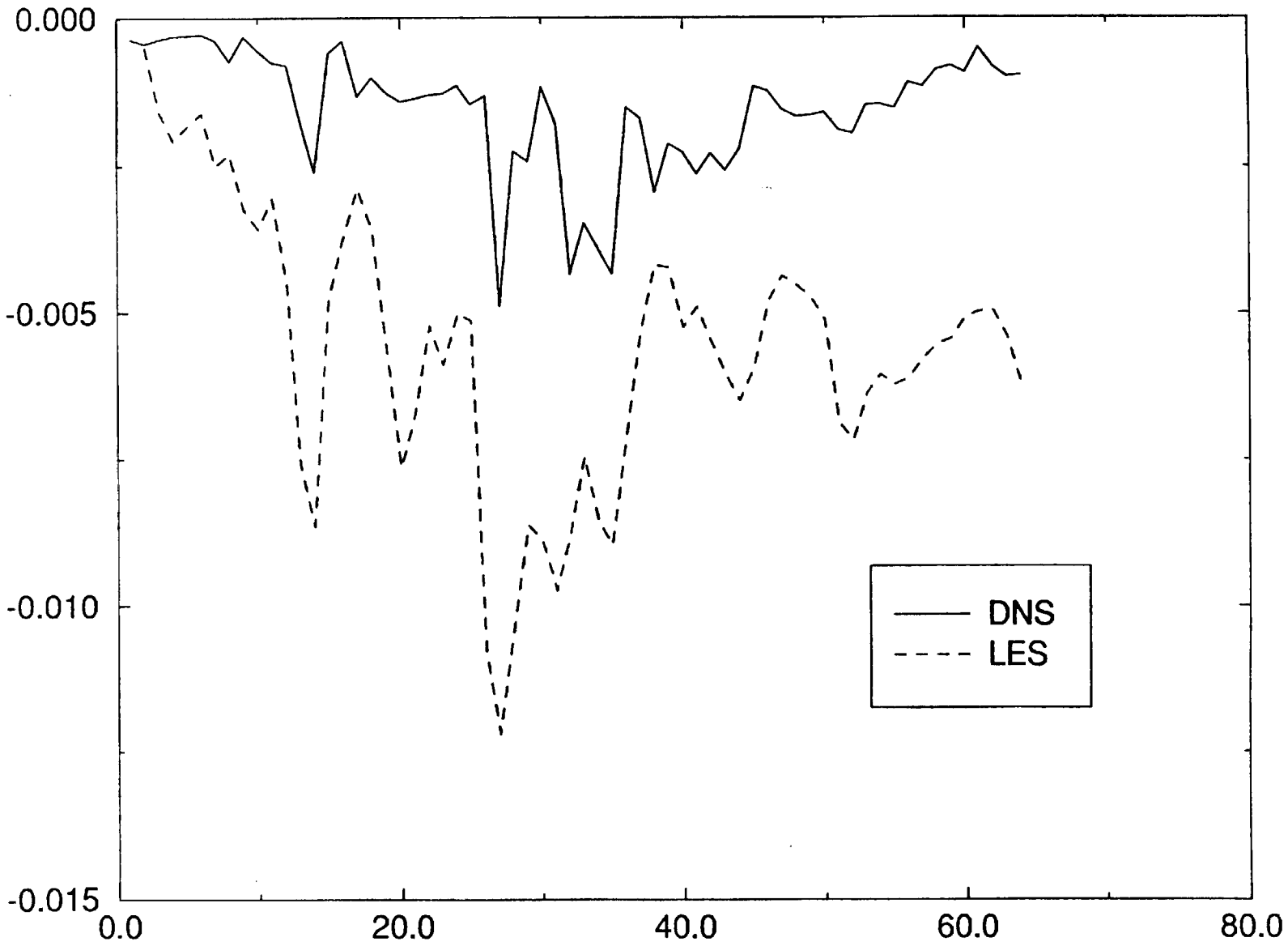
Total Covariance: Da=10
0.000
-0.005
-0.010
-0.015
0.0
20.0
40.0
60.0
80.0
DNS
LES

FIGURE 14

5 Appendix III

This appendix provides a report, albeit incomplete, in validating the use of PF generated family of PDF's in Reynolds averaging procedures. We realize that this report is incomplete and we apologize for that. However, we feel it is necessary to include this summary to show our current status in this particular aspect of our work. We are presently analyzing our results, and we hope to have this report completed in the near future.

This appendix has been prepared by Mr. George Sabini, an undergraduate Research Aid, who is a new-comer to our group and is assisting us in this project.

Modeling of Turbo-Chemical Fluctuations in a Reacting Scalar Mixing Layer

by

G. J. Sabini, S. H. Frankel, C. K. Madnia and P. Givi

Abstract

Single-point Probability Density Function (PDF) methods have proven very useful for modeling of turbo-fluctuations in statistical descriptions of turbulent reacting flows. In this work, results are presented of statistical predictions of an incompressible, turbulent, parallel mixing layer under the influence of a non-premixed, isothermal chemical reaction of the type $A + B \rightarrow$ Products. The self-similar region of the reacting layer is considered. This flow configuration has been the subject of numerous previous investigations, and abundant experimental data are available providing the basis for appraising the performance of turbulence closures. The effects of hydrodynamics on scalar transport are modeled by means of conventional turbulent closures, and the influences of scalar-scalar fluctuations are taken into account by assumed PDF methods. Based on earlier findings, several members of the *Pearson Family* of PDF's are considered: namely, a Dirichlet density for non-equilibrium chemistry flow, and a Beta density of the first kind for the flow under chemical equilibrium. The predicted results are compared with those obtained based on a joint Gaussian PDF, which has been employed in most previous analytical investigations. All the analytic results are also compared with the experimental data of Saetran *et al* (1989) and of a reacting flow and Bilger *et al* (1991) of a reacting flow under similar fluid mechanical-chemical conditions. The outcome of this comparative study indicates that the Pearson family of PDF's are indeed superior for predicting the influence of turbulence on the reactant conversion rate. In particular, it is shown that the Dirichlet distribution if parameterized with the scalar energy, provides the most reasonable means of modeling the joint PDF of the scalar. The extent of agreement improves as the magnitude of the Damköhler number is increased. This is demonstrated by detailed comparisons of predicted results with laboratory data.

Key Words:

Scalar Mixing Layer, Turbulent Reacting Flows, Dirichlet Distribution, Probability Density Function.

Introduction:

In our previous works (Madnia *et al.*, 1991a, Frankel *et al.*, 1992) we have demonstrated that the Beta density provides a very good means of approximating the probability distribution of a conserved scalar quantity in both homogeneous and nonhomogeneous turbulent flows. Closed form analytic expressions have been obtained for the statistics of the passive scalar field, and with the assumption of fast chemistry, for the reactive scalar field as well. These relations are valid for any value of the stoichiometric coefficient.

In this work we intend to investigate the validity of our model in predicting the statistical behavior of the passive and reactive scalar fields in a homogeneous mixing layer, often referred to as a thermal or scalar mixing layer. Results obtained with our model will be compared to the experimental data of Saetran *et al.* (1991). In order to obtain the passive scalar statistics we shall follow the eddy viscosity approach detailed by Libby (1975) to solve the passive scalar mean and variance transport equations in this simple flow. With the specification of the first two moments of the conserved scalar our model is capable of predicting the equilibrium statistics of the reacting scalar field.

We will then extend this work to treat nonequilibrium, that is, finite rate, chemically reacting flowfields. This will be done by assuming a Dirichlet distribution for the joint PDF of the reacting scalars. For the second order reaction under consideration here, this PDF is also known as the joint Beta PDF. The specification of this PDF requires the knowledge of first moments of both of the reactants and turbulent scalar energy Q (which is the sum of the scalar variances), or the reactant means and covariance. The information with regard to these statistics is determined from the solution of modeled transport equations. One of the pleasing features of the choice of the Dirichlet PDF is that it results in simple closed form expressions for both the chemical source term and the chemical source/sink terms appearing in the mean and scalar energy transport equation. As before all results of the investigation obtained with the PDF model will be compared to the experimental data of Saetran *et al.* (1991), as well as to the solution of the same transport equations using a Joint Gaussian PDF, which has been employed in previous calculations.

Description:

A scalar mixing layer is formed when traditional grid generated turbulence is augmented with a scalar gradient. This can be in the form of either temperature, obtained as a result of heating half the grid (Libby, 1975) or by including two different species (Bilger, 1991). This simple flow configuration, because of its convenience, is of interest to study in order to gain insights and test modeling assumptions for more complex flows, such as nonhomogeneous shear layers. Experiments have been conducted by a number of researchers in order to study the statistical behavior of the passive scalar (Libby, 1975; LaRue and Libby, 1981; LaRue *et al.*, 1981, Gibson *et al.*, 1989). Reacting scalar measurements were obtained by Saetran *et al.* (1989) and recently discussed by Bilger *et al.* (1991). Theoretical and modeling contributions originated with Libby (1975), Newman *et al.* (1981) and Elghobashi and Launder (1983), and concentrated on traditional moment methods for closure. These numerous investigations have been concerned with predicting the behavior of the scalar mean and intensity. Particular difficulties have been noted in predicting the peak intensities for the passive and reacting scalars (Saetran *et al.*, 1989). When dealing with reacting flowfields the added difficulties encountered by the nonlinear chemical source terms make PDF methods the method of choice in such situations (Pope, 1985,1991; Givi, 1989).

Libby (1975) discusses the diffusion of temperature in the downstream region of a partially heated grid. In order to predict the passive scalar statistics in the mixing layer he utilizes the eddy viscosity assumption to obtain an analytic solution for the conserved scalar mean and to close the transport equation for the conserved scalar variance. With the grid flow assumptions of a homogeneous velocity field, temporally invariant statistics, high Reynolds number, and boundary layer assumptions he comes up with an ordinary differential equation for the passive scalar variance. This equation has the two usual constants in front of the turbulent fluctuation and dissipation terms which are normally chosen to provide a best match to experimental results (Spalding, 1972). This linear equation is discretized using central differences and the resulting linear system of equations is solved using a tridiagonal solver.

With the provision of the conserved scalar mean and variance, knowledge of the conserved scalar PDF would allow us to predict the limiting values for the reacting scalar statistics. Frankel *et al.* (1992) (see also Madnia *et al.*, 1992) used a Beta density and obtained closed

form, analytic expression for the maximum rate of reactant conversion in a nonhomogeneous shear layer. The model predictions compared favorably with those obtained from DNS. The derivations of the analytic expression for the statistics of the reacting scalar are rather involved (see Frankel, 1992). Here, we only present the final results for the second moment of the reacting scalar,

$$< A^2 >= \frac{f_s^\alpha (1-f_s)^{\beta-2}}{B(\alpha,\beta)} \left[\frac{\alpha+1-f_s(\alpha+\beta+2)}{(\alpha+\beta)(\alpha+\beta+1)} \right] + \frac{(1-\mathcal{I}_{f_s}(\alpha,\beta)}{(1-f_s)^2} \left[f_s^2 - \frac{2\alpha f_s}{(\alpha+\beta)} + \frac{\alpha(\alpha+1)}{(\alpha+\beta)(\alpha+\beta+1)} \right]$$

$$< B^2 >= \frac{f_s^{\alpha-2} (1-f_s)^{\beta}}{B(\alpha,\beta)} \left[\frac{f_s(\alpha+\beta+2)-(\alpha+1)}{(\alpha+\beta)(\alpha+\beta+1)} \right] + \frac{\mathcal{I}_{f_s}(\alpha,\beta)}{f_s^2} \left[f_s^2 - \frac{2\alpha f_s}{(\alpha+\beta)} + \frac{\alpha(\alpha+1)}{(\alpha+\beta)(\alpha+\beta+1)} \right]$$

Here, $B(\alpha,\beta)$ is the Beta function, and α and β are related to the first two moments of the random field (Frankel *et al.*, 1991). $\mathcal{I}_{f_s}(\alpha,\beta)$ is the Incomplete Beta Function, and f_s denotes the stoichiometric value of the Shvab- Zeldovich variable, f. For unity normalized concentrations at the free streams, $f_s = 0.5$. Thus, with these formulas for reacting scalar mean and variance we can compare our fast chemistry predictions with the experimental data of Saetran *et al.* (1989). This will follow in the next section.

In order to treat the nonequilibrium chemistry we employ an assumed Dirichlet distribution for the joint PDF of the reacting scalars. This results in analytic closed form expressions the chemical source and source/sink terms in the mean and scalar energy equation. The form of the Dirichlet distribution is

$$P_{AB}(\Psi', \Psi'') = \frac{\Gamma(p_1+p_2+p_3)}{\Gamma(p_1)\Gamma(p_2)\Gamma(p_3)} (\Psi')^{p_1-1} (\Psi'')^{p_2-1} (1-\Psi'-\Psi'')^{p_3-1}$$

where $\Psi' \geq 0$, $\Psi'' \geq 0$, $\Psi' + \Psi'' \leq 1$ and $p_1, p_2, p_3 > 0$. The parameters p_1, p_2, p_3 can be determined from any three of the following quantities: $<A>$, $<B>$, $<A'^2>$, $<B'^2>$, $<A'B'>$, and $<A'^2> + <B'^2>$. Here we select the scalar means and the sum of the scalar

variances, or the reacting scalar energy, Q, and we also perform a second closure using the reactant means and covariance.

The Joint Gaussian distribution used for comparison is expressed as

$$P_{AB}(\Psi', \Psi'') = \frac{e^{\frac{1}{2(1-\rho^2)}\left[\frac{(\Psi' - <A>)^2}{<A'^2>} - 2\rho\frac{(\Psi' - <A>)(\Psi'' - <B>)}{\sqrt{<A'^2><B'^2>}} + \frac{(\Psi'' - <A>)^2}{<A''^2>}\right]}}{2\pi\sqrt{< A'^2 >< B^2 >}\sqrt{1-\rho^2}}$$

where ρ is the correlation coefficient, defined as $<A'B'> / <B'^2><A'^2>$.

Presentation of Results:

Computations of the conserved scalar mean and variance were performed with the constants in front of the turbulent fluctuation and dissipation terms as 0.89 and 5.72, respectively. The production constant is the same as suggested by LaRue *et al.* (1981) but the dissipation level had to be increased from their value of 2.25. This is because the peak intensity in the experiment of Saetran *et al.* (1989) is about 30% less than the peak intensity of LaRue *et al.*. Figures 1 and 2 show the the conserved scalar mean and standard deviation plotted against the similarity variable η, normalized by the mixing layer thickness δ. δ is the distance between the points where the mean is 0.1 and 0.9 (Saetran *et al.*, 1989). Excellent agreement with the experimental data is observed. With the first two moments all higher order moments of the conserved scalar are available from simple analytic expressions (Statistics, 19xx). In figures 3 and 4 the skewness and kurtosis versus transverse distance are shown for both the model and the experimental data. While the general trends are encouraging, note that local minima and maxima are not captured.

The participating chemical species used to obtain the reacting scalar data are nitric oxide and ozone. Two cases were examined by Saetran *et al.*, a low and a high Damköhler number case. The experimental results for the high Damköhler number case were deemed close to the fast chemistry equilibrium limit and are chosen for comparison in this study. Thus, using the values of the conserved scalar mean and variance, as discussed, we can now assess our model predictions for the reacting scalar statistics. Figure 5 shows the mean reactant concentrations normalized by their inlet values. Also shown is the Beta density solution obtained from our closed form expressions for reactant conversion. The agreement is quite good. In figure 6 we show the standard deviations of the reactant concentrations versus transverse distance. Here again we note the excellent agreement with experimental data

in both the peak intensity level and the overall distribution. Another important quantity in modeling of turbulent reacting flows is the unmixedness or normalized concentration covariance. With the Beta density a closed form expression for the unmixedness has been obtained (Madnia *et al.*, 1991; Frankel *et al.*, 1992). Figure 7 shows a comparison of the unmixedness between our predictions and the experimental data with encouraging result.

Obviously the reason for the good agreement between our model predictions and the experimental data is the necessary agreement between our assumed Beta PDF and the experimentally measured PDFs. Bilger *et al.* (1991) provides further experimental data, specifically the conserved and reacting scalar PDFs. These are presented in figure 8. The agreement between the measured PDFs and the Beta PDF provides the rationale for our previously discussed statistical concordance. Due to the excellent agreement and attractive simplicity of our closed form expressions for the entire statistical behavior of the scalar mixing layer field, and previous agreements in both homogeneous and non-homogeneous environments, we heartily recommend usage of these formulas for predictions of the limiting bounds of the reactant conversion under warranted conditions.

Of greater interest is the prediction of species concentration for finite rates of reactant conversion. With the assumed Dirichlet distribution, analytic expressions for the statistics of the scalar field allow closure of the chemical source terms in the mean and scalar energy transport equations. The three parameters of the Dirichlet distribution are $p_1 = <A>a$, $p_2 = <B>a$, and $p_3 = (1- <A> - <B>)a$, where a depends on whether the third specified quantity is the species covariance or the scalar energy. With the scalar energy as the specified quantity,

$$a = \frac{<A>\,(1- <A>)+ <B>\,(1- <B>)}{<A'^2> + <B'^2>} - 1$$

and specifying the covariance,

$$a = -(\frac{< A'B' >}{< A >< B >} + 1)$$

In a scalar mixing layer with homogenous turbulence and the assumptions of stationary flow, self similarity, and high Reynolds number, the transport equation of Q is

$$\alpha\frac{d^2Q}{d\eta^2} + \frac{\eta}{2}\frac{dQ}{d\eta} + 2(\frac{d<A>}{d\eta})^2 + 2(\frac{d<B>}{d\eta})^2 - \gamma Q + 2X(\overline{\dot{\omega}_A A'} + \overline{\dot{\omega}_B B'}) = 0$$

where η is the similarity transformation variable, X is the downstream location normalized by the turbulence grid mesh size, and α and γ are the constants in front of the turbulent fluctuation and dissipation terms. The analogous equation for the species covariance is

$$\alpha\frac{d^2<A'B'>}{d\eta^2}+\frac{\eta}{2}\frac{d<A'B'>}{d\eta}+2\frac{d<A>}{d\eta}\frac{d<B>}{d\eta}-\gamma<A'B'>+X(\overline{\dot{\omega}_A A'}+\overline{\dot{\omega}_B B'})=0$$

The derivatives were approximated with second order central finite differences at fifty gridpoints between the boundaries of $\eta = 4$ and $\eta = -4$. The statistical closures in terms of the scalar means and energy result in a system of coupled non-linear equations which were solved with a Newton-Rapson scheme with a convergence criterion of 1×10^{-5}.

For purposes of comparison, in addition to the Dirichlet and the Joint Gaussian models, also used is a mean-chemistry model, in which fluctuations are ignored in the chemical source terms of the transport equations The solutions of all the closure models for the mean reactant concentrations versus the normalized similarity variable. are shown in figures 9 and 10, for the the low and high Damköhler number cases, respectively. In order to make a better evaluation of the merits of each model than is possible with the mean concentration profiles, presented in figures 11 and 12 (for the same respective case) are the mean product profiles. The Dirichlet model parameterized with scalar energy provides the most accurate measure of peak product generation, while the mean chemistry model overpredicts the reactant conversion (especially in the center of the mixing layer, where the reaction occurs most vigorously).

Figures 13 and 14 show the total scalar energy of the high and low Damköhler number cases for all models. The Dirichlet model parameterized with scalar energy captures the reduction of scalar energy in the center of the mixing layer (where the bulk of the reaction occurs), whereas the other models do not. The negative of the unmixedness (in this case equal to the covariance, because the intial reactant concentrations are normalized to unity) are shown for Da=0.3 and Da=1.81, respectively, in figures 15 and 16.

Bilger (1991) provides experimental data of the skewness and kurtosis of mixture fraction for a variety of Damköhler numbers. For all the cases presented, it appears that these moments are invariant with Damköhler number. Figures 17 and 18 present the skewness, and 18 and 19 the kurtosis, of the two cases of finite rate chemistry (again, Da=0.3 and

Da=1.81). In both mixture fraction moments, the higher Damköhler number case better reproduces the experimental data.

Again the reason for the favorable results of our model is the agreement between our assumed PDFs and the measured PDFs. Bilger provides experimental data of the joint PDFs of the concentrations of the two reactants. Joint PDFs of the species concentrations according to the Dirichlet model are presented in figures 21 and 22.

Figures 23 and 24 show the contribution to the scalar energy transport equation of the dissipation, production and chemical terms for the two cases of Damköhler number. In a recent paper, Baurle *et al.* (1992) use an assumed Dirichlet distribution for concentration in supersonic turbulent combustion. They find that the chemical source acts as a sink which effectively reduces the total scalar energy, and is not consistent with the experimental data. We can draw the same conclusion from our results. For the high Damköhler number, the chemical term is a greater sink than the low Damköhler case, almost matching the dissipation term at its peak. Hence the better match in peak intensities of total scalar energy for the low Damköhler number case.

As a result of the encouraging agreement for predictions of finite rates of reactant conversion in the scalar mixing layer and of mixture fraction moments with using the scalar energy-parameterized Dirichlet distribution, we extend our recommendation, in the absence of better alternatives, to this model.

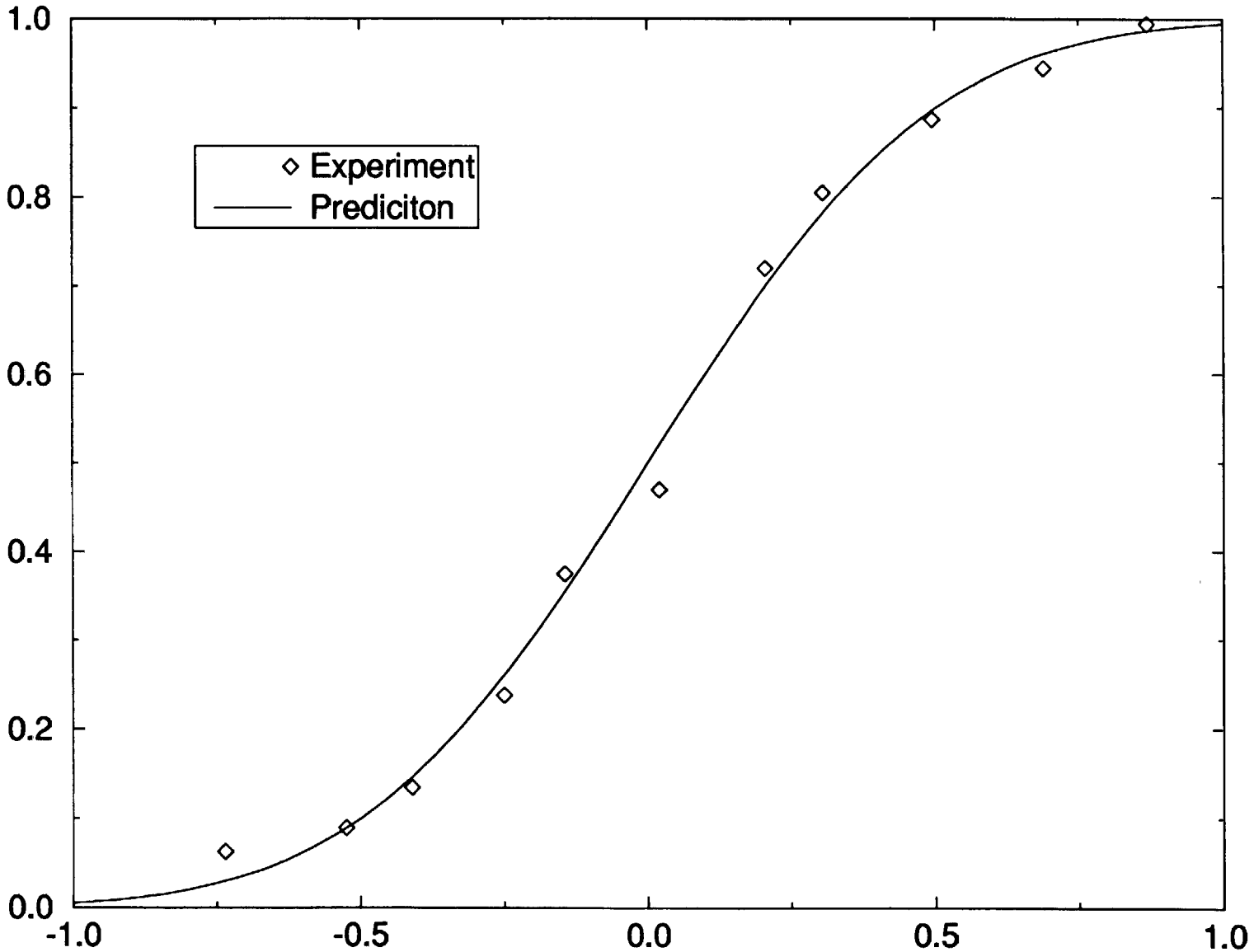

Figure 1

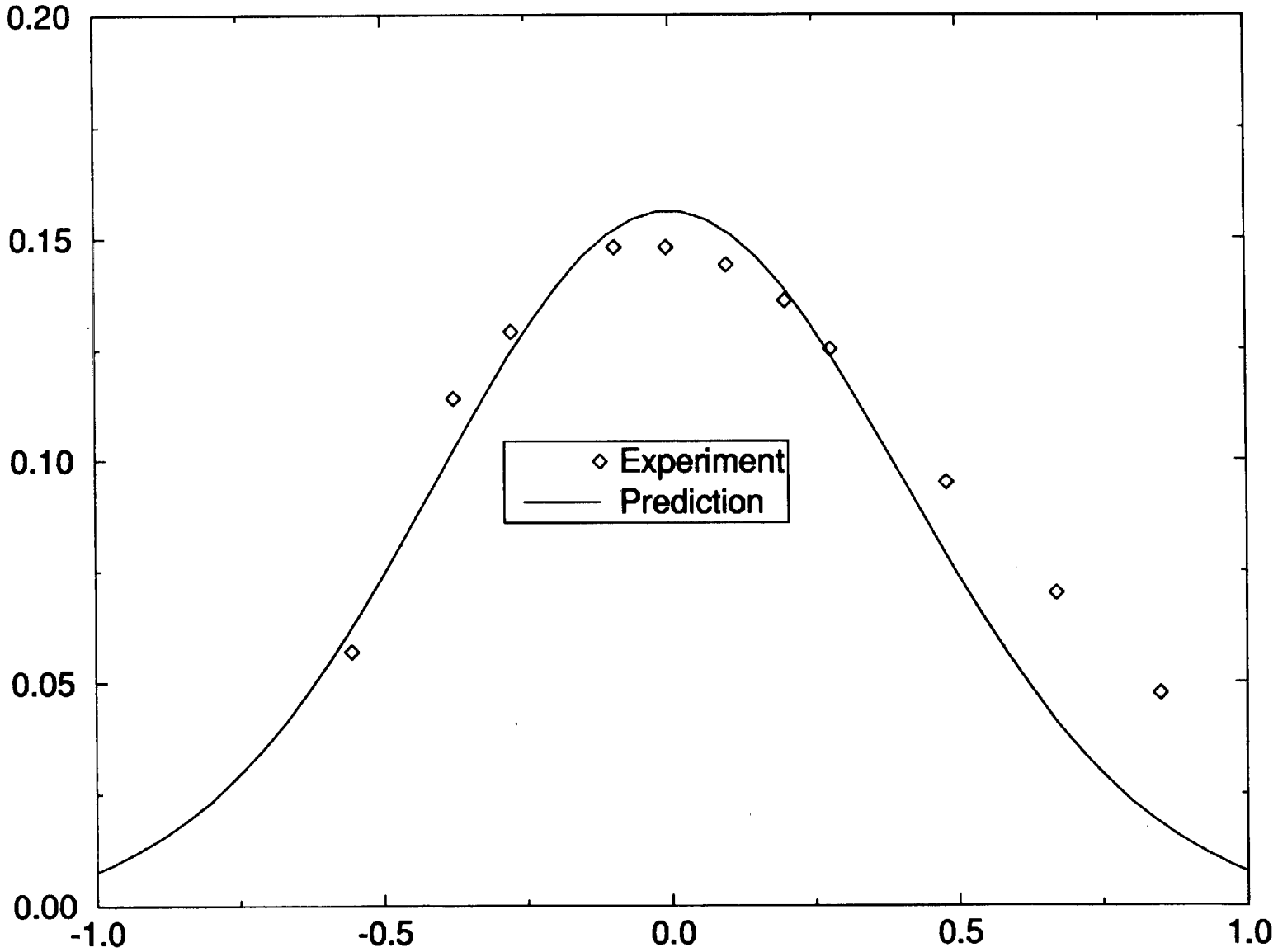

Figure 2

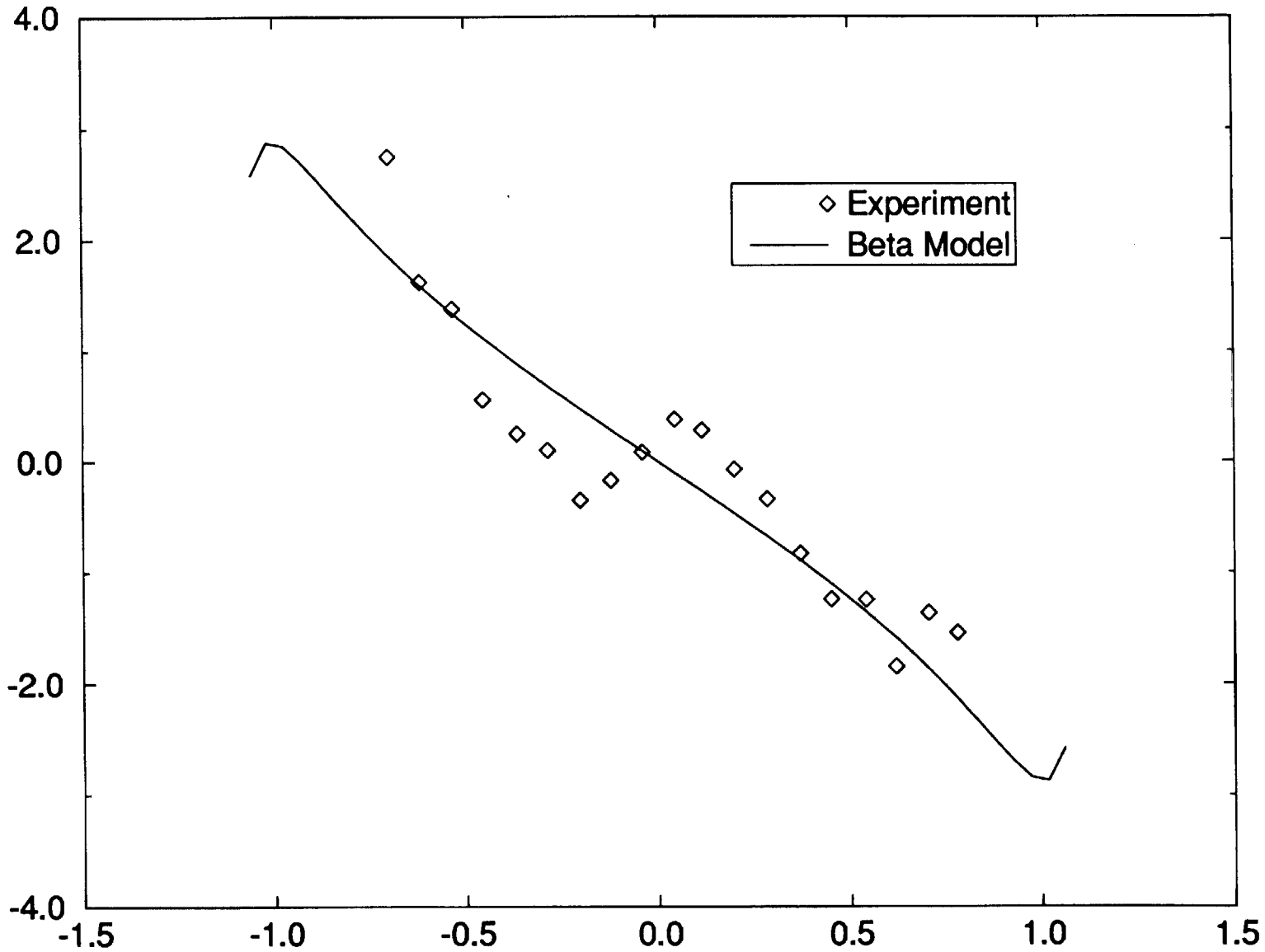

Figure 3

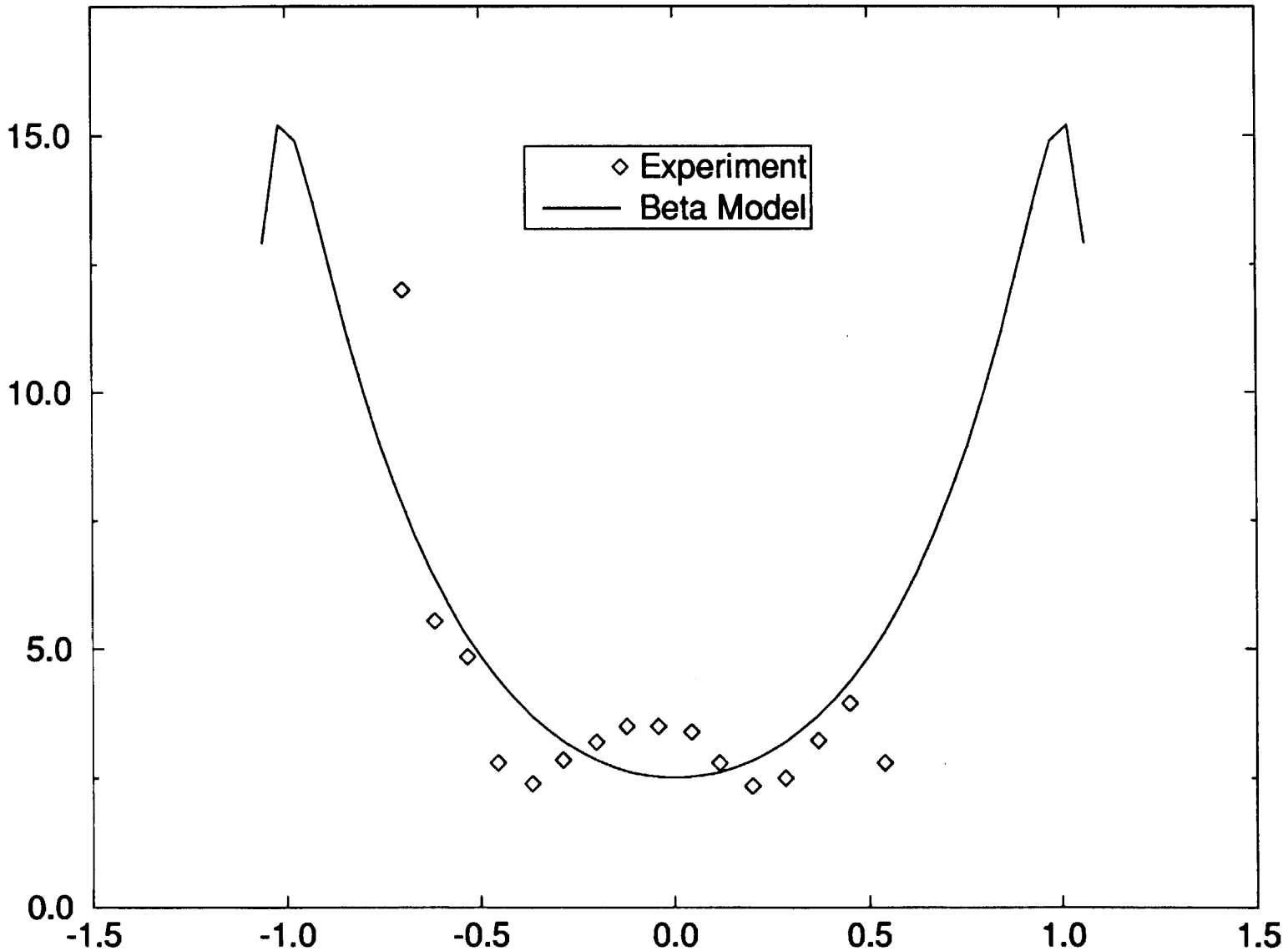

Figure 4

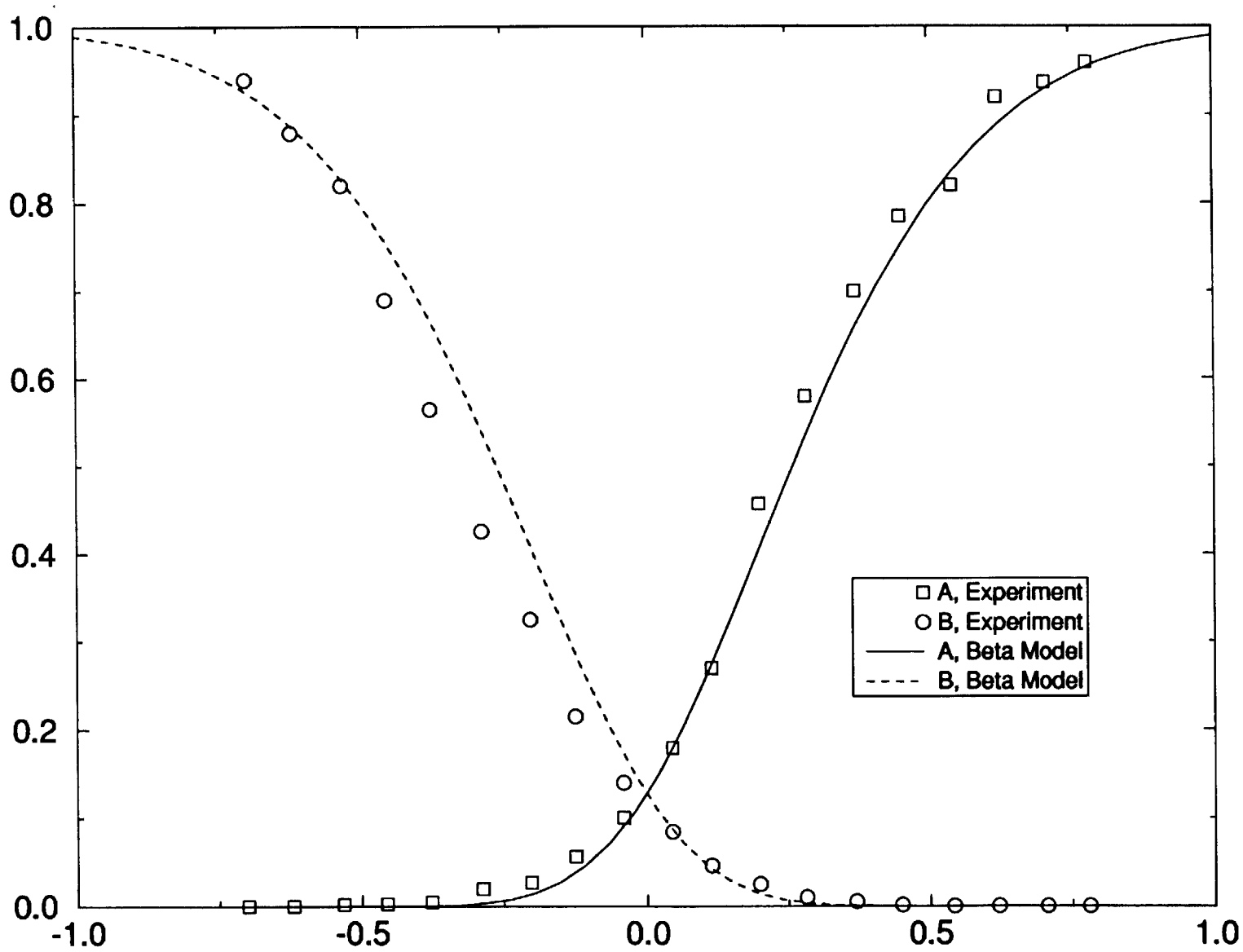
1.0
0.8
0.6
0.4
0.2
0.0
-1.0
-0.5
0.0
0.5
1.0
A, Experiment
B, Experiment
A, Beta Model
B, Beta Model

Figure 5

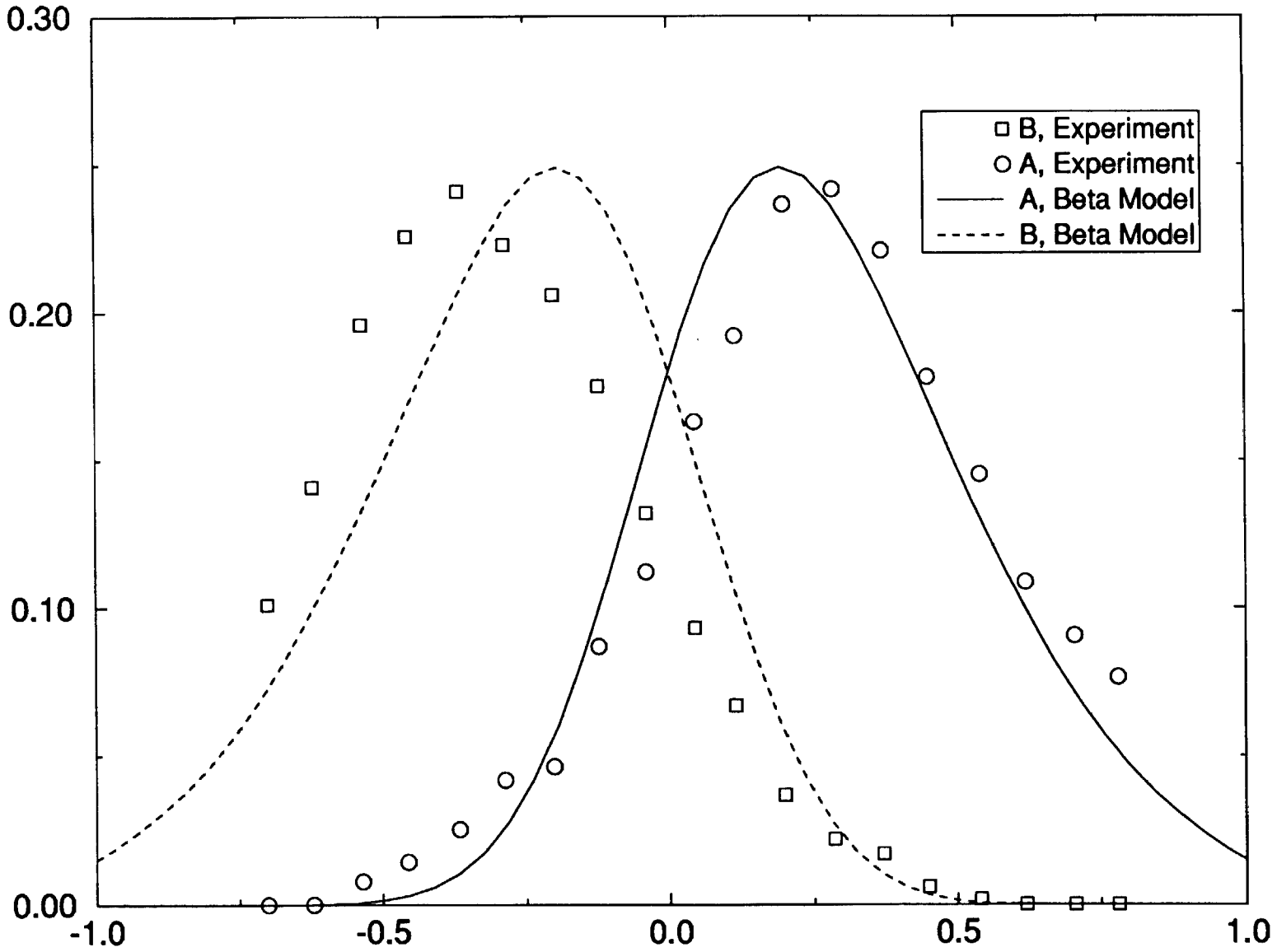
0.30
0.20
0.10
0.00
-1.0
-0.5
0.0
0.5
1.0
B, Experiment
A, Experiment
A, Beta Model
B, Beta Model

Figure 6

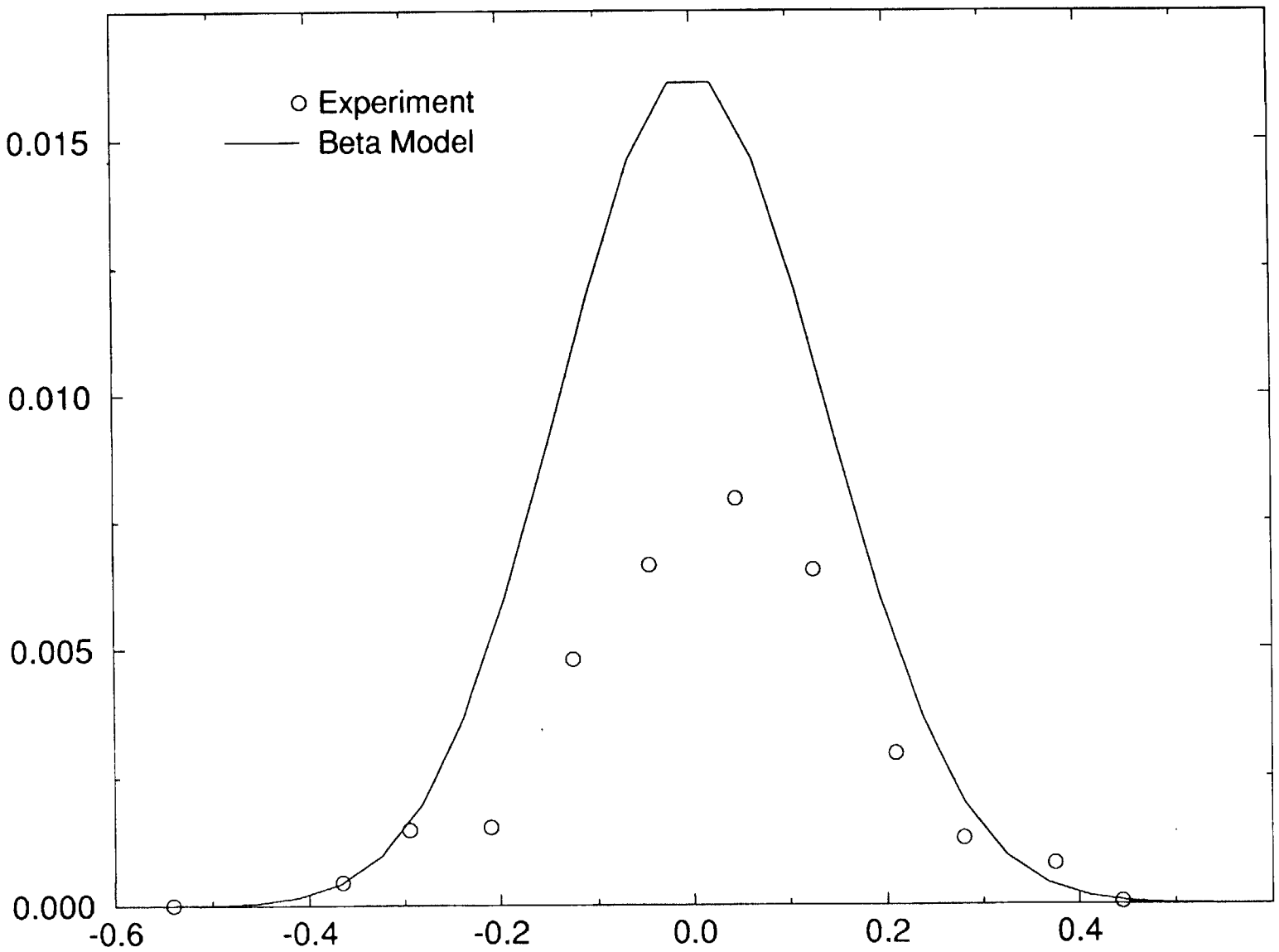

Figure 7

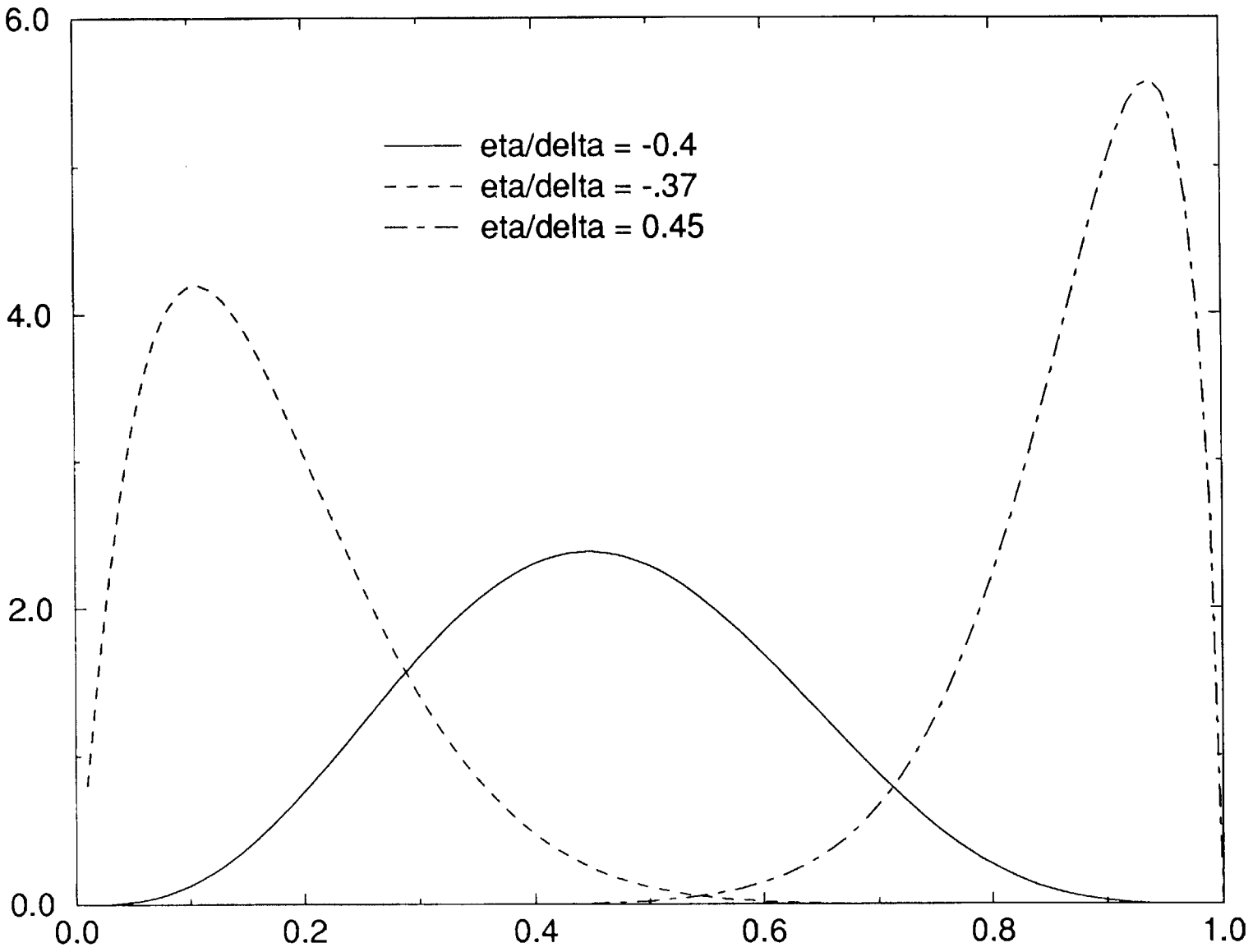
6.0
4.0
2.0
0.0
0.0
0.2
0.4
0.6
0.8
1.0
eta/delta = -0.4
eta/delta = -.37
eta/delta = 0.45

Figure 8

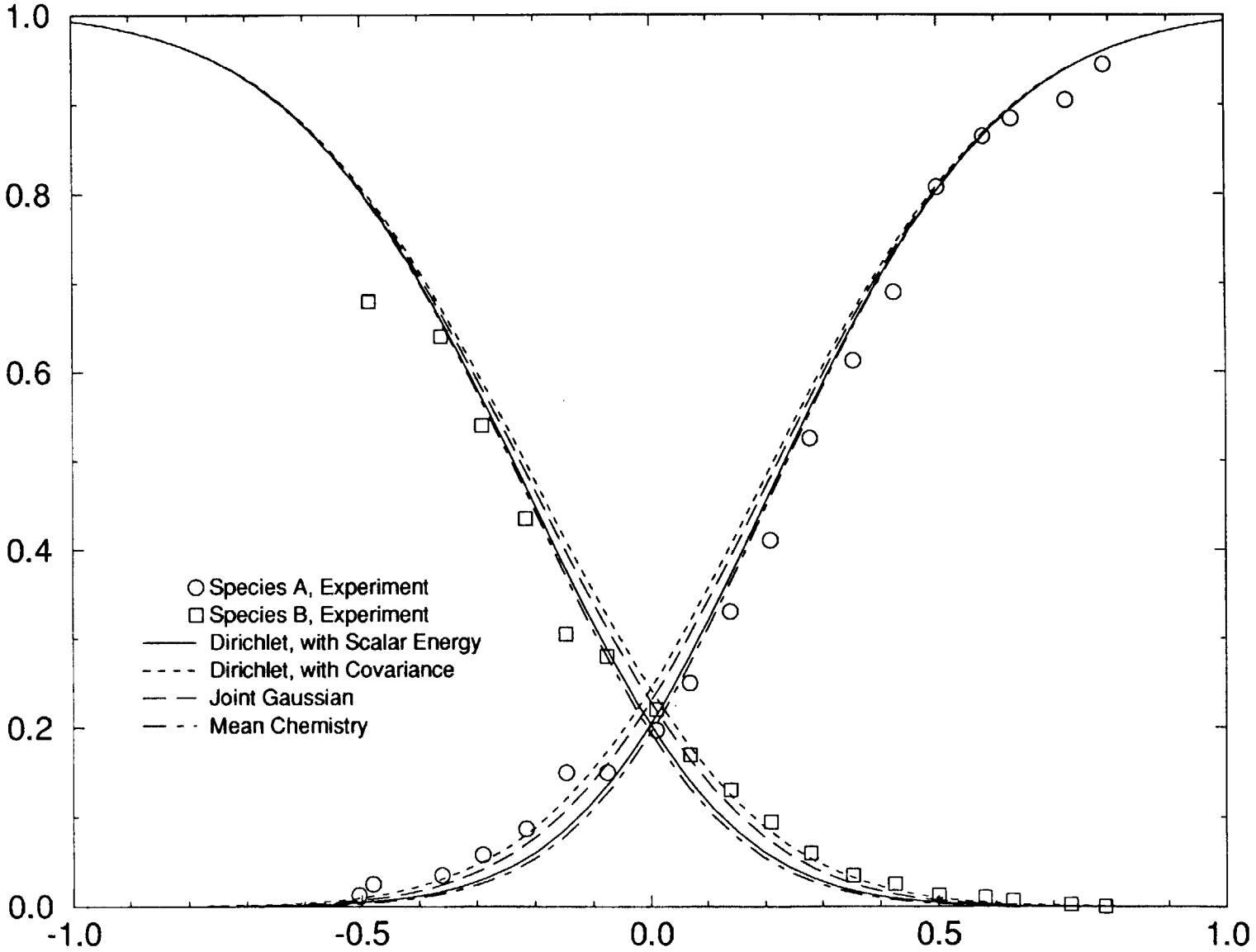
1.0
0.8
0.6
0.4
0.2
0.0
-1.0
-0.5
0.0
0.5
1.0
Species A, Experiment
Species B, Experiment
Dirichlet, with Scalar Energy
Dirichlet, with Covariance
Joint Gaussian
Mean Chemistry

Figure 9

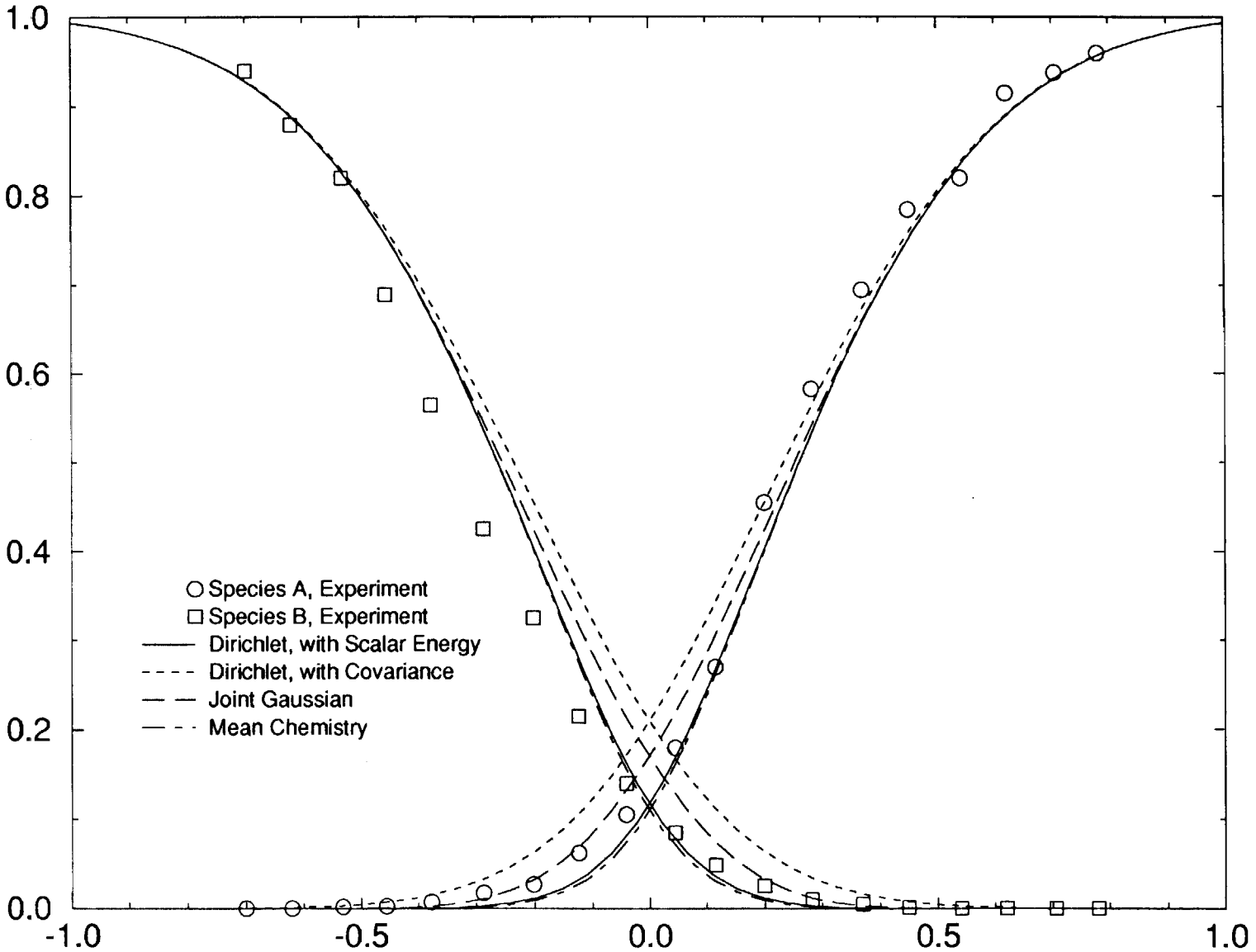
1.0
0.8
0.6
0.4
0.2
0.0
-1.0
-0.5
0.0
0.5
1.0
Species A, Experiment
Species B, Experiment
Dirichlet, with Scalar Energy
Dirichlet, with Covariance
Joint Gaussian
Mean Chemistry

Figure 10

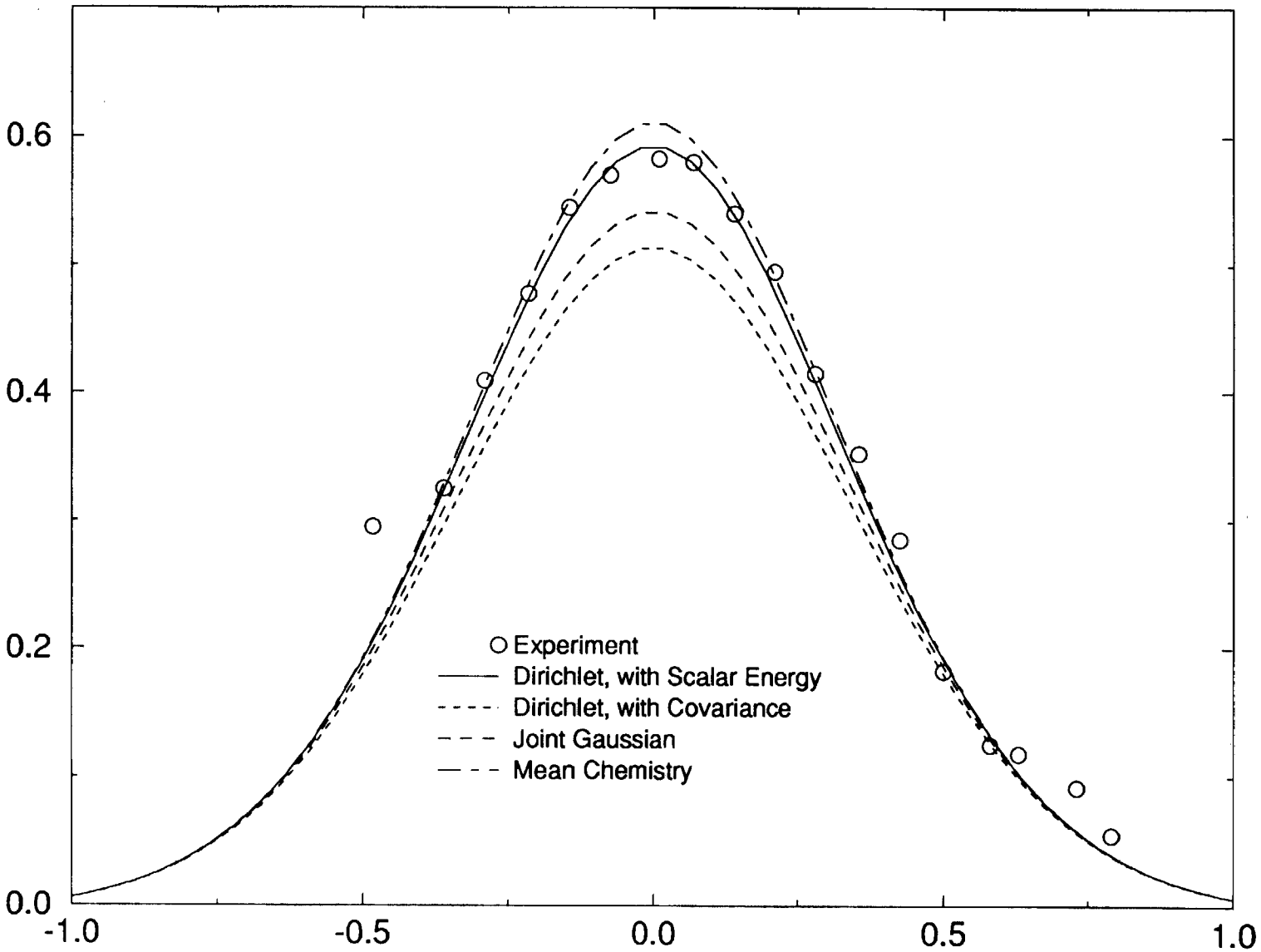
0.6
0.4
0.2
0.0
-1.0
-0.5
0.0
0.5
1.0
Experiment
Dirichlet, with Scalar Energy
Dirichlet, with Covariance
Joint Gaussian
Mean Chemistry

Figure 11

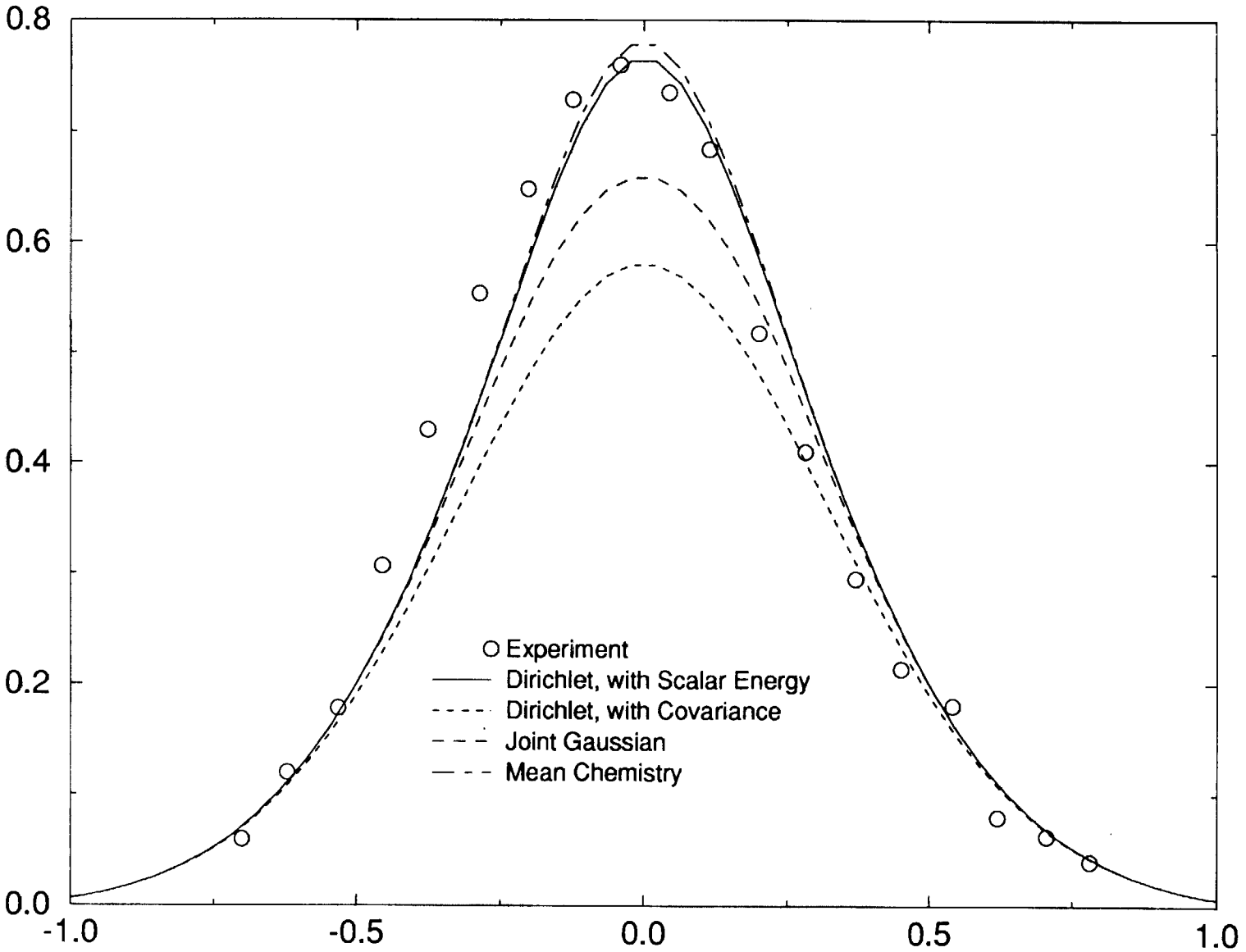
0.8
0.6
0.4
0.2
0.0
-1.0
-0.5
0.0
0.5
1.0
Experiment
Dirichlet, with Scalar Energy
Dirichlet, with Covariance
Joint Gaussian
Mean Chemistry

Figure 12

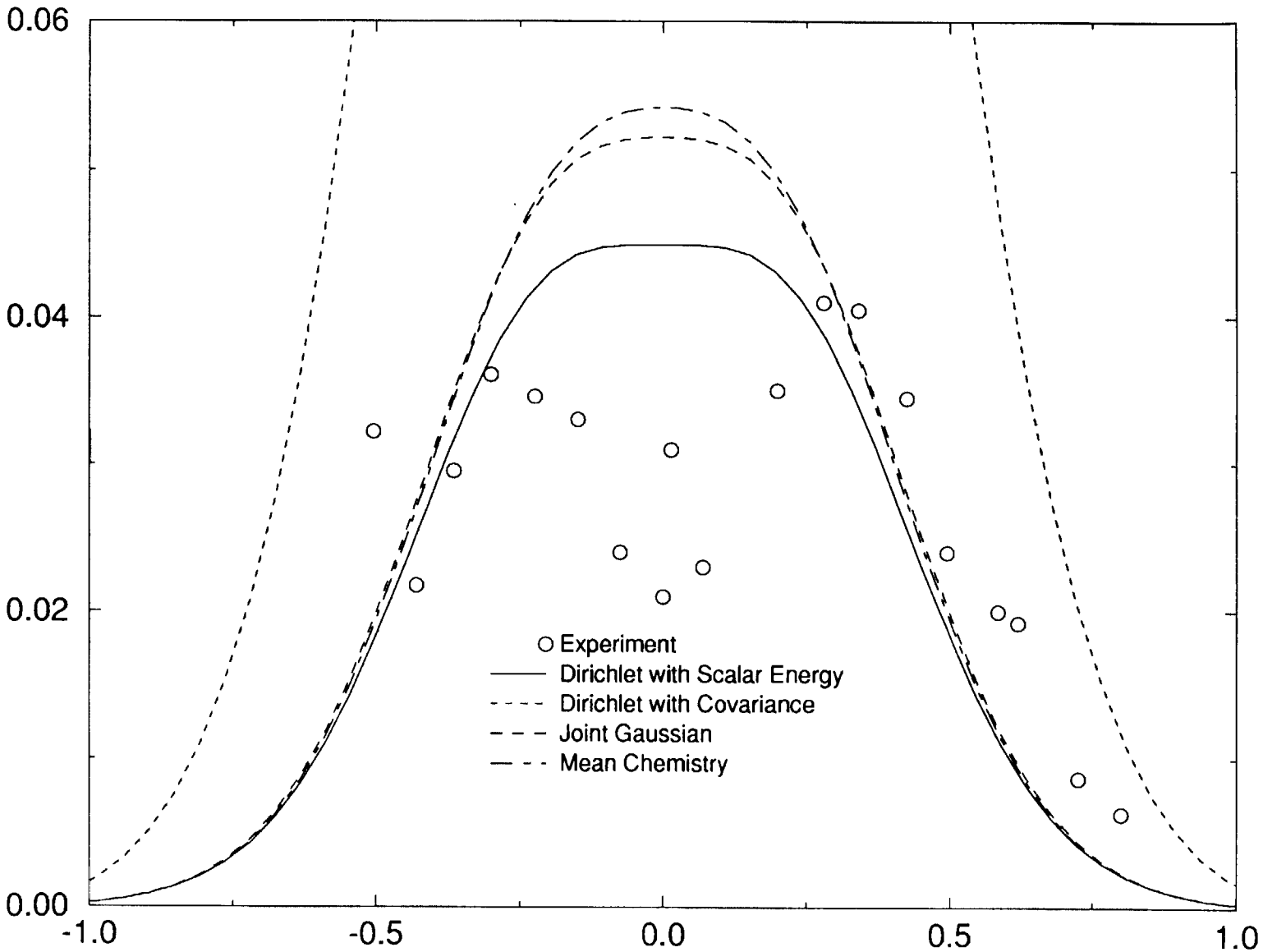
0.06
0.04
0.02
0.00
-1.0
-0.5
0.0
0.5
1.0
Experiment
Dirichlet with Scalar Energy
Dirichlet with Covariance
Joint Gaussian
Mean Chemistry

Figure 13

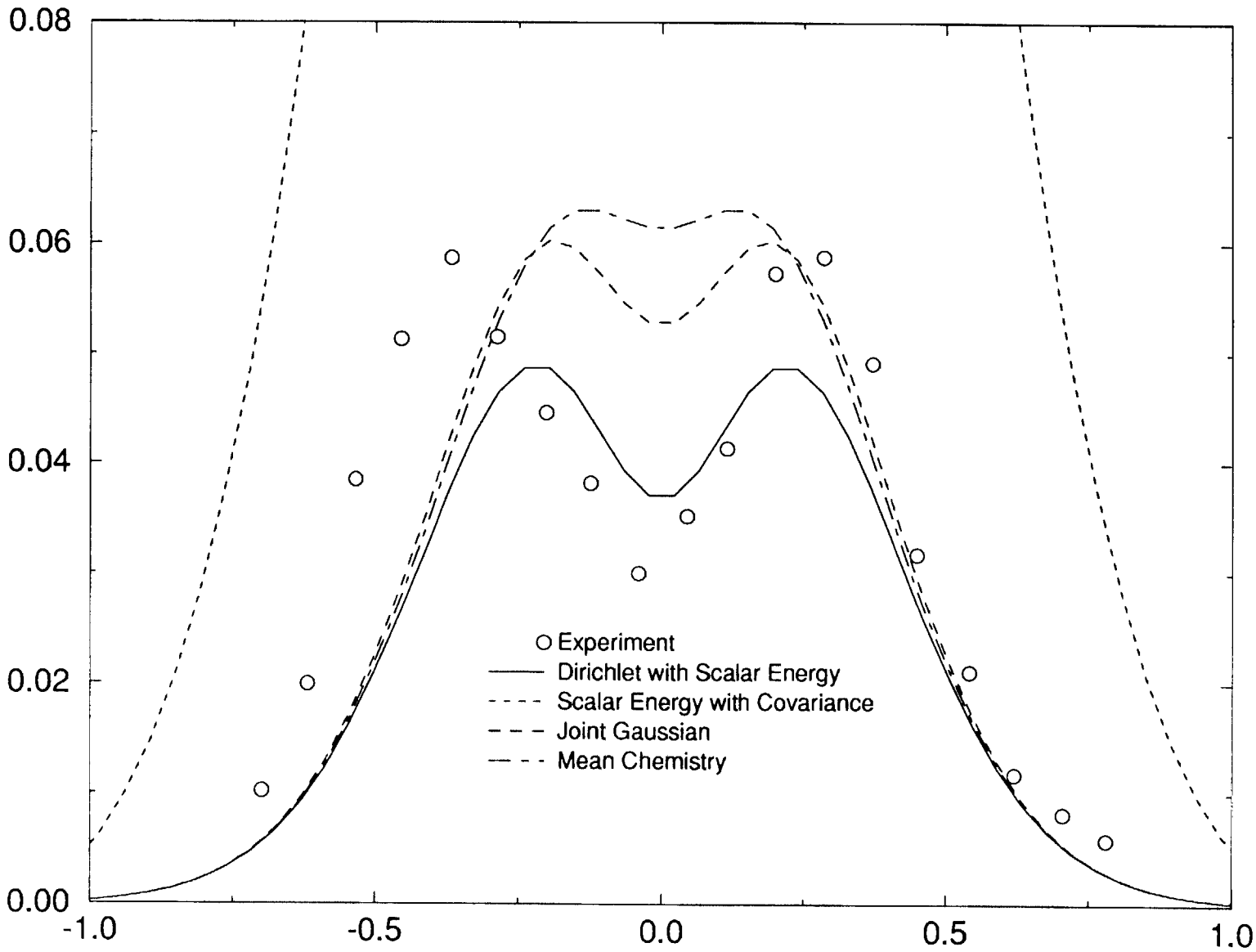
0.08
0.06
0.04
0.02
0.00
-1.0
-0.5
0.0
0.5
1.0
Experiment
Dirichlet with Scalar Energy
Scalar Energy with Covariance
Joint Gaussian
Mean Chemistry

Figure 14

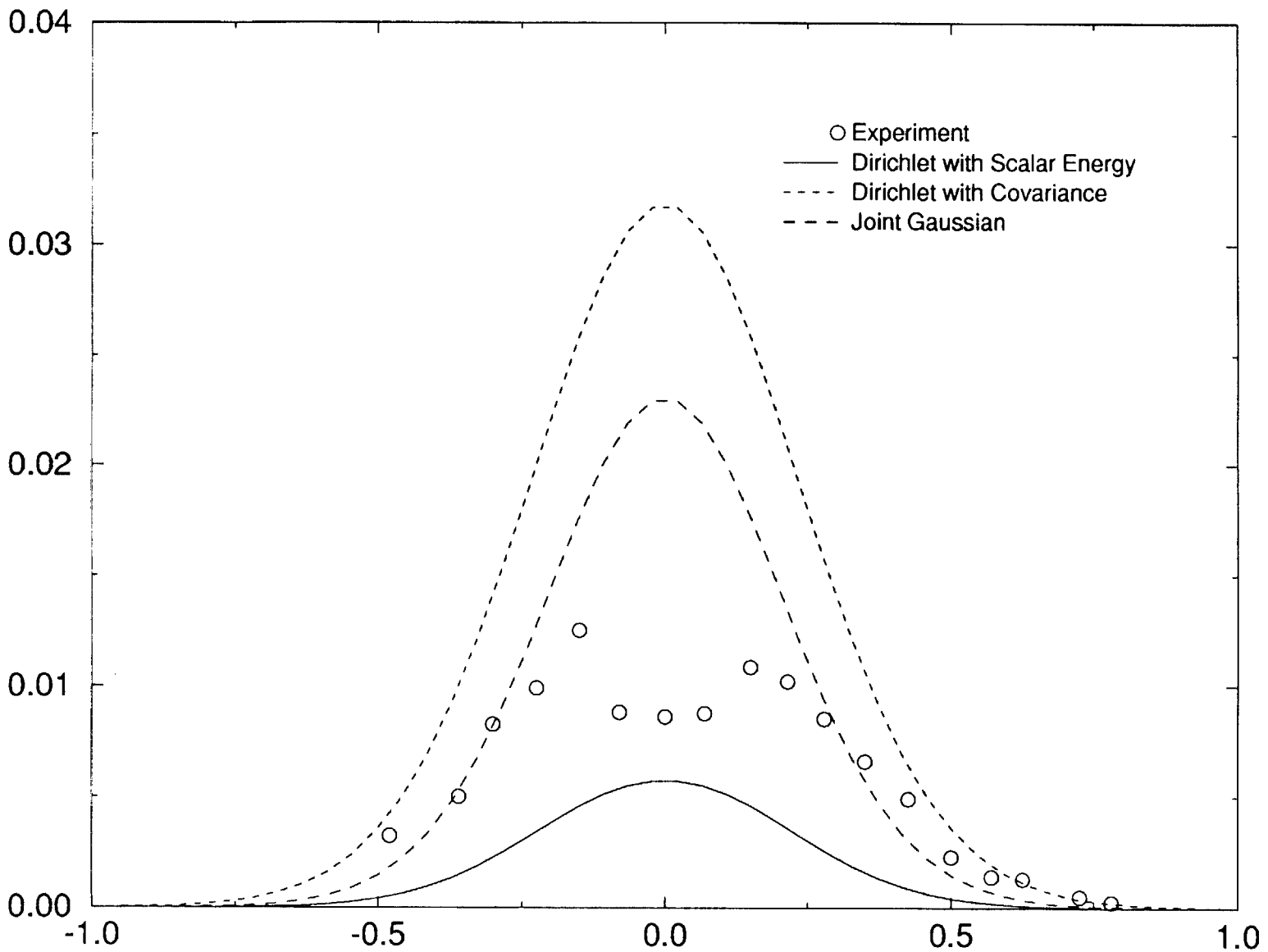
0.04
0.03
0.02
0.01
0.00
-1.0
-0.5
0.0
0.5
1.0
Experiment
Dirichlet with Scalar Energy
Dirichlet with Covariance
Joint Gaussian

Figure 15

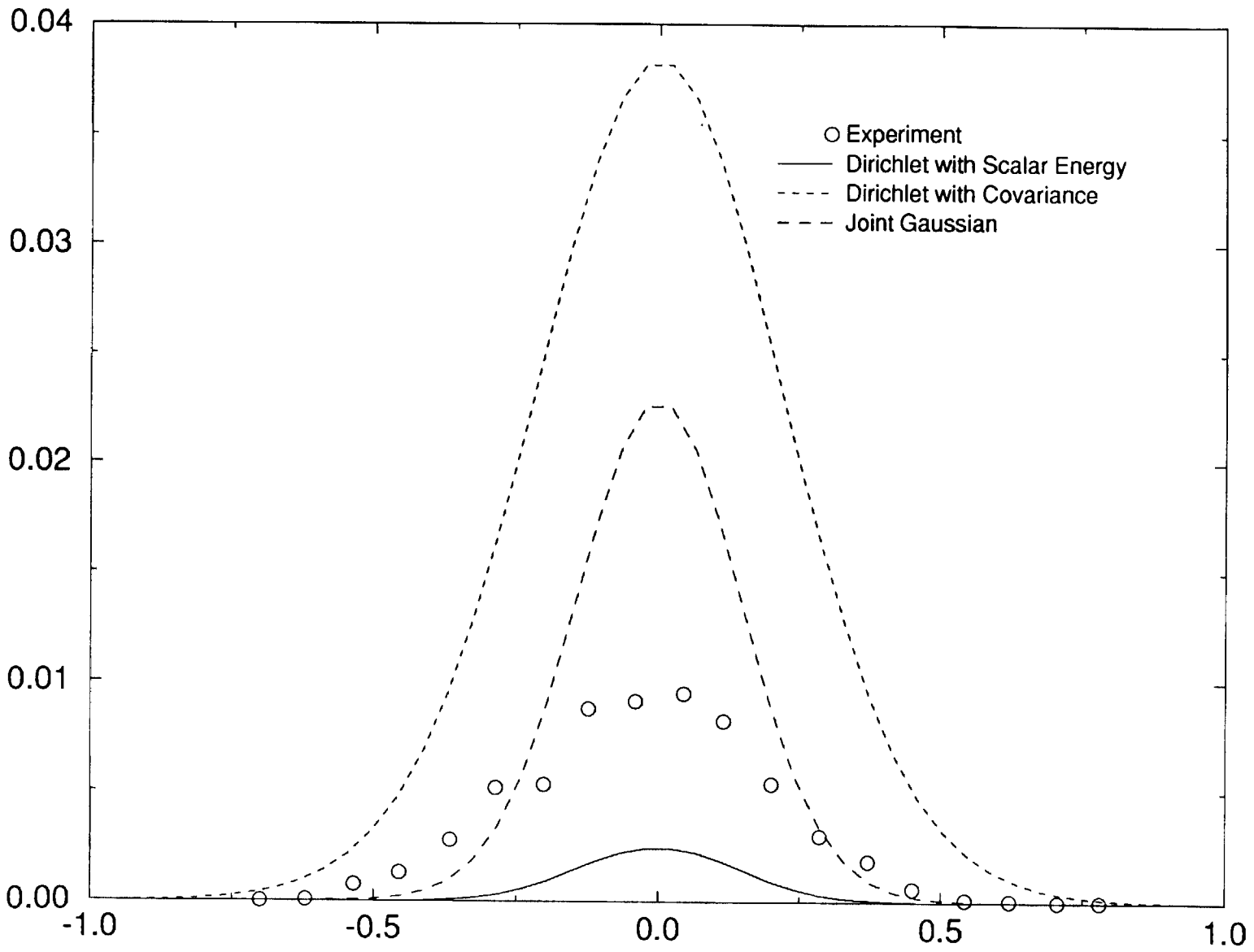
0.04
0.03
0.02
0.01
0.00
-1.0
-0.5
0.0
0.5
1.0
Experiment
Dirichlet with Scalar Energy
Dirichlet with Covariance
Joint Gaussian

Figure 16

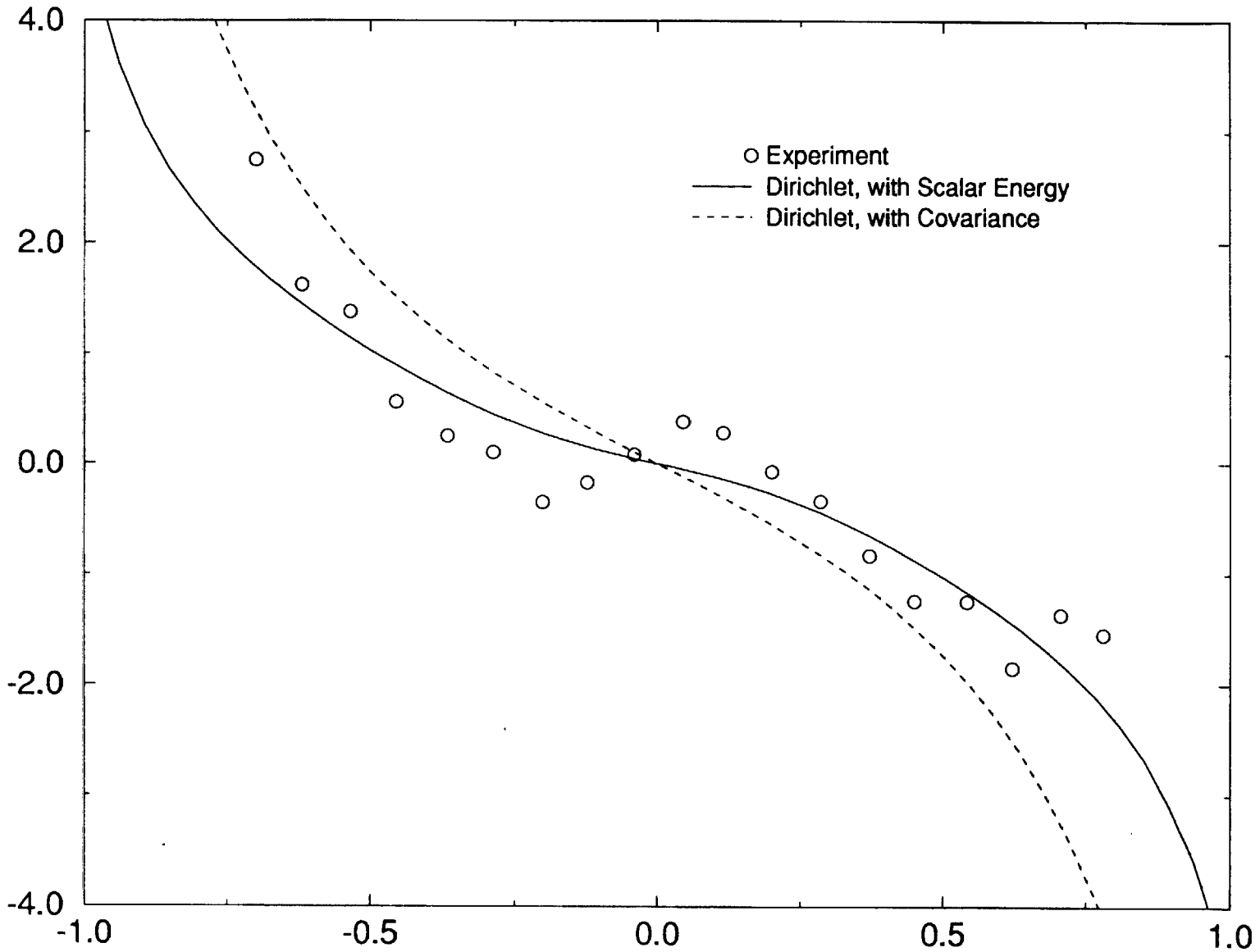
4.0
2.0
0.0
-2.0
-4.0
-1.0
-0.5
0.0
0.5
1.0
Experiment
Dirichlet, with Scalar Energy
Dirichlet, with Covariance

Figure 17

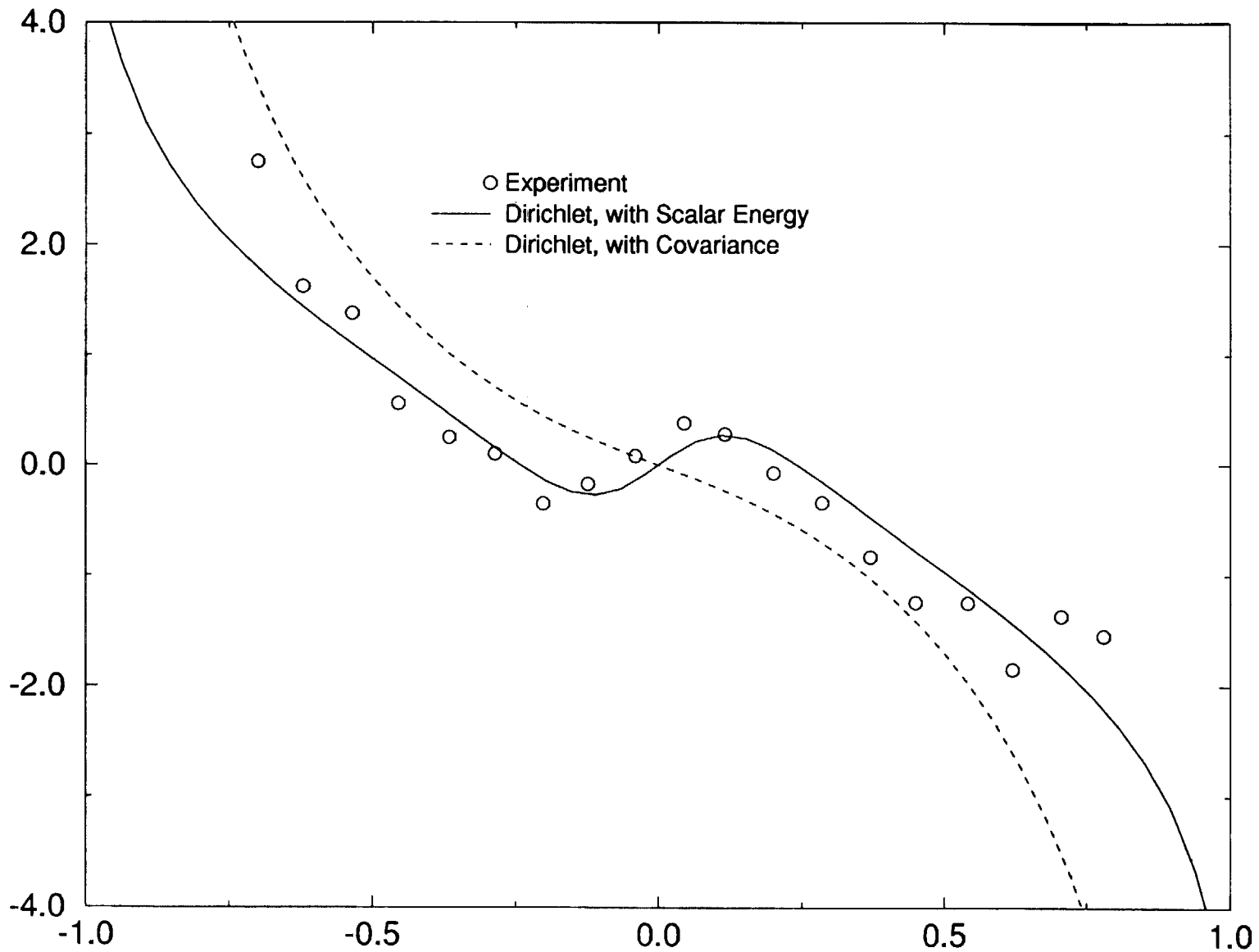
4.0
2.0
0.0
-2.0
-4.0
-1.0
-0.5
0.0
0.5
1.0
Experiment
Dirichlet, with Scalar Energy
Dirichlet, with Covariance

Figure 18

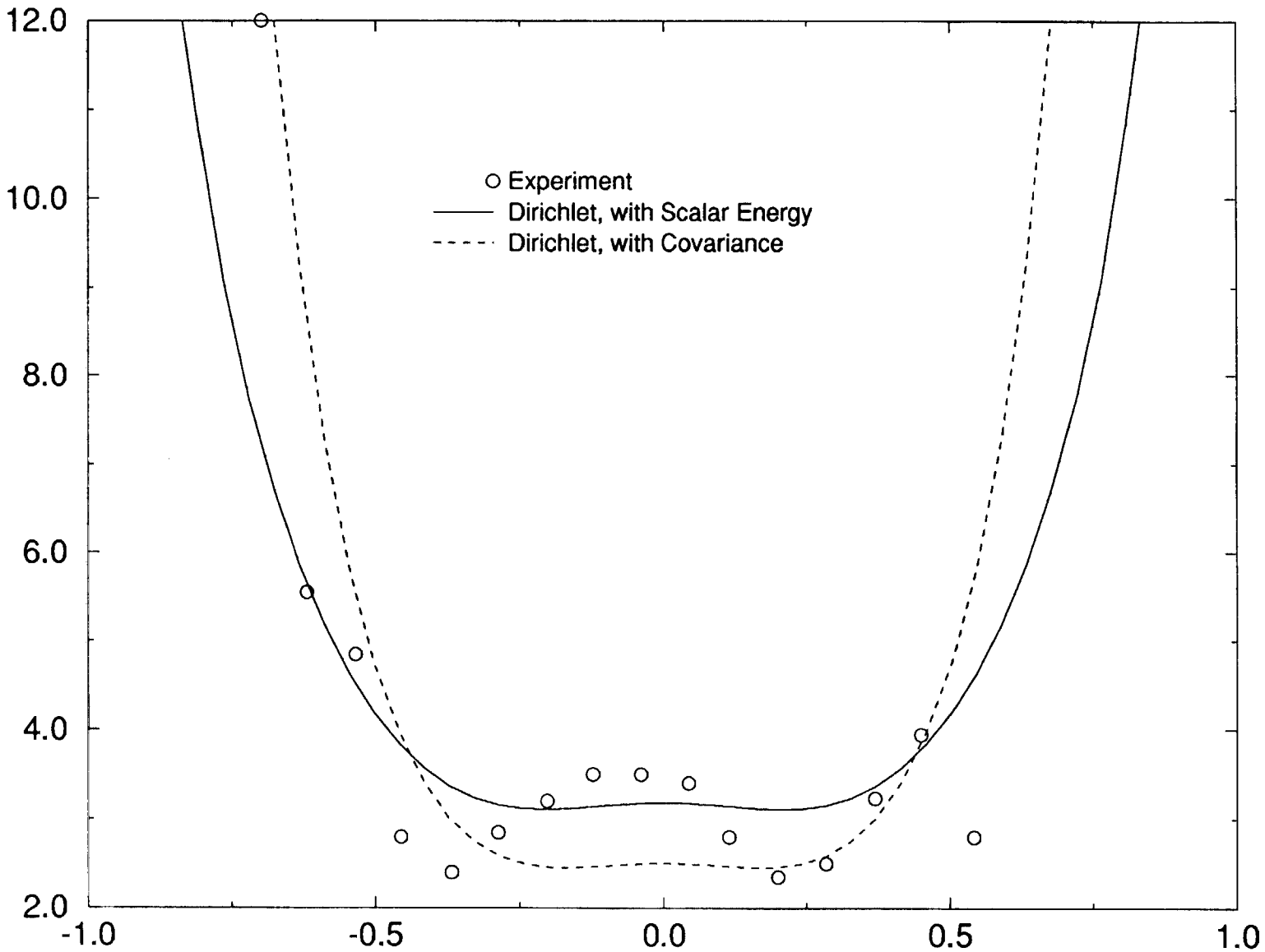
12.0
10.0
8.0
6.0
4.0
2.0
-1.0
-0.5
0.0
0.5
1.0
Experiment
Dirichlet, with Scalar Energy
Dirichlet, with Covariance

Figure 19

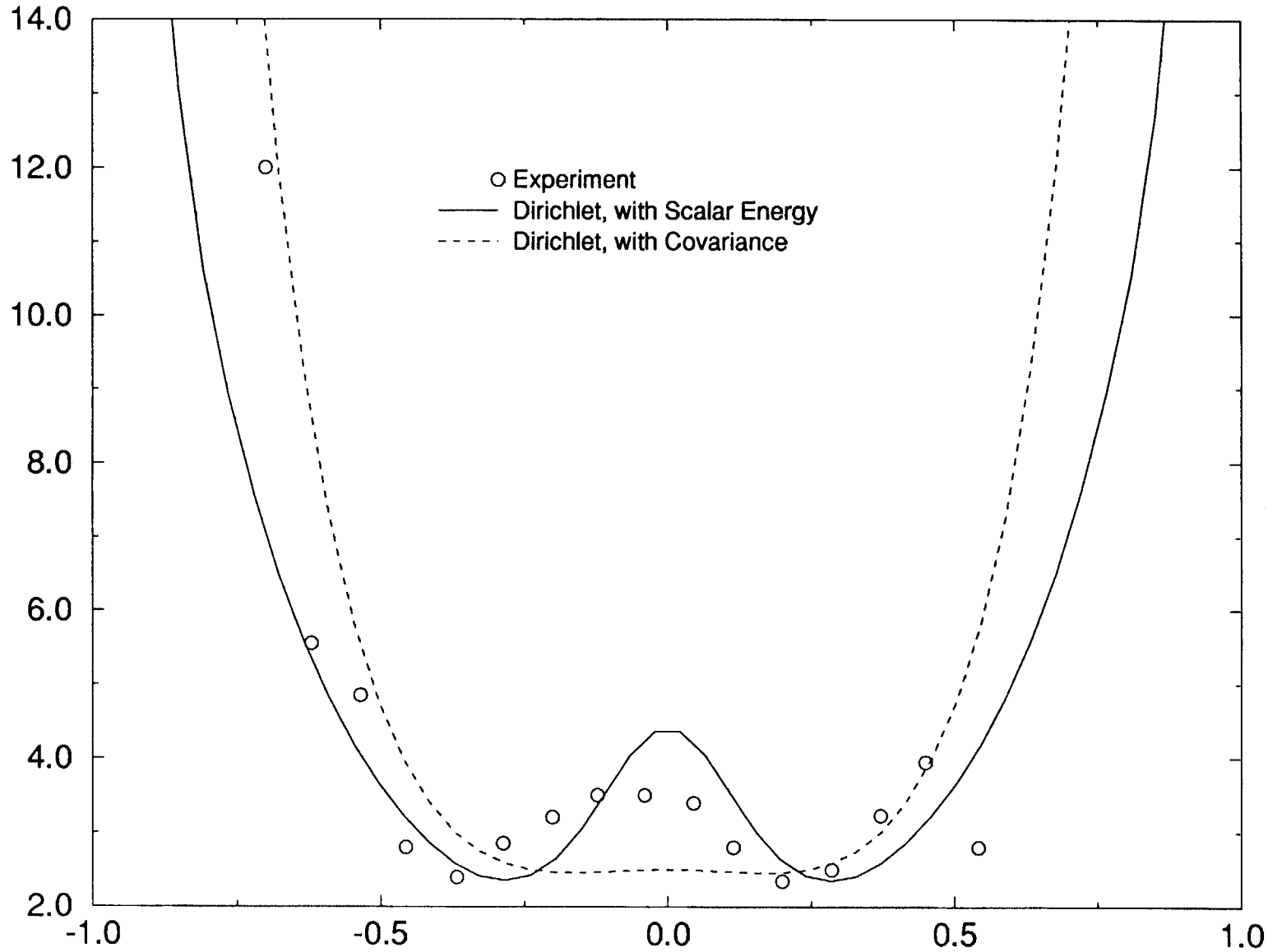
14.0
12.0
10.0
8.0
6.0
4.0
2.0
-1.0
-0.5
0.0
0.5
1.0
Experiment
Dirichlet, with Scalar Energy
Dirichlet, with Covariance

Figure 20

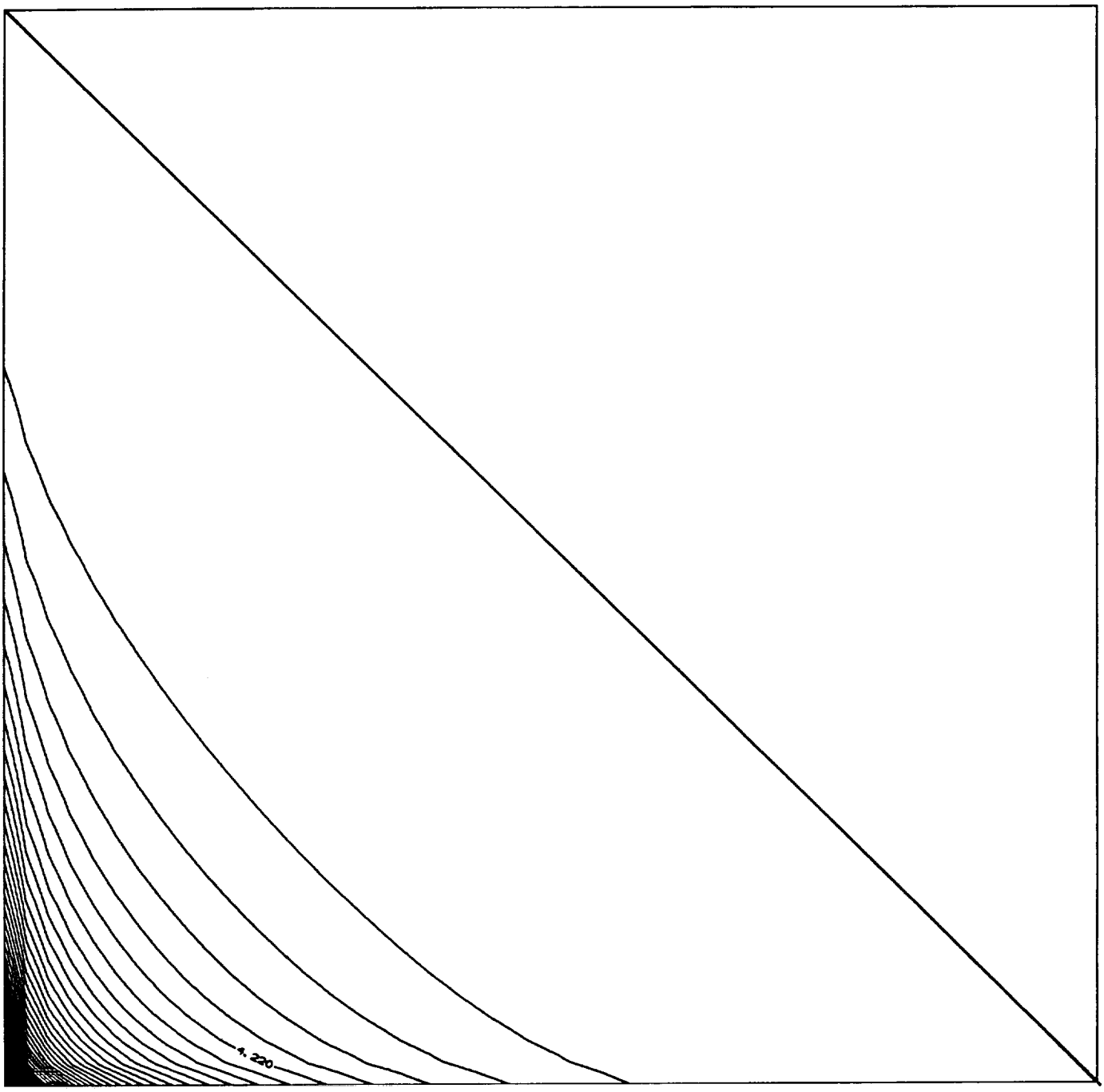

Figure 21

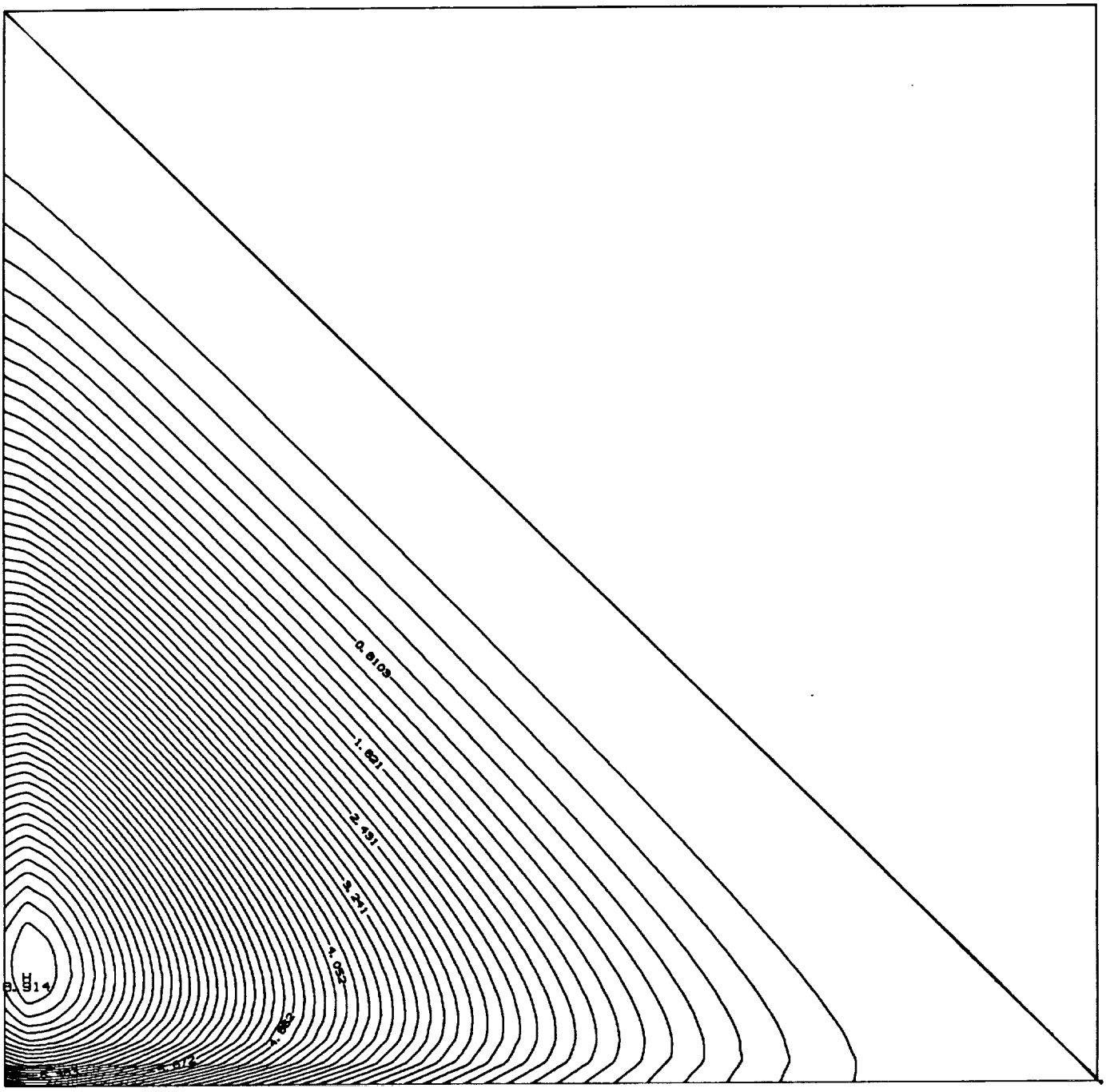

Figure 22

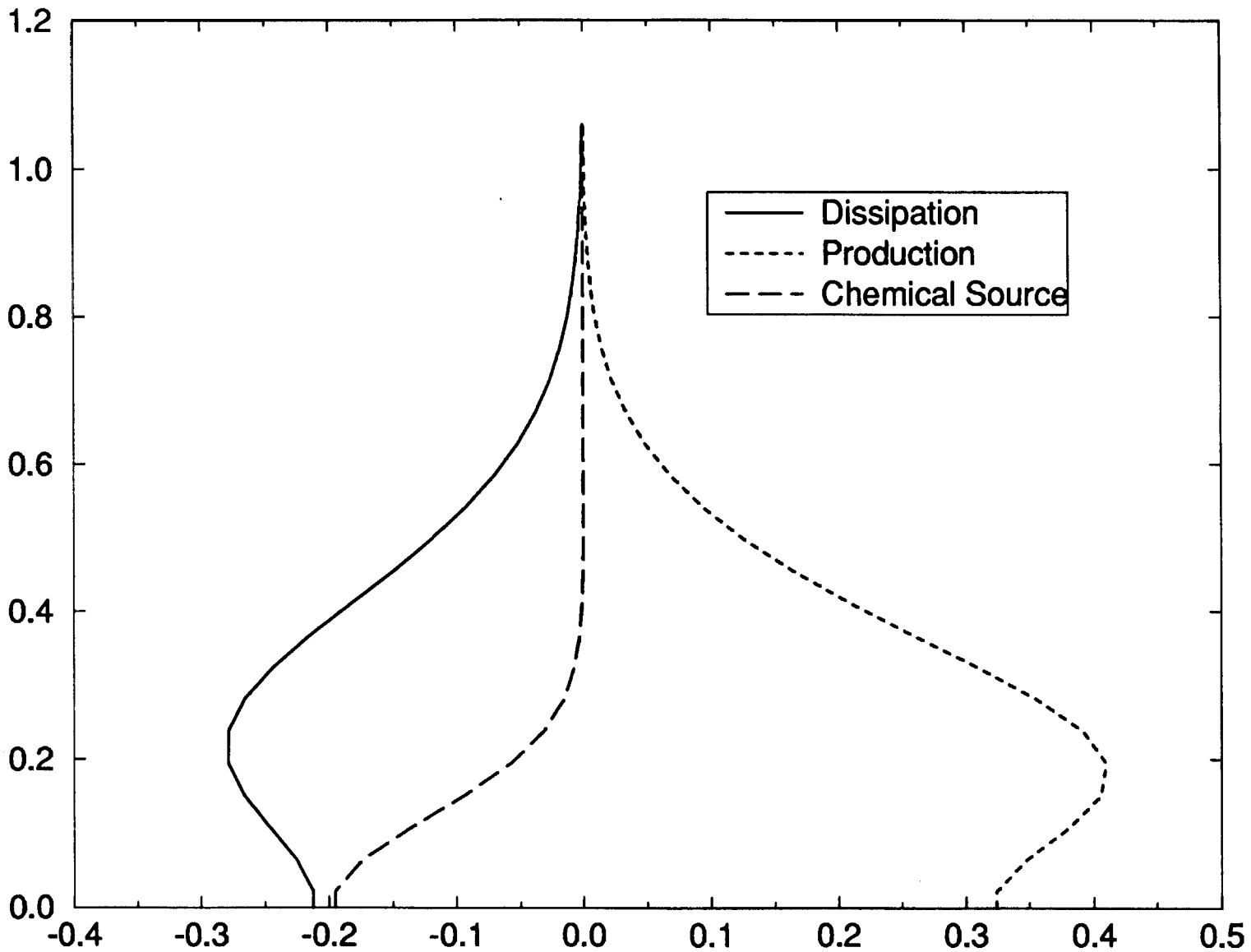
1.2
1.0
0.8
0.6
0.4
0.2
0.0
-0.4
-0.3
-0.2
-0.1
0.0
0.1
0.2
0.3
0.4
0.5
Dissipation
Production
Chemical Source

Figure 23

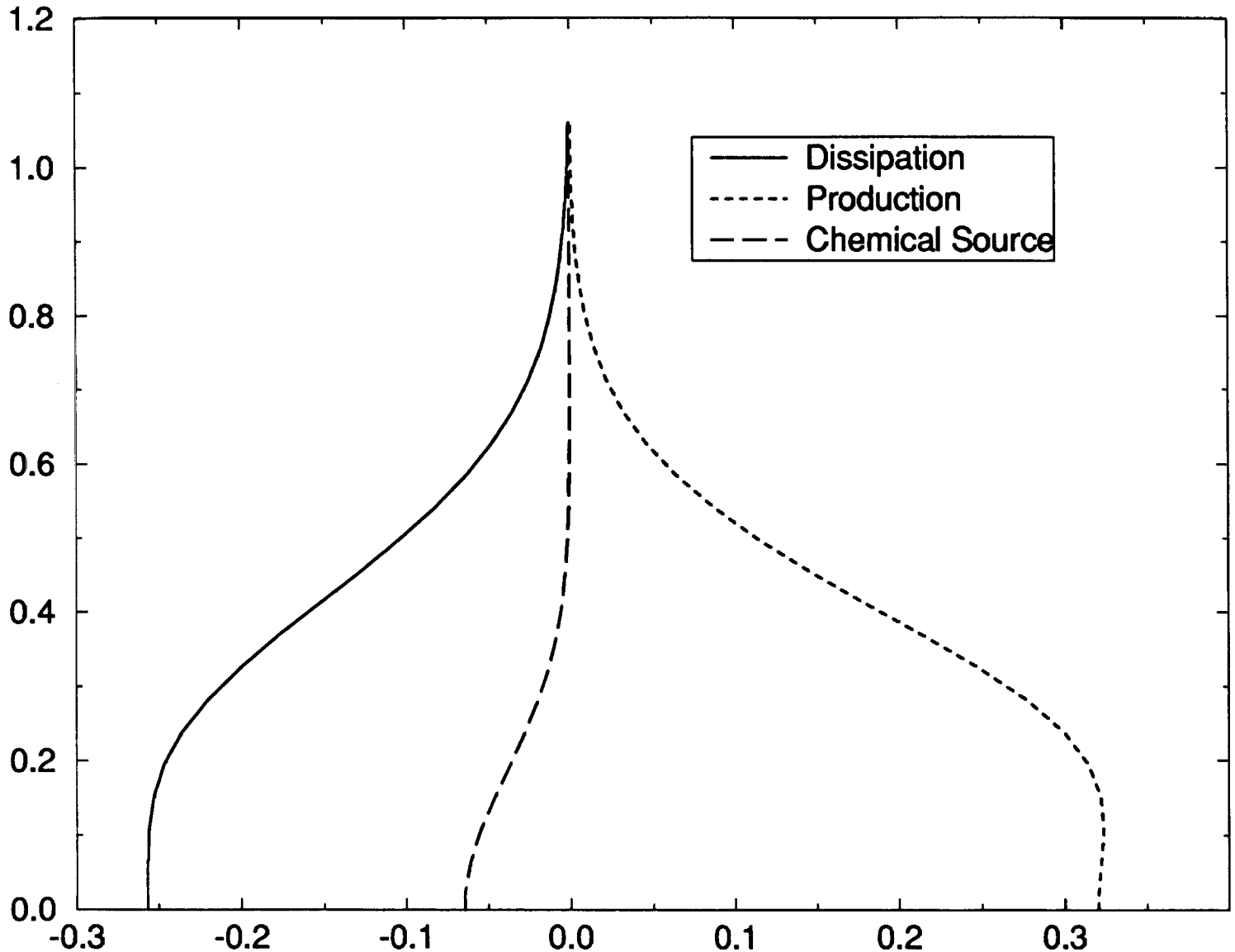
1.2
1.0
0.8
0.6
0.4
0.2
0.0
-0.3
-0.2
-0.1
0.0
0.1
0.2
0.3
Dissipation
Production
Chemical Source

Figure 24